

VOLATILITY IN EMERGING MARKETS

Introduction

The great majority of empirical studies have focused on asset markets in the US and other developed economies. The purpose of this research is to determine to what extent the findings of other researchers in relation to the characteristics of asset volatility in developed economies applies also to emerging markets. The important characteristics observed in asset volatility that we wish to identify and examine in emerging markets include clustering, (the tendency for periodic regimes of high or low volatility) long memory, asymmetry, and correlation with the underlying returns process. The extent to which such behaviors are present in emerging markets will serve to confirm or refute the conjecture that they are universal and not just the product of some factors specific to the intensely scrutinized, and widely traded developed markets.

The ten emerging markets we consider comprise equity markets in Australia, Hong Kong, Indonesia, Malaysia, New Zealand, Philippines, Singapore, South Korea, Sri Lanka and Taiwan focusing on the major market indices for those markets. After analyzing the characteristics of index volatility for these indices, the research goes on to develop single- and two-factor REGARCH models in the form by Alizadeh, Brandt and Diebold (2002).

Data and Methodology

The equity indices under consideration in this research are the following:

1. ASX200 Australian Stock Exchange 200
2. CAS Colombo All Share (Sri Lanka)

3. HSI Hang Seng Index (Hong Kong)
4. JSX (Indonesia)
5. KLSE (Malaysia)
6. KOSPI (South Korea)
7. NZSE 40 (New Zealand)
8. PSE (Philippines)
9. STI Straights Times Index (Singapore)
10. TWI Taiwan Weighted Index

The data used in this research comprises observations (Open, High, Low and Close prices) from inception of each index to 14th August 2002. In the case of the longest established index, the Australian ASX200, this dataset comprises 3,035 observations from Feb 1990. However, for a number of the more-recently established indices, such as the Columbo All Share (CAS) Index, data is available only from very much later (Aug 1998 in the case of the CAS) and the dataset is correspondingly very much smaller. Where appropriate, for instance in calculating correlations, the dataset is truncated to the 967 observations from 20-Aug-1998. Summary statistics for the daily returns series is shown in Table 23 below. These indicate a wide disparity in returns, and in the distribution of returns over the sample indices. Many of the indices show negative average returns over the sample period, largely due to the regional decline in Asian markets after the crisis in 1997, and several of the series show exceptionally high levels of skewness (CAS) and kurtosis (CAS, KLSE, NZSE, PSE and STI).

Returns	ASX200	KOSPI	CAS	HSI	JSX	KLSE	NZSE	PSE	STI	TWI
Count	3038	1565	1181	967	1205	2081	2434	1220	3121	1192
Mean	4.8%	-6.5%	-3.1%	7.9%	-12.1%	-6.5%	4.2%	-19.2%	0.7%	-15.8%
Min	-7.4%	-12.7%	-5.4%	-9.3%	-12.7%	-24.2%	-13.3%	-9.7%	-9.2%	-9.9%
Max	6.1%	8.4%	18.3%	8.6%	13.1%	20.8%	9.5%	16.2%	12.9%	8.5%
Stdev	13.0%	39.7%	17.8%	29.3%	34.9%	31.0%	15.3%	29.7%	21.5%	30.6%
Skew	-0.4	-0.1	3.7	0.0	0.3	0.5	-1.0	1.0	0.1	0.0
Kurtosis	4.9	1.8	62.6	2.2	4.9	29.4	20.9	10.9	9.0	1.5

Table 1 Summary Statistics for Emerging Market Index Returns

The chart in figure below gives sense of the relative performance of the various markets from August 1998 (with Aug 1998 = 100)¹. The series broadly separate into two groups. The first, comprising the HSI, JSX, KLSE, KOSPI, and STI indices show rapid recovery from their 1987 crisis lows and wide variation over the four year sample period. The second, larger group of the remaining indices are very much more stable.

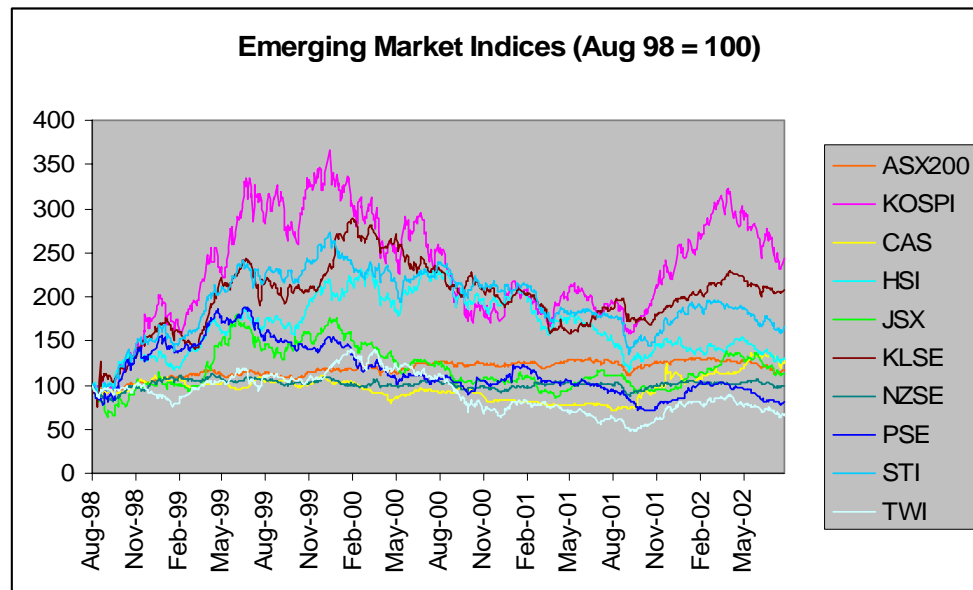


Figure 1 Emerging Market Indices from 1998

The table of correlations below gives an indication of the linkages between the various indices. The ASX has significantly high correlations with most of the other indices (approximately 0.19 at the 5% confidence level), with the exception

¹ Full time series plots are shown in Appendix 4 to this chapter.

	ASX200	KOSPI	CAS	HSI	JSX	KLSE	NZSE	PSE	STI	TWI
ASX200	1									
KOSPI	0.38	1								
CAS	0.05	0.02	1							
HSI	0.51	0.49	0.08	1	5					
JSX	0.22	0.20	0.03	0.27	1					
KLSE	0.25	0.16	0.05	0.27	0.19	1				
NZSE	0.45	0.27	0.01	0.31	0.18	0.17	1			
PSE	0.28	0.24	0.06	0.28	0.26	0.11	0.27	1		
STI	0.04	0.06	0.02	0.07	0.02	0.02	0.02	0.05	1	
TWI	0.21	0.28	0.10	0.25	0.13	0.12	0.20	0.14	0.02	1

of the CAS, STI and TWI indices. The STI has the least number of significant correlations of all of the indices.

Table 2 Returns Correlations for Emerging Market Indices

The inter-relationships are perhaps more easily assimilated by means of a cluster diagram. From here it is evident that the closest grouping comprises the more developed Australian and New Zealand indices, while the South Korean, Malaysian and Indonesian equity indices (representing some of the least developed economies) group at the largest Euclidean distance.

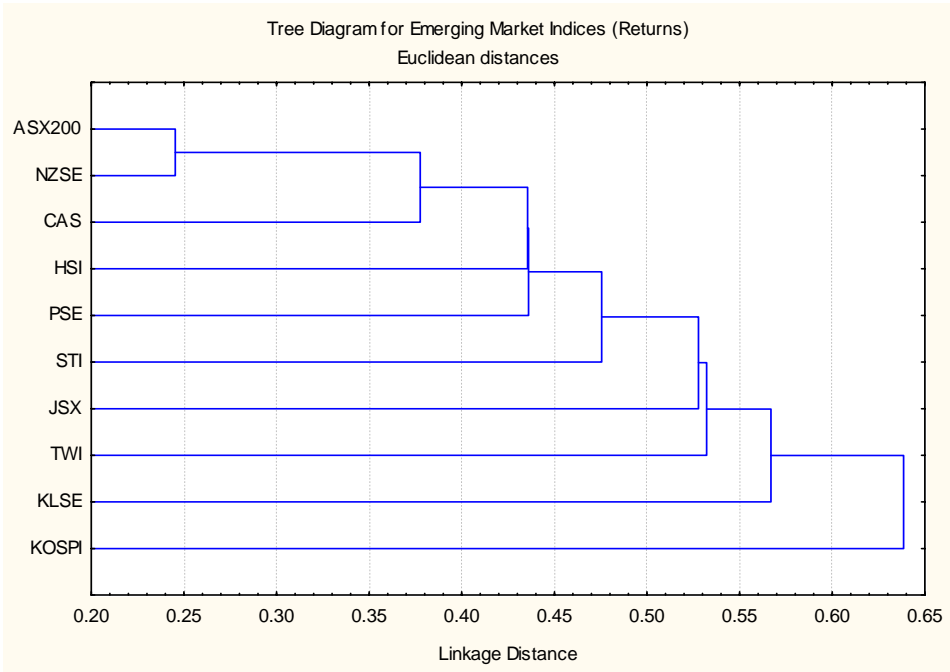


Figure 2 Dendrogram for Returns Processes of Emerging Market Equity Indices

It is not the intention in this study to focus too deeply on the inter-relationships between the returns processes in these markets, but rather the volatility processes. For this purpose we extract volatility estimates use daily values of the log range, D_t , as in Alizadeh, Brandt and Diebold (2002) (see Chapter 2).

$$D_t = \ln \left(\max_{\tau \in [t, t+1]} s_\tau - \min_{\tau \in [t, t+1]} s_\tau \right) \quad (5.1)$$

where s_t is the log index price.

We know this is to a very good approximation distributed as

$$D_t \sim N[0.43 + \ln h_t, 0.29^2] \quad (5.2)$$

The simulation studies in Chapter 2 indicate that the log-range is a robust estimator which is largely unaffected by sample size, low sampling frequency and market microstructure effects. This is important as, not only is the sample size small and sampling frequency low in this study, it is entirely possible that market microstructure effects are exaggerated in emerging markets when compared to their counterparts in developed economies.

As we progress to consider volatility modeling and forecasting, we adopt the framework of Alizadeh, Brandt and Diebold (2002), and consider 1- and 2-factor REGARCH models of the form

$$\ln h_t - \ln h_{t-1} = k_h (\mathcal{G} - \ln h_{t-1}) + \phi_h X_{t-1}^D + \delta_h R_{t-1} / h_{t-1} \quad (5.3)$$

where the returns process R_t is conditionally Gaussian: $R_t \sim N[0, h_t^2]$ and the process innovation is defined as the standardized deviation of the log range from its expected value:

$$X_{t-1}^D = (D_{t-1} - 0.43 - \ln h_{t-1}) / 0.29$$

For the two-factor range-based REGARCH model, the conditional volatility dynamics) are as follows:

$$\ln h_t - \ln h_{t-1} = k_h (\ln q_{t-1} - \ln h_{t-1}) + \phi_h X_{t-1}^D + \delta_h R_{t-1} / h_{t-1} \quad (5.4)$$

$$\ln q_t - \ln q_{t-1} = k_q (\mathcal{G} - \ln q_{t-1}) + \phi_q X_{t-1}^D + \delta_q R_{t-1} / h_{t-1} \quad (5.5)$$

where $\ln qt$ can be interpreted as a slowly-moving stochastic mean around which log volatility $\ln ht$ makes large but transient deviations (with a process determined by the parameters k_h , ϕ_h and δ_h).

The parameters θ , k_q , ϕ_q and δ_q determine the long-run mean, sensitivity of the long run mean to lagged absolute returns, and the asymmetry of absolute return sensitivity respectively.

The intuition is that when the lagged absolute return is large (small) relative to the lagged level of volatility, volatility is likely to have experienced a positive (negative) innovation. Unfortunately, as we explained above, the absolute return is a rather noisy proxy of volatility, suggesting that a substantial part of the volatility variation in GARCH-type models is driven by *proxy noise* as opposed to true information about volatility. In other words, the noise in the volatility proxy introduces noise in the implied volatility process. In the context of volatility forecasting, this noise in the implied volatility process deteriorates the quality of the forecasts through less precise parameter estimates and, more importantly, through less precise estimates of the current level of volatility to which the forecasts are anchored.

Two key elements absent from the Alizadeh, Brandt and Diebold (2002) REGARCH modeling framework are possible long memory effects and interactions between the various volatility processes. We take two approaches to estimating long memory features. The first is the procedure developed by Mandelbrot (1968) in which the Hurst exponent of the series is estimated from the log-linear relationship between the rescaled-range of the series, (R/S_N) , and the number of observations N for varying time intervals (see Chapter 1 for details). The second approach is to develop explicit univariate models of the individual log-volatility processes in which the degree of fractional integration is estimated directly. Here we adopt the ARFIMA-GARCH framework described in Chapter 3, and set out in equations 3.4 to 3.7.

Extending the analysis to the multivariate framework, we model interactions between log volatility processes using two procedures. The first involves a simple extension to the familiar ARFIMA-GARCH model, in which we bring in as regressors concurrent and lagged observations of a related log volatility process. This is the procedure adopted in the analysis of the relationship between the log volatility for the Australian and New Zealand stock indices, which in principle we might expect to show evidence of causality in the sense of Granger (1969).

The general form of the model is as follows:

$$(1-L)^d \Phi(L)(Y_t - \gamma_0 - \pi_{1t}x_{1t}) = \gamma_{1t} + \pi_{2t}x_{2t} + \theta(L)(\pi_{3t}x_{3t} + u_t) \quad (5.6)$$

In which $u_t = h_t^{1/2} e_t$ where error terms $e_t \sim \text{iid } N(0,1)$ and h_t , $\phi(L)$ and $\theta(L)$ are defined as before (see equations 3.5 – 3.7)

Regressors can enter into the ARFIMA model framework in three ways:

Type 1 regressors (x_1) can be thought of as exhibiting “error dynamics”, since a transformation allows the model to be recast with only the error term u_t entering in lagged form.

A model with Type 2 regressors (x_2) exhibits “structural dynamics” since it has a distributed lag representation.

Type 3 regressors (x_3) act as a component of the error term, adjusting its mean systematically, and is often used for implementing a GARCH-M model.

In this analysis we are concerned primarily with distributed lag effects, in which the ASX200 log volatility process enters as a Type 2 regressor.

Systems of Equations

Now let Y_t denote an $N \times 1$ vector of jointly determined variables. We can generalize equation 5.6 in this form:

$$\Delta^d \Phi(L)(BY_t - \gamma_{01} - \Pi_1 x_{1t}) = \gamma_{02} + \Pi_2 x_{2t} + \gamma(L)x_{7t-1} + \Theta(L)(\Pi_3 x_{3t} + u_t) \quad (5.7)$$

With

$$u_t = \hat{H}_t^{-1/2} e_t \quad \hat{H}_t = \text{diag}(h_t)$$

and $e_t \sim iid(0, C)$

where C is a fixed correlation matrix with units on the diagonal.

In the error-correction model framework x_{7t} is a $N \times 1$ vector with

$$x_{7t} = BY_t - \gamma_{01} - \Pi_1 x_{1t}$$

In the fractional vector error correction model (F-VECM)

$$\gamma(L) = \alpha(L)\beta'$$

In which $\alpha(L)$ is a polynomial matrix having a typical element

$$\alpha_{ji}(1-L)^{d_{1j}-d_{3ji}}$$

Here the parameters d_{3ji} measure the order of fractional cointegration.

Linear combinations βx_7 are potentially cointegrated in the sense that they are integrated to order $d_{1j} - d_{3ji} < d_{1j}$.

Analysis and Research Findings

Volatility Characteristics

Summary Statistics

Charts of the log-range processes for the sample series show clear evidence of the typical behavior normally associated with asset volatility processes, specifically volatility clustering and time-varying conditional volatility. The log-range volatility chart for the South Korean KOSPI index is typical (see Appendix 4 in this chapter for plots for other stocks).

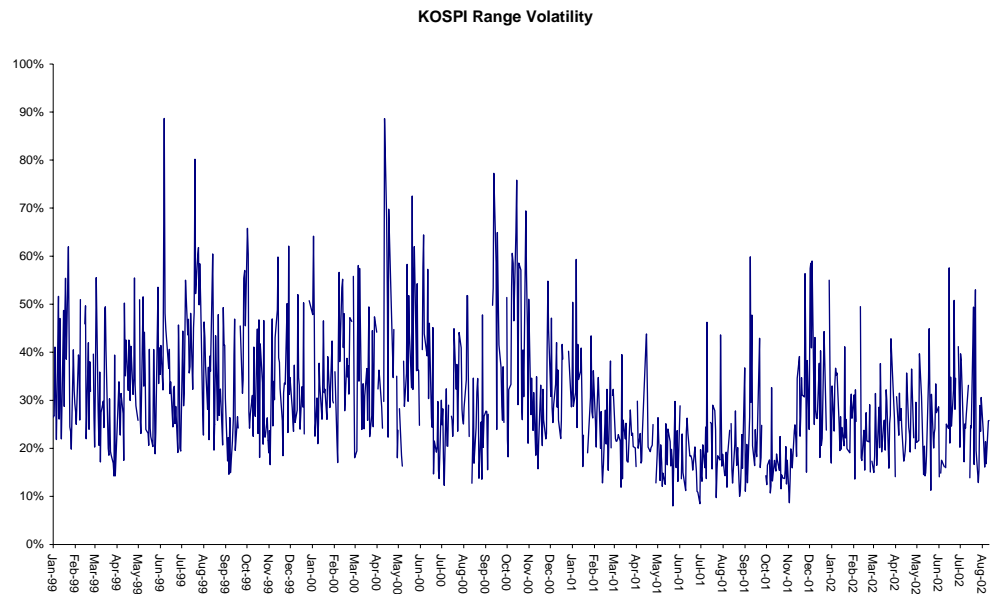


Figure 3 Volatility in the South Korean KOSPI Index 1999-2002

Here we can easily identify many of the typical characteristics of volatility seen in studies of volatility processes in developed markets: volatility clustering, trending (the result of long memory), mean reversion and, possibly, regime shifts.

Summary statistics for the Log-Range processes are shown in Table 26 following. The range in average levels of index volatility is substantial – from 8.4% for the Australian ASX 200 Index to 25.3% for the South Korean KOSPI Index. So too is the variation in the levels of index volatility, with standard deviations ranging from 44% (Hang Seng Index) to 73% (Columbo All Share Index). There are indications of some degree of skewness and kurtosis in the distribution of the log-range series, but in most cases these are quite modest.

Log Range	ASX200	KOSPI	CAS	HSI	JSX	KLSE	NZSE	PSE	STI	TWI
Count	3035	1565	906	965	1204	2080	2432	1219	2485	1191
Mean	-4.81	-3.71	-5.08	-4.03	-3.94	-4.28	-4.77	-4.24	-4.46	-4.01
Range Vol	8.4%	25.3%	6.4%	18.4%	20.0%	14.4%	8.8%	14.8%	12.0%	18.7%
Min	-6.70	-5.70	-6.65	-5.41	-5.60	-6.11	-7.29	-5.59	-6.43	-5.43
Max	-2.25	-2.36	-1.68	-2.54	-1.59	-1.27	-2.02	-1.64	-2.04	-2.35
Stdev	48.9%	52.4%	73.3%	43.8%	60.4%	66.7%	54.7%	55.4%	62.1%	46.8%
Skew	0.22	-0.18	0.58	0.06	0.31	0.31	0.28	0.45	0.19	0.11
Kurtosis	0.51	-0.15	0.54	0.01	0.03	0.33	0.67	0.26	0.10	0.01

Table 3 Summary Statistics for Log-Range Processes

Distribution tests of the log-range processes indicate the near-Normality of log volatility for several of the series. The chart below showing the histogram of the HSI log-volatility series is illustrative. Standard tests for non-Normality (Kolmogorov-Smirnov, Lilliefors, and the more powerful Shapiro-Wilk test) all fail at the 5% significance level to reject the null hypothesis that the log-volatility process follows a Gaussian distribution.

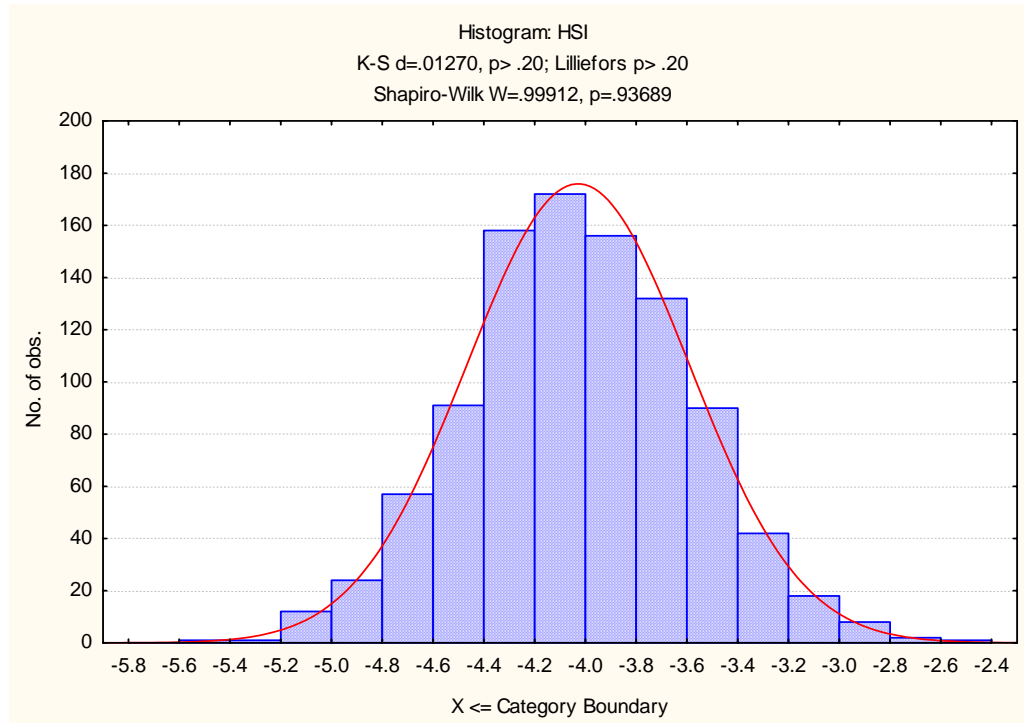


Figure 4 Histogram of Log-Volatility for Hang-Seng Index

For many other assets distribution tests tend to reject the null hypothesis. However the departures from normality (skewness, excess kurtosis) are typically quite small and in most cases test failure is simply the result of the sensitivity of the tests in samples with a large number of degrees of freedom. In other cases, however, non-normality may be the product of significant regime shifts in the process (see section following).

Volatility Asymmetry

One important characteristic of many volatility processes is that of volatility asymmetry, which is described in some detail in Chapter 1. Asymmetry typically arises from a feedback mechanism in the following way. Substantial good news

produces a large positive shock in the return process, which produces an uplift in the stock price. However, the rise in volatility increases the return required by investors, which tends to dampen the ensuing price increase. On the other hand, significant bad news produces both a downturn in the stock price and an increase in volatility. The increase in risk means that investors require a higher rate of return, which tends to drive the price down further, amplifying the process volatility. The result is that volatility tends to be negatively correlated with asset returns.

In our analysis we carried out preliminary testing for asymmetry effects by segregating the volatility series into days on which returns were positive, versus days in which they were negative. The results are summarized in Table 26.

Log Range +	ASX200	KOSPI	CAS	HSI	JSX	KLSE	NZSE	PSE	STI	TWI
Count	1569	762	447	482	579	1003	1254	565	1179	545
Mean	-4.82	-3.71	-5.10	-4.03	-4.03	-4.32	-4.77	-4.28	-4.45	-4.06
Range Vol	8.3%	25.3%	6.3%	18.4%	18.3%	13.8%	8.8%	14.3%	12.1%	17.9%
Min	-6.42	-5.70	-6.65	-5.15	-5.60	-6.11	-7.29	-5.59	-6.20	-5.26
Max	-2.56	-2.46	-1.95	-2.69	-2.01	-1.57	-2.33	-1.64	-2.04	-2.57
Stdev	47.7%	51.5%	75.4%	42.7%	62.3%	68.3%	54.6%	55.3%	62.3%	48.7%
Skew	0.10	-0.28	0.58	0.12	0.39	0.36	0.09	0.54	0.22	0.19
Kurtosis	0.18	0.09	0.38	-0.07	0.08	0.39	0.40	0.54	-0.01	-0.18

Log Range -	ASX200	KOSPI	CAS	HSI	JSX	KLSE	NZSE	PSE	STI	TWI
Count	1458	799	457	483	620	1075	1167	653	1230	645
Mean	-4.79	-3.71	-5.06	-4.03	-3.86	-4.24	-4.76	-4.21	-4.46	-3.97
Range Vol	8.6%	25.4%	6.6%	18.4%	21.7%	14.9%	8.8%	15.3%	12.0%	19.5%
Min	-6.70	-5.27	-6.61	-5.41	-5.26	-5.85	-6.10	-5.52	-6.43	-5.43
Max	-2.25	-2.36	-1.68	-2.54	-1.59	-1.27	-2.02	-2.31	-2.08	-2.35
Stdev	50.1%	53.3%	71.2%	44.8%	57.3%	65.0%	55.1%	55.3%	62.0%	44.7%
Skew	0.33	-0.10	0.59	0.01	0.32	0.29	0.47	0.39	0.13	0.07
Kurtosis	0.78	-0.35	0.76	0.08	0.05	0.30	0.94	0.07	0.16	0.28

Table 4 Comparison of Summary Statistics for Log Range for days on which returns are positive (+) or negative (-)

Visual comparison of average levels of volatility during up-days versus down-days appears to indicate that there are asymmetry effects for a number of the indices,

including the JSX, KLSE and TWI, with average downside volatility exceeding average upside volatility by several percentage points.

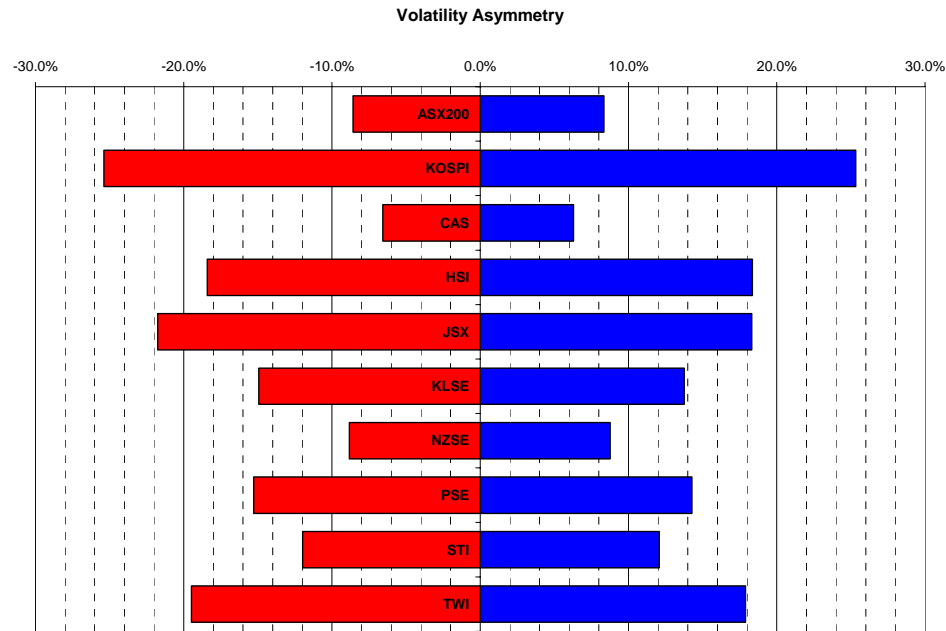


Figure 5 Volatility Asymmetry in Emerging Market Indices

Paired t-tests (with unequal variances) were used to determine whether there were significant differences in the average levels of volatility (as measured by the log-range) in the two samples. For the majority of indices the differences were not statistically significant, the exceptions being the JSX, KLSE, PSE and TWI indices. In these markets, we conclude, volatility asymmetry effects are likely to be important.

Stat Tests	ASX200	KOSPI	CAS	HSI	JSX	KLSE	NZSE	PSE	STI	TWI
F-Stat	1.10	1.07	1.12	1.10	1.18	1.10	1.02	1.00	1.01	1.19
F-Test Variance	3.0%	16.6%	11.2%	14.5%	2.0%	5.8%	37.0%	49.7%	44.7%	1.8%
Sg	48.9%	52.4%	73.4%	43.8%	59.8%	66.6%	54.8%	55.3%	62.2%	46.6%
T-Stat	1.59	0.09	0.91	0.11	4.96	2.79	0.31	2.15	0.30	3.15
T-Test Means	11.3%	93.0%	36.5%	91.4%	0.0%	0.5%	75.4%	3.2%	76.2%	0.2%

Table 5 T-Tests for Mean Upside Volatility vs. Mean Downside Volatility

Long Memory

Long-term serial autocorrelation is a standard feature of many asset processes, including volatility processes, as empirical research has often demonstrated (refer to Chapter 1 for details). Examination of the autocorrelations in the Log-Volatility processes reveals the typical pattern of slow decay and significant coefficients at long lags.

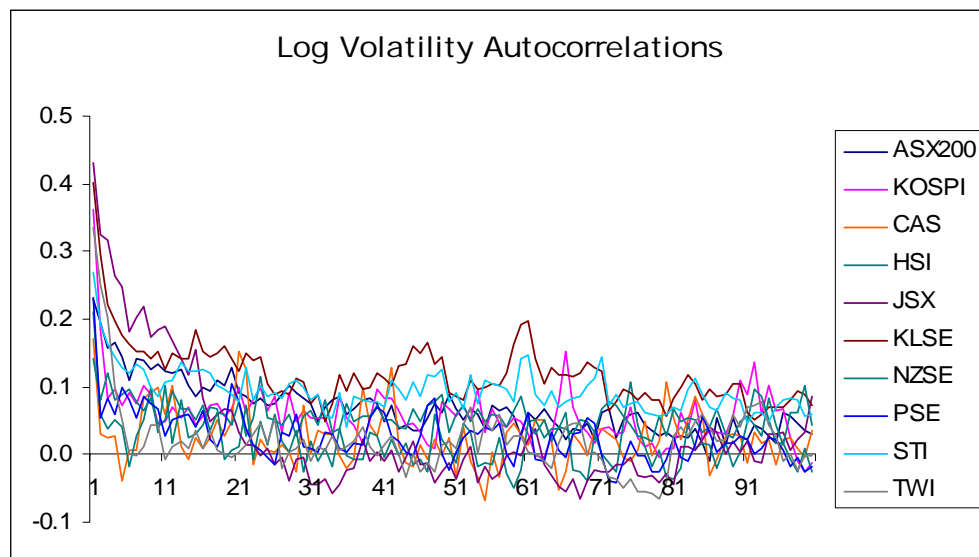


Figure 6 Log-Volatility Autocorrelations

The long memory characteristics of the sample stocks were tested using the following procedure, due to Mandelbrot. First, a standard ARMA(1,1) model was fitted to each volatility series in order to remove any short term correlation in the processes, which might otherwise contaminate long-memory estimates. Using the residuals from the ARMA models, the rescaled range in each series was estimated for periods of $N = 126$ to 1512 days. By regressing the log of the rescaled range against $\log(N)$ estimate were obtained of the Hurst exponent, H , being the slope of the regression line. An estimate of H in excess of 0.5 indicates

the presence of a power scaling law and volatility persistence, with fractional integration parameter $d = H-0.5$. Our initial findings in this area indicate volatility persistence for most of the sample indices, with Hurst exponent estimates in the region of 0.58 to 0.86. The initial findings suggest that long memory effects are especially important in the volatility processes for the Australian and South Korean Indices, but much less so for the Hang Seng and other indices (see Table 29). A more accurate method of estimating the degree of fractional integration in the volatility processes is utilized in the latter half of this study.

	ASX200	KOSPI	CAS	HSI	JSX	KLSE	NZSE	PSE	STI	TWI
H	0.86	0.79	0.67	0.58	0.66	0.63	0.60	0.71	0.65	0.66
d	0.36	0.29	0.17	0.08	0.16	0.13	0.10	0.21	0.15	0.16
SE	0.04	0.08	0.07	0.03	0.07	0.05	0.04	0.03	0.05	0.02
R²	97%	87%	89%	97%	87%	92%	93%	98%	94%	99%

Table 6 Hurst Exponent Estimates

The log-log rescaled range plot for PSE, shown in the figure below, is illustrative.

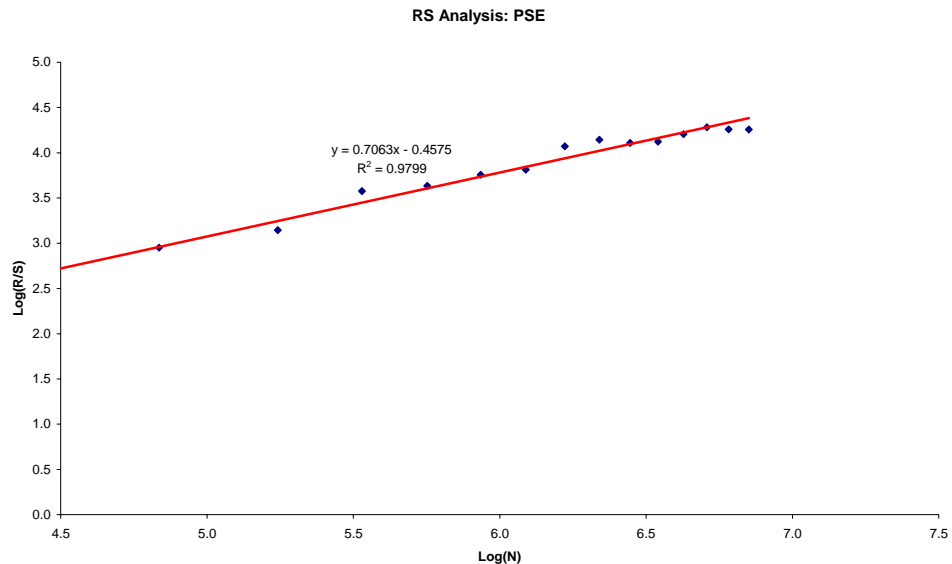


Figure 7 Rescale Range Analysis Plot for PSE Index

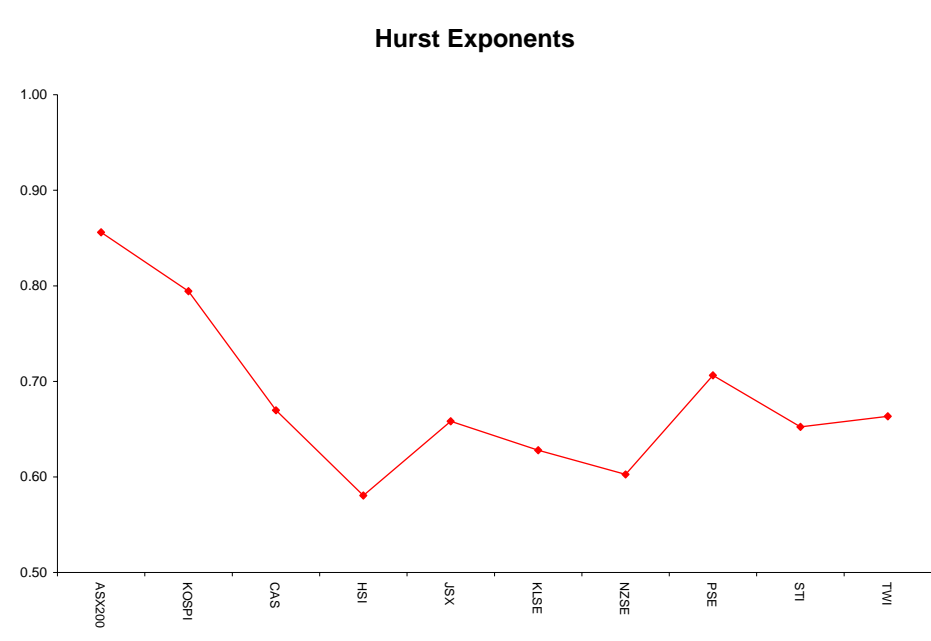


Figure 8 Estimated Hurst Exponents for Emerging Market Index Volatility Processes

Regime Shifts

For a stable process there should be a consistent relationship between the log range and log absolute returns. A plot of the difference between the two will appear stationary in the approximate range from 0.5 – 0.8, if the process is stable. A trending plot, or one with very substantial variation, indicates process instability.

One of the few examples of process instability detected by this method is shown in the plot for CAS (see Figure 51). The ASX 200 Index, by contrast, in common with almost all of the sample stocks shows a stationary difference plot. Plots for all of the sample indices are given in Appendix. 4.

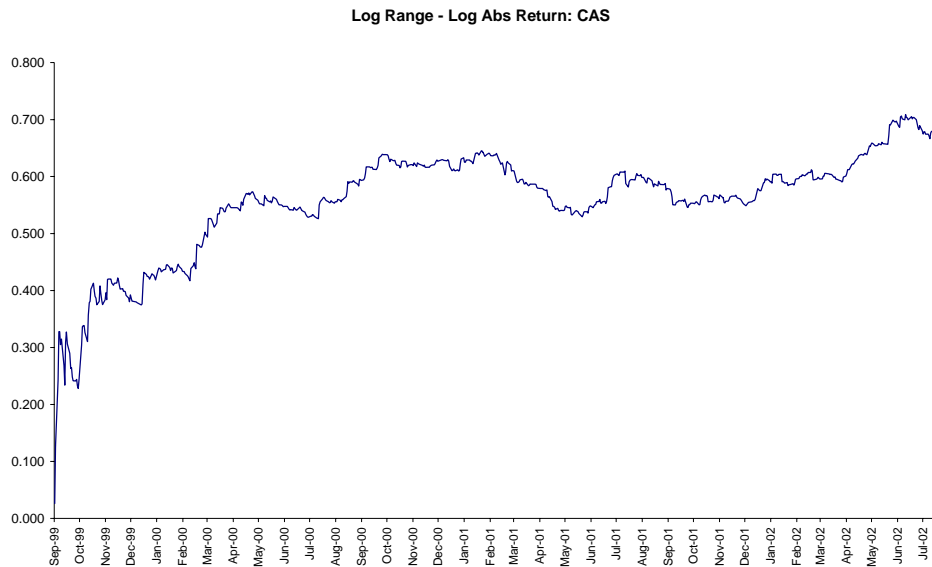


Figure 9 Log Rage - Log Absolute Returns: CAS

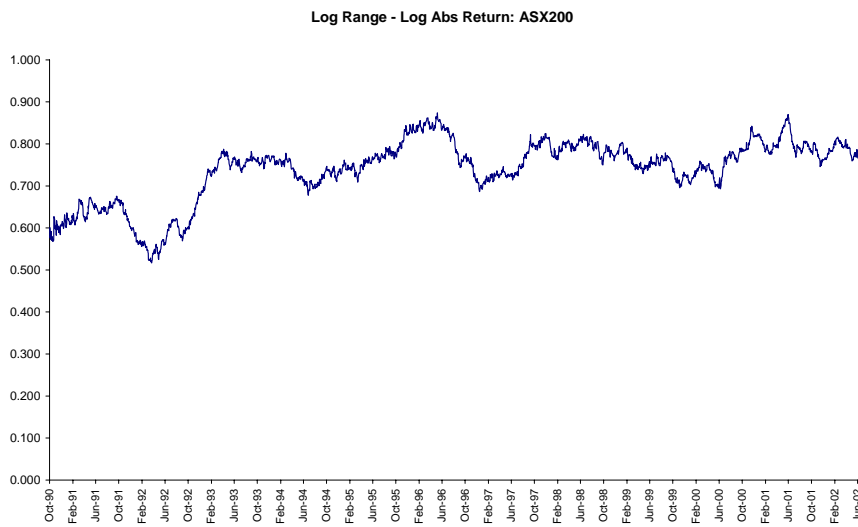


Figure 10 Log Rage - Log Absolute Returns: ASX 200

Another widely used method for detecting process regime shifts is by means of calculating the Iterated Cumulative Sums of Squares (ICSS) over the entire sample period. As detailed in Chapter 1, the ICSS statistic D_k is a Brownian Bridge process, which is constrained to be zero for the first and last observations in the sample period, but elsewhere behaves like a random Brownian motion process. If $\max_k \sqrt{(T/2)} |D_k|$ exceeds 1.36, the 95th percentile of the asymptotic distribution, then we take k^* , the value of k at which the maximum value is attained, as an estimate of a change point in the process. Note that while the ICSS provides a reliable way of detecting structural change, it gives no information as to the cause, or as to the precise nature of the change. The shift may be the result of a change in one or another of the distribution moments of the process and it may be permanent or temporary: it is entirely plausible that a process might exhibit higher than average volatility for, say, a period of several weeks, only to revert once again to its long run mean. In such a situation the ICSS test should indicate not one but two separate regime shifts.

ICSS tests were carried out on all of the sample indices (see Appendix 4 in this chapter). Most of the series begin after 1997, the time of the crisis in Asian financial markets. Those emerging market indices with longer histories tend to show evidence of a volatility regime shift during 1997, and this group includes the South Korean KOSPI Index, the Malaysian KLSE Index, the Australian ASX 200 Index and the New Zealand NZSE Index. In a number of cases we see evidence of a secondary regime shift in 2001 around the time of the 9/11 attack – the Colombo All Share Index is a case in point.

ICSS: KOSPI

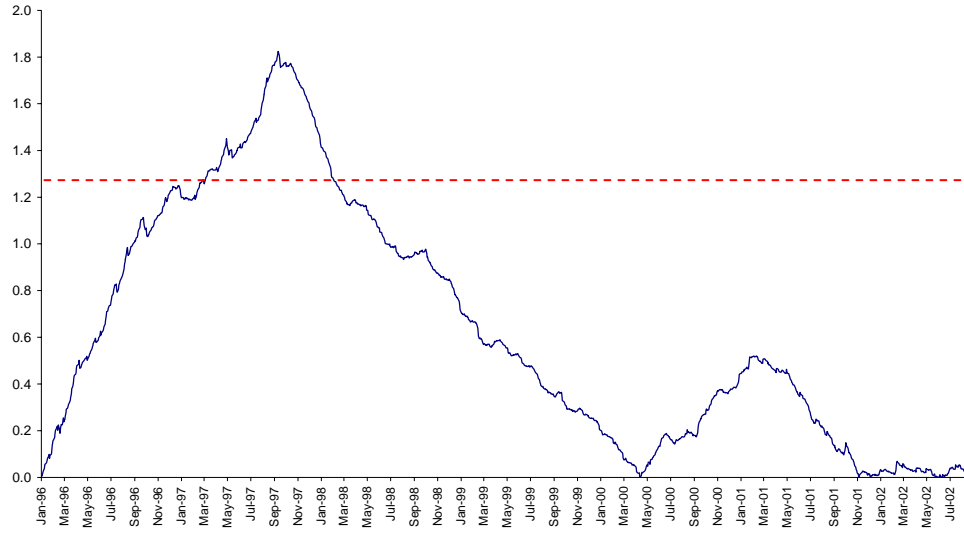


Figure 11 Regime Shifts in the KOSPI Index Volatility Process

ICSS: KLSE

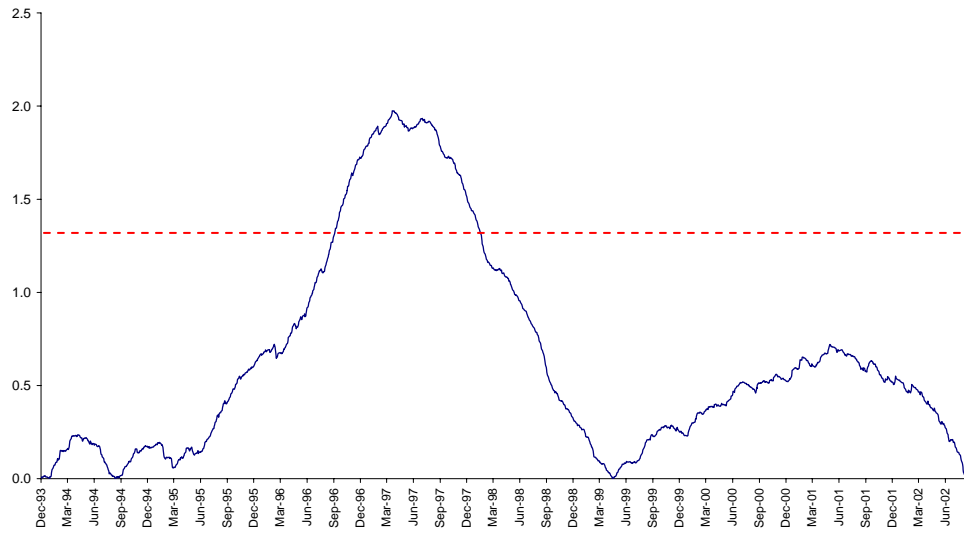


Figure 12 Regime Shifts in the KLSE Index Volatility Process

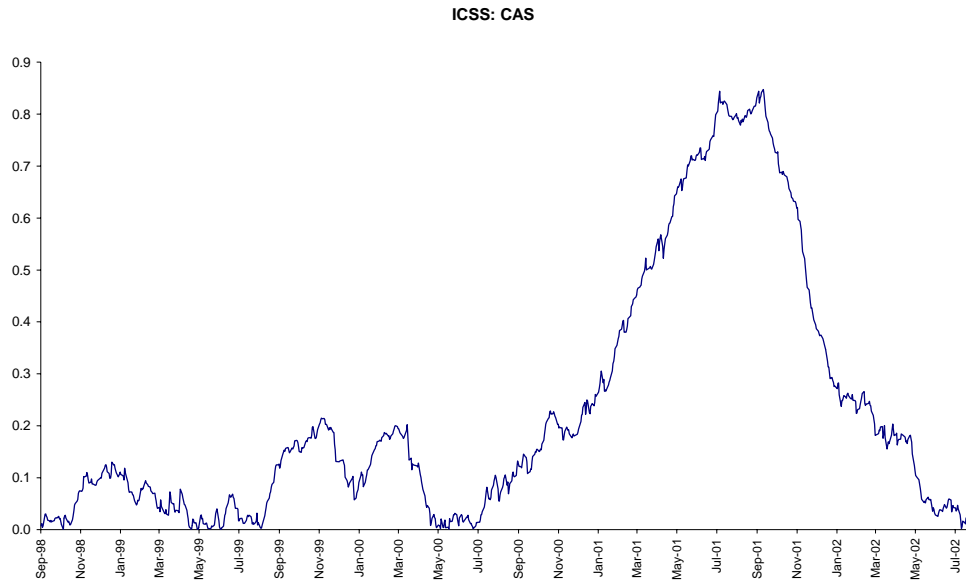


Figure 13 Regime Shift in the CAS Index Volatility Process

The conclusion is that the Asian crisis almost certainly resulted in a significant upward shift in the average level of process volatility for a number of the emerging market indices examined in this study for a period lasting several months. A further volatility regime shift occurred for many emerging markets around the time of the WTC attacks in September 2001. Whether the changes produced by the crisis were transient or permanent is difficult to judge without further analysis.

Multivariate Analysis

Just as with the returns processes, we find evidence of significant correlations between many of the volatility processes in the merging markets under consideration in this study (Table 30). The inter-relationships are better illustrated in a cluster diagram (Figure 56)

	ASX200	KOSPI	CAS	HSI	JSX	KLSE	NZSE	PSE	STI	TWI
ASX200	1.00									
KOSPI	0.13	1.00								
CAS	0.04	0.01	1.00							
HSI	0.24	0.27	-0.03	1.00						
JSX	0.20	0.19	-0.10	0.23	1.00					
KLSE	0.17	0.30	-0.08	0.28	0.31	1.00				
NZSE	0.30	0.14	-0.02	0.23	0.18	0.21	1.00			
PSE	0.20	0.23	-0.01	0.21	0.21	0.21	0.14	1.00		
STI	0.25	0.34	0.06	0.42	0.27	0.34	0.25	0.31	1.00	
TWI	0.01	0.03	0.04	0.02	-0.13	-0.05	0.01	-0.01	0.01	1.00

Table 7 Volatility Correlations

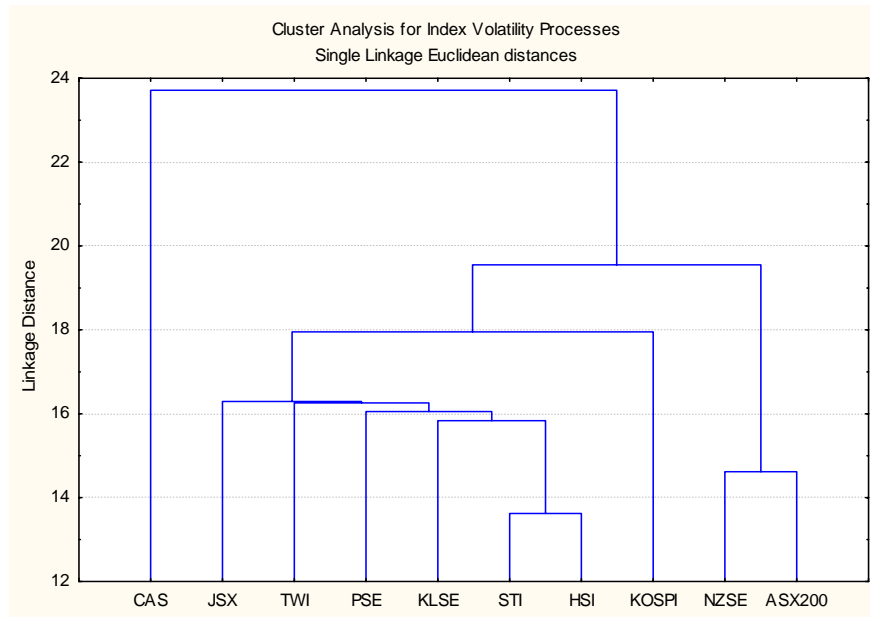


Figure 14 Cluster Dendrogram for Volatility Processes

Here we can identify two distinct clusters: in the first group are the indices for the more developed New Zealand and Australian markets, while the second group includes all of the other indices, excepting the KOSPI and CAS indices, which appear as “outliers”. Within the second group, the volatility processes of the Hong Kong and Singapore indices appear to be the most closely linked pair of indices in the sample universe, a finding which is perhaps unsurprising considering their geographical proximity and position as prominent financial centers in the Asian region. The clear distinction in the average levels of volatility between the two groups is illustrated in the k-means cluster plot in Figure 57, in which the consistently lower levels of volatility in the Australian/New Zealand index grouping is evident.

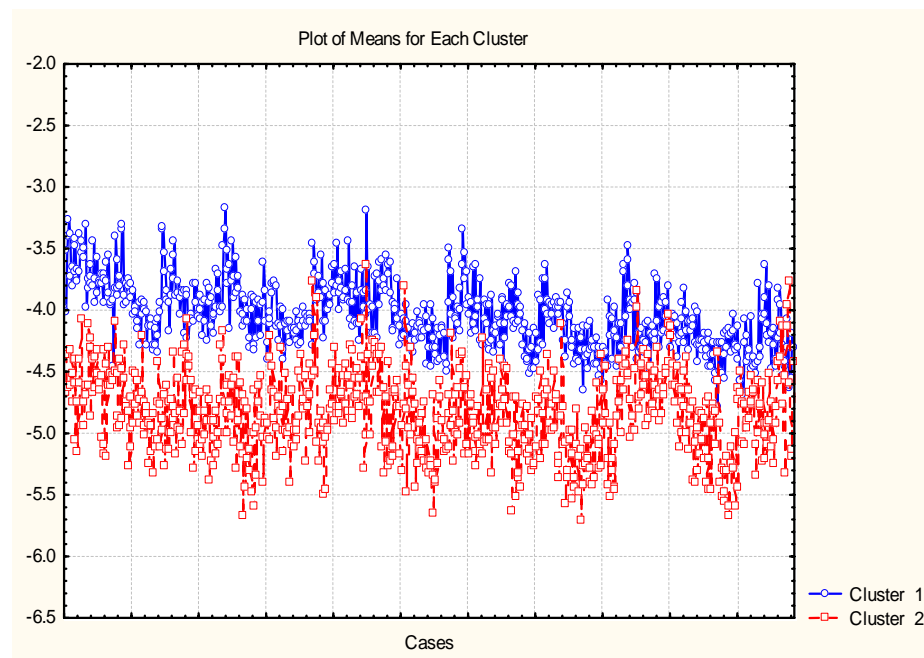


Figure 15 k-Means Cluster Plot of Index Volatility Processes

Another multivariate method used to explore the interrelationships in the volatility process is principal components analysis. Based on the accepted norm of using a value of 1.0 for the cutoff eigenvalue, we can see evidence of (at least) three common factors driving the volatility processes in the sample indices, which between them account for almost 50% of the total common variation. (Similar findings are made when the same method is used to analyze the volatility processing of equity indices in developed economies).

Eigenvalues Extraction: Principal components				
Value	Eigenvalue	% Total variance	Cumulative Eigenvalue	Cumulative %
1	2.719153	27.19153	2.719153	27.19153
2	1.150398	11.50398	3.869551	38.69551
3	1.000514	10.00514	4.870065	48.70065

Table 8 Principal Components Analysis of Index Volatility

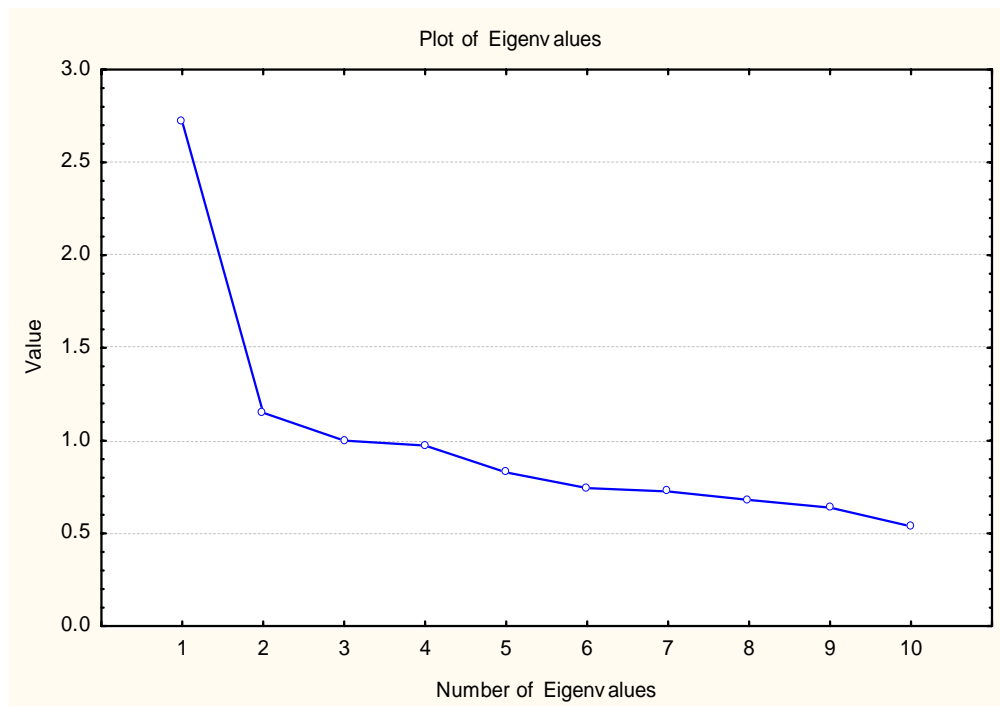


Figure 16 Plot of Eigenvalues

Examination of the factor loadings (varimax normalized) again suggests two primary groupings amongst the volatility processes for the sample indices (see Figure 59). The first group again contains the Australian and New Zealand Indices. The second group, contains all of the other indices, excepting two “outliers”, the Sri Lankan CAS index and the Taiwanese index.

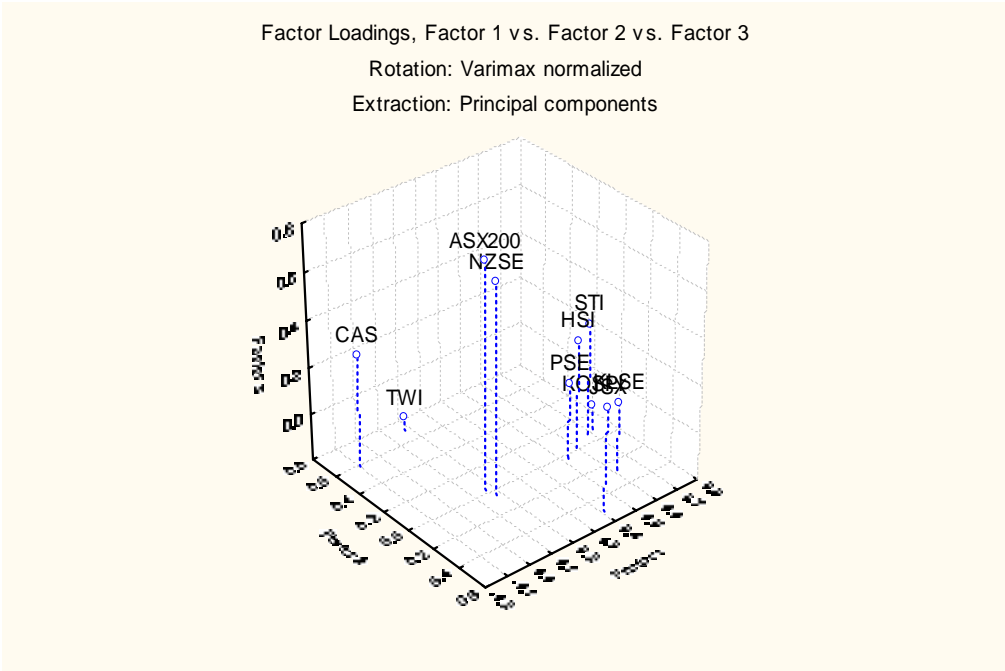


Figure 17 Factor Loadings

Volatility Modeling

REGARCH Model Estimation and Analysis

In this section of the research we apply the model framework of Alizadeh, Brandt and Diebold (2002) to construct single- and two-factor REGARCH models of the log-volatility processes of the sample indices. The models were constructed using the entire log-volatility data series for each index, with an expanding window used to provide period-by-period parameter estimates and ex-ante forecasts. Summary results are summarized in Table 32.

In general, the two-factor models typically provide a slightly better fit to the data than single factor models, but in many cases the improvement in model fit is marginal. The best models appear to be the two-factor models for the CAS, JSX, KOSPI and PSE indices, which not only provide relatively low Mean Absolute Percentage Errors, but for which portmanteau tests also indicate no significant autocorrelations in the residuals or squared residuals. The chart in Figure 60 below plots the estimates transient $\{h_t\}$ and mean $\{q_t\}$ processes for the Sri-Lankan CAS Index. Noteworthy are the trending behavior of the mean process, the rapid mean-reversion of the transient process and the attempt by the model to adapt to the regime shift in the process that occurred in 1997.

Models for other indices exhibit signs of lack of fit, in the form of residual autocorrelations or residual ARCH effects in the error process. The R-squares for the model range from as low as 20% for the ASX 200 models to as high as 51% for the two-factor model for the CAS index. Theory shows that in a GARCH framework model R-squares are often misleading and therefore preference should be given to other diagnostic tests such as MAPE, Theil's-U and Direction Prediction Indicator, which are defined and discussed in Chapter 2.

	<i>MODEL</i>	<i>Adj R²</i>	<i>MAPE</i>	<i>Theil's U</i>	<i>DP</i>	<i>κh</i>	<i>θ</i>	<i>φh</i>	<i>δh</i>	<i>κq</i>	<i>φq</i>	<i>δq</i>	<i>Comments</i>
ASX200	REGARCH 1	19.8%	7.1%	0.74	72.8%	0.0271	-5.1179	0.0264	-0.0252				Residual ARCH effects
	REGARCH 2	19.7%	7.1%	0.74	72.7%	0.147	-5.001	0.0383	-0.0260	0.0020	0.0042	-0.0172	Residual ARCH effects
CAS	REGARCH 1	49.8%	8.3%	0.79	70.8%	0.0635	-4.2361	0.0958	-0.0108				Residual autocorrelations
	REGARCH 2	51.4%	8.2%	0.78	69.9%	0.173	-4.664	0.0714	-0.0213	0.0016	0.0288	-0.0043	Good fit, well specified model, high R-sq
HSI	REGARCH 1	29.0%	10.4%	0.75	68.5%	0.1598	-5.5056	0.0973	0.0190				Residual autocorrelations
	REGARCH 2	29.4%	10.3%	0.75	69.4%	0.528	-5.497	0.1036	0.0234	0.0671	0.0469	0.0062	Residual autocorrelations
JSX	REGARCH 1	21.7%	7.9%	0.71	70.9%	0.0013	-4.0341	0.0258	-0.0068				Good fit, well specified model
	REGARCH 2	21.6%	7.9%	0.71	72.3%	0.242	-4.017	0.0323	-0.0102	0.0005	0.0228	-0.0059	Good fit, well specified model
KLSE	REGARCH 1	31.7%	10.8%	0.83	68.4%	0.1283	-4.3935	0.0978	-0.0013				Good fit, well specified model, high R-sq
	REGARCH 2	32.9%	10.6%	0.82	69.6%	0.507	-4.432	0.1114	-0.0010	0.0244	0.0326	-0.0141	Good fit, well specified model, high R-sq
KOSPI	REGARCH 1	33.7%	8.4%	0.77	70.7%	0.0516	-3.9947	0.0635	-0.0136				Good fit, well specified model, high R-sq
	REGARCH 2	33.0%	8.5%	0.78	71.3%	0.546	-4.483	0.0729	-0.0096	0.0123	0.0486	-0.0054	Good fit, well specified model, high R-sq
NZSE	REGARCH 1	21.5%	8.4%	0.78	71.7%	0.0483	-5.1981	0.0446	-0.0106				Residual ARCH effects
	REGARCH 2	21.9%	8.3%	0.77	71.9%	1.419	-5.199	0.0703	-0.0065	0.0487	0.0473	-0.0113	Residual ARCH effects
PSE	REGARCH 1	27.5%	9.3%	0.75	70.3%	0.0561	-4.6791	0.0593	-0.0016				Good fit, well specified model
	REGARCH 2	27.5%	9.2%	0.75	70.6%	0.260	-4.686	0.0653	0.0005	0.0367	0.0371	-0.0051	Good fit, well specified model
STI	REGARCH 1	40.9%	8.8%	0.82	69.0%	0.0456	-4.9130	0.0684	-0.0161				Residual autocorrelations & ARCH effects
	REGARCH 2	42.2%	8.7%	0.81	70.0%	0.245	-5.028	0.0839	-0.0177	0.0040	0.0177	-0.0049	Residual ARCH effects
TWI	REGARCH 1	23.8%	8.3%	0.78	69.8%	0.1361	-4.4533	0.0737	-0.0252				High R-sq, Residual ARCH effects
	REGARCH 2	23.5%	8.3%	0.79	69.7%	0.173	-4.664	0.0714	-0.0213	0.0016	0.0288	-0.0043	High R-sq, Residual ARCH effects

Table 9 REGARCH Model Estimation

κ_h	0.1731
ϕ_h	0.0714
δ_h	-0.0213
κ_q	0.0016
θ_q	-4.6644
ϕ_q	0.0288
δ_q	-0.0043

Sample Stats	
T	1565
SumSq Err	208.3
Likelihood	4948.8
Adj R ²	51.4%
AIC	-2.008
BIC	-1.984
Av Dt	-3.708
Av ln(ht)	-4.148
Diff	0.439
SD ln(ht)	0.390
Mean Xt	0.032
SD Xt	1.258

MSE	13.3%
MAD	29.5%
MAPE	8.2%
Theil's U	0.78
DP	69.9%

Errors et	
Mean	0.009
Stdev	0.365
Skew	0.10
Kurtosis	-0.19
JB	0.00%
Box-Pierce	42.0%
ARCH-LM	48.2%
Sign Bias	-0.70
Sign Bias -	-5.41
Sign Bias +	4.26
D-W	2.01

Mean Rt/ht	-0.037
SD Rt/ht	1.404
Sign Bias	0.68
Sign Bias -	-21.09
Sign Bias +	13.45
D-W	1.83

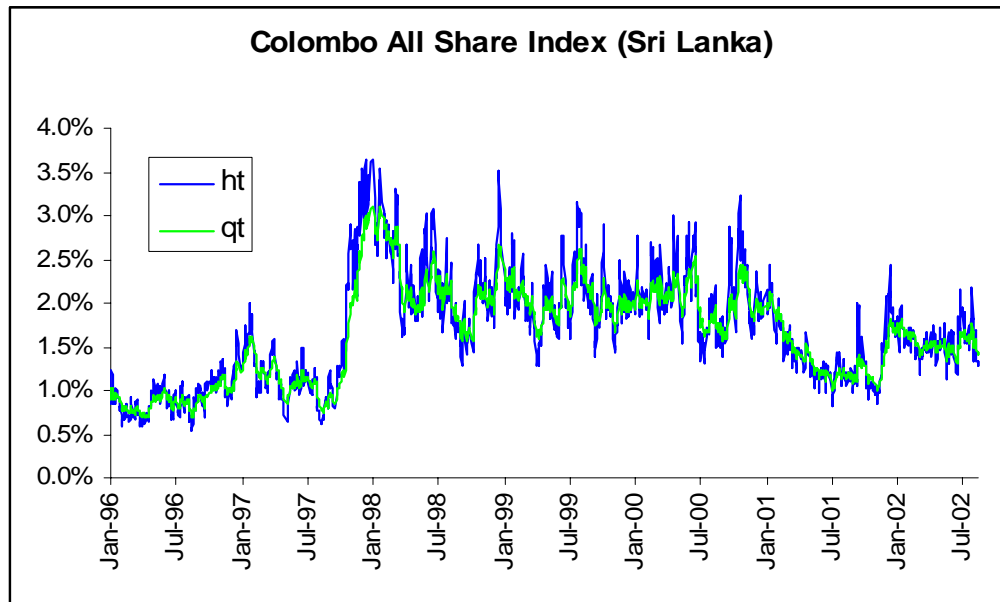
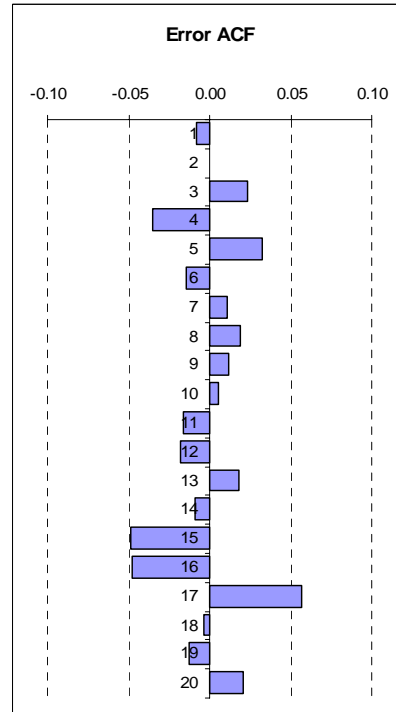


Figure 18 Estimated Transient and Mean Volatility Processes for the CAS Index

In the two-factor models, return shocks tend to affect the transient volatility process (h_t) far more than the mean process (q_t), as the ϕ_h parameter tend to be an order of magnitude larger than the equivalent ϕ_q parameter.

For several of the sample stocks the mean-reversion property, which is minimal in the single-factor model, becomes much more prominent in the equivalent two-factor model. A good example here would be PSE: for the single factor model the estimate for the k_h mean reversion parameter is only 0.056, compared with 0.26 for the equivalent parameter in the two-factor model. For this index, and for others such as KLSE, the two-factor model not only provides a slightly better overall fit, but also more clearly delineates important properties of the underlying processes.

Mean reversion is of the order of ten times faster in the transient process $\{h_t\}$ than in the mean process $\{q_t\}$, as the relative size of the k_h and k_q parameters indicates. The half-life of transient volatility shocks ranges from less than half a day (CAS Index) to around 1.2 days (KOSPI Index). One interpretation is that some markets disperse transient volatility shocks more efficiently than others.

Confirming the earlier analysis, volatility asymmetry appears to be important in some markets, such as the Australian and Sri Lankan markets, but not in others, such as the Malaysian and Philippines markets. Based on modeling experience in other markets, we would expect ex-ante to find that volatility asymmetry is a more important component of transient volatility than long-run volatility. This is true for several of the sample indices, including the ASX 200, CAS, HSI, KLSE, KOSPI, STI and TWI indices. However, for the JSX, NZSE and PSE indices the reverse relationship holds.

In most cases where the explanatory power of the models is substantial, the MAPE is low enough, and the percentage direction prediction is high enough, to suggest that volatility forecasts produced by the models will be useful (assuming that out-of sample accuracy is comparable). The ability of the models to successfully time the volatility market is indicated by direction prediction coefficients of 70% or higher (see Figure 61). Likewise, the low values of the Thiel's-U statistic indicates that these models performed very well in comparison to the random walk predictor (forecast for next period is the observed value for previous period, i.e. a random walk).

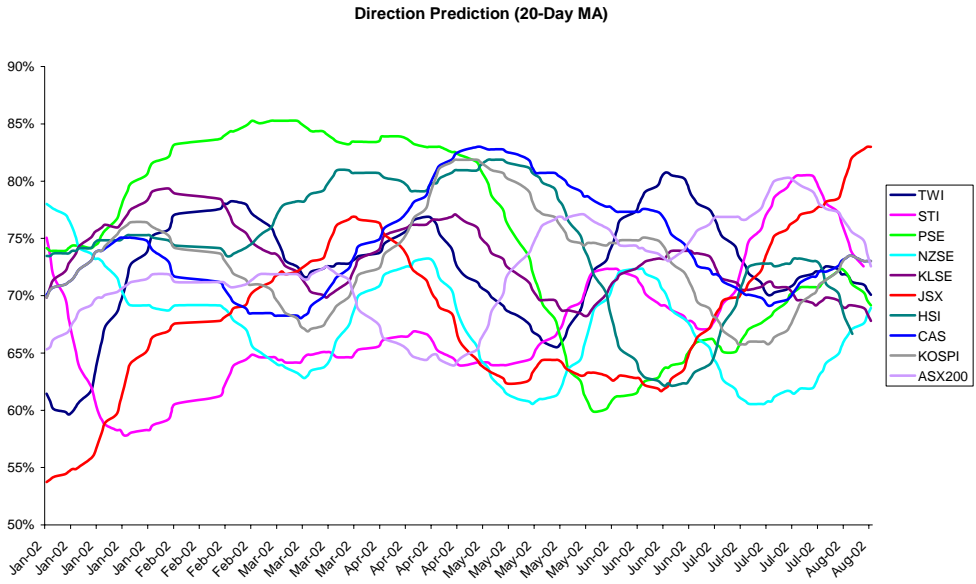


Figure 19 Direction Prediction Accuracy (20-Day MA)

Model Testing

Out-of-sample tests of the single-factor REGARCH models for the sample stocks were constructed as follows. Each model was estimated using a rolling 750-day window, forecasting ahead for non-overlapping 1-, 5- and 20-day periods. Out-of-sample forecasts were then compared with actual log-range (volatility) during each period. In addition, the model R-squares were calculated over each of the sub-samples and the evolution of the R-squares was tracked over time. Finally, for comparison purposes both the symmetric and asymmetric versions of the single-factor REGARCH models were compared, to gauge the importance of the additional asymmetry parameter. In almost every case the out-of-sample model R-squares were slightly higher for the asymmetric models than for the symmetric models, at least for sustained periods, confirming the earlier finding that asymmetry is indeed an important component of volatility processes in general.

Ex-ante, of course, the expectation would be that model R-squares would be lower for the test periods than for the entire sample, because we have fewer degrees of freedom in the estimation process. In addition, one would expect forecast accuracy to decline over long forecasting horizons. For a stationary process model parameters and R-squares should be relatively invariant over time. However, difficulties in the estimation process can lead to variability in the parameter estimates and hence in the model R-squares. Moreover, model parameters and R-squares may also fluctuate due to changing market conditions and it is by no means uncommon to see model R-squares trending upwards or downwards over sustained periods of time. This can happen, for instance, as a result of some fundamental changes in the structure of the company, or the markets in which it operates, which can make volatility inherently more or less forecastable than during earlier periods. There are several instances of such behavior in the sample indices. A clear example is provided by the sample stock

PSE (see chart in Figure 62). Here the model R-squares decline steadily from around 39% in July 1999 to around 7% in August 2002. Similar patterns of declining model power are seen in the case of KLSE, while in other cases such as the JSX Index the reverse pattern is seen.

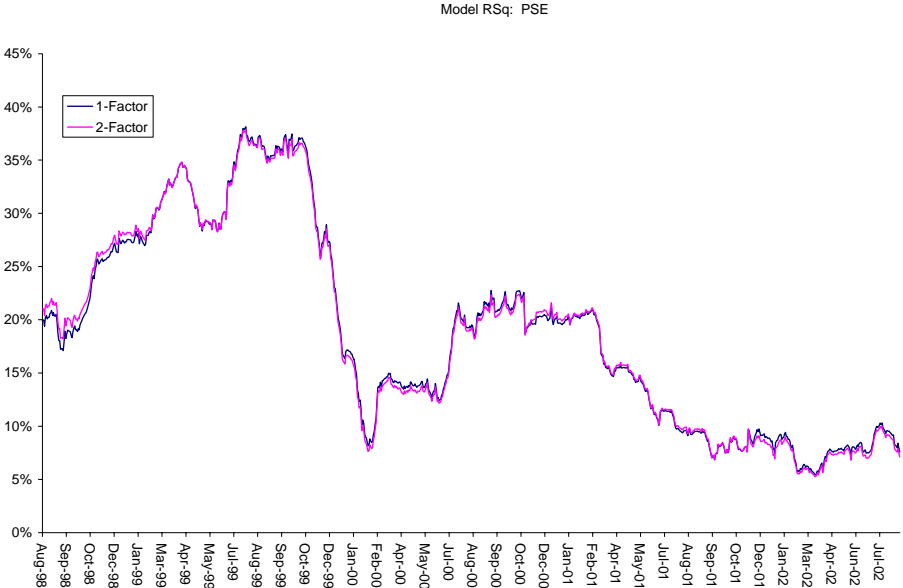


Figure 20 Model R-Squared for PSE Index

A third category of behavior is characterized by one (or several) step changes in the model R-squares. A case in point is the HSI index, where the model r-squares increase by as much as five-fold in the four months following September 2001 (see Figure 63). Similar step-changes are seen in the model R-squares for the ASX 200, CAS, KOSPI, NZSE, PSE and STI indices.

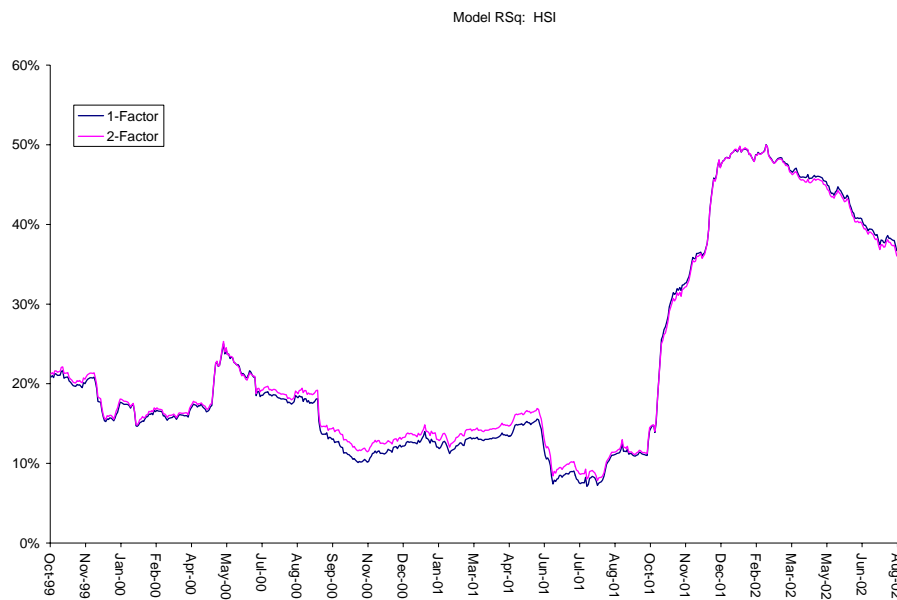


Figure 21 Model R-Squares for HIS Index

One common factor appears to be the events in the USA during September 2001. For many of the sample assets, for instance the ASX200 index, the steady improvement in model R-squares dates from this period. One plausible explanation is that volatility autocorrelation, and hence predictability, tends to rise during periods of high volatility, such as pertained in US markets in the aftermath of the events of September 11th, 2001. However, this theory fails to explain why for some indices US market volatility should have such a substantial impact, while for others, JSX for instance the effect is muted to the point of being almost negligible. One possible explanation is that variants of some of the indices trade as on the US, London or other international exchanges; another is that certain of the companies that comprise the universe for some of the indices operate to a

significant degree in US and international markets, while others, say in Sri Lanka, operating more locally, are less directly exposed to global events that induce asset volatility. A more extensive study and possibly more complex multivariate models would be required to provide definitive answers to these questions.

Another related aspect of the analysis was to examine the evolution of the model parameters over the sample periods. Here the aim is to gain insight as to the robustness of the model and how the importance of the various model parameters might fluctuate as market conditions change. To carry out the analysis the model parameters were restated in later sample periods relative to their value in the initial sample period.

The pattern in the case of the ASX 200 index is very interesting (see Chart 64 below). Here we see a steady decline in the size of the asymmetry parameter ϕ until the period around September 2001, when there is a sudden reversion to around 90% of its initial value. Model R-squares, which had been tailing off in the preceding months begin an upward trend around this time, which continues despite the steady erosion in the size of the asymmetry parameter thereafter. A plausible theory is that the events of September 2001 induced greater predictability in the ASX200 volatility process by means of increased asymmetry. Intuitively this makes some sense – it is credible that investors should be far more concerned about downside shocks than upside shocks at that time, and the option volatility skews certainly reflected that view. Unfortunately for this theory, subsequent events appear to be unresponsive: the steady decline in the asymmetry parameter since December '01 has not been matched by lower model R-squares.

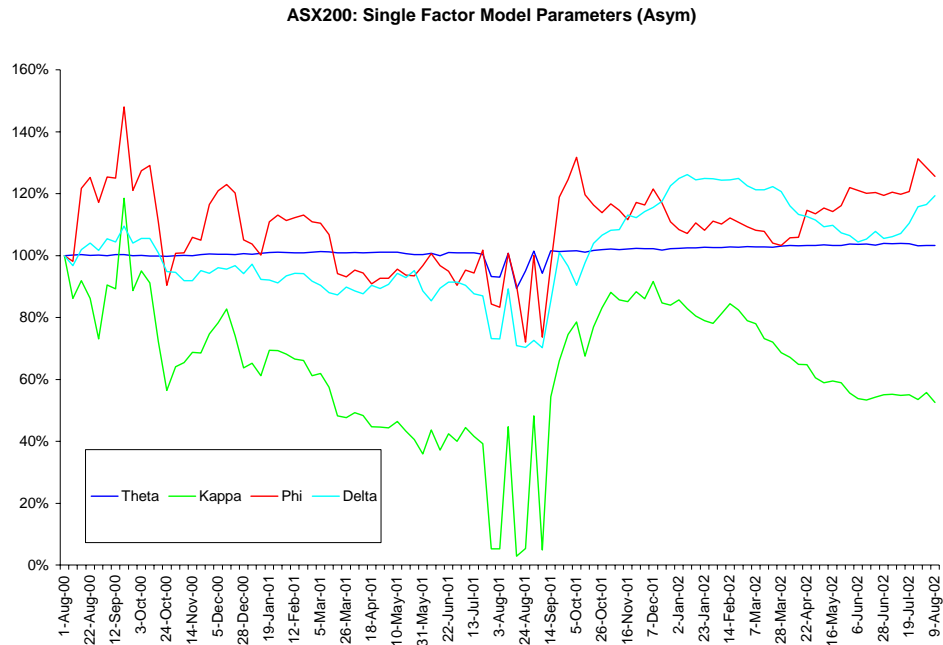


Figure 22 Single-Factor REGARCH Parameter Estimates for the ASX 200 Index

A series of parallel out-of-sample tests for the two-factor models were constructed, corresponding to those carried out for the single factor versions. In almost every case the out-of-sample model R-squares were consistently higher for the asymmetric two-factor models than for the corresponding single factor equivalent, confirming the general superiority of the former class of models.

Parameter analysis of the two-factor REGARCH models is, of course, made much more challenging by the increased complexity of the model. Overall, it can be said that the additional intricacy of the two-factor models at least enables us to circumvent some of the lack-of-fit issues that arise with the single factor models.

In the single factor model for the ASX200 index we found a sudden increase in the estimated mean reversion parameter in September 2001, around the time

when the model R-squares began to trend upwards. However, for the two factor model no such explanation offers itself – the parameter estimates are mostly stable or downward trending. The same is true of the two factor model for the KOSPI index, except for periods when there is a sudden resurgence in the level of the estimated long-term volatility asymmetry parameter $\delta\text{-}q$ (see Figure 65).

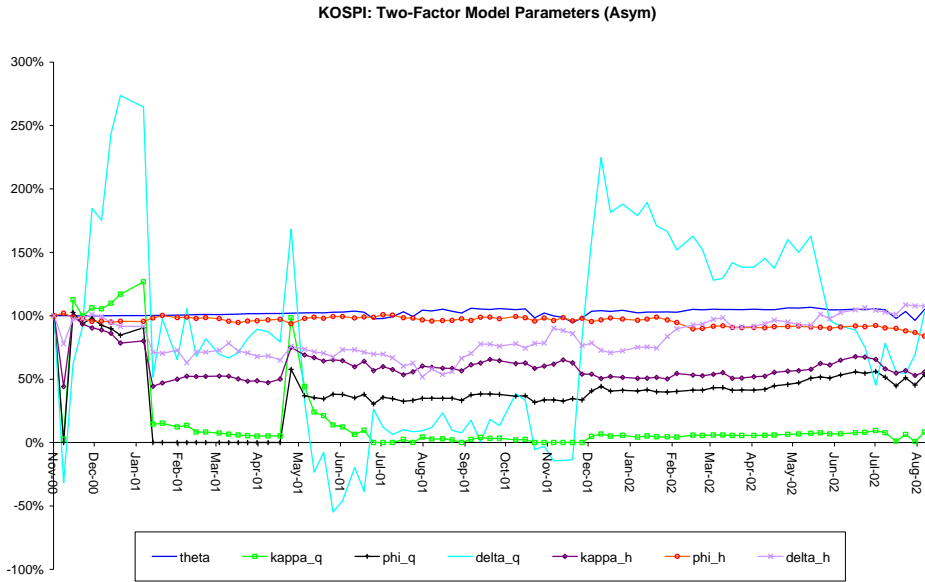


Figure 23 Parameter Estimates for 2-Factor REGARCH Model for KOSPI Index

Univariate ARFIMA-GARCH Models

As discussed in the introductory section of this chapter, the REGARCH model framework does not allow for long memory effects which the preliminary analysis suggests are present in each of the index volatility series. In this section we consider ARFIMA-GARCH models of the form described in the introduction. The full results are shown in Tables 32 and 33 (analysis for the CAS index is omitted as there is insufficient data).

With few exceptions (the most notable being the significant Jarque-Bera test statistic, indicating non-Normality in the error process), none of the models exhibits signs of lack of fit or parameter instability. Portmanteau tests of the residuals and squares of the residuals indicate no significant autocorrelations up to lag 40, with the sole exception of residuals from the HSL log-volatility model. Only in the case of the NZSE and STI Indices does the Forecast Test 2 give an indication of parameter instability. Using the Akaike Information Criterion (AIC) as the principal criterion for model selection, of the nine log volatility models are fitted with a fully specified version of the model, all parameters being significant at the 1% level. Only in the case of the KOSPI index does the best-fitting model omit all GARCH effects, while remainder include GARCH(1,1) error processes and at least the intercept and fractional integration parameters of the ARFIMA component of the model. Without exception, the degree of fractional integration is substantially higher than estimated previous using the Mandelbrot method. Only in the case of the KLSE index does the estimated fractional differencing parameter indicate non-stationary (being > 0.5). Long memory effects appear of greatest importance in the KLSE, STI and NZSE series. Volatility persistence is around half these levels in these series for the HSI and TWI processes. Charts of the model residuals and forecasts are shown in Appendix 4 to this chapter.

	ASX200	KOSPI	HSI	JSX
Log Likelihood	-1792.660	-662.649	-419.080	-818.779
Akaike	-1799.660	-666.649	-424.080	-823.779
R-Sq	0.157	0.489	0.126	0.323
Residual SD	0.447	0.368	0.389	0.479
Residual Skewness	0.184	0.150	0.031	0.323
Residual Kurtosis	3.365	2.866	2.930	3.272
Jarque-Bera	32.9021 {0}	7.0681 {0}	0.330 {0.847}	24.383 {0}
Box-Pierce (40)	42.107 {0.379}	45.995 {0.237}	77.633 {0}	35.414 {0.676}
Box-Pierce ² (40)	43.7589 {0.314}	43.462 {0.326}	37.327 {0.591}	47.749 {0.186}
Fcst Test 1	98.7072 {0.517}	90.096 {0.75}	112.816 {0.179}	83.463 {0.883}
Fcst Test 2	-0.0998 {0.92}	-0.765 {0.444}	.808 {0.419}	-1.438 {0.15}

	KLSE	NZSE	PSE	STI	TWI
Log Likelihood	-1303.140	-1625.970	-764.322	-1644.410	-585.131
Akaike	-1310.140	-1632.970	-770.322	-1651.410	-590.131
R-Sq	0.504	0.215	0.278	0.408	0.231
Residual SD	0.455	0.480	0.464	0.471	0.400
Residual Skewness	0.164	0.184	0.449	0.212	0.177
Residual Kurtosis	3.244	3.648	4.009	3.200	3.297
Jarque-Bera	14.591 {0}	54.998 {0}	88.747 {0}	22.676 {0}	10.417 {0.005}
Box-Pierce (40)	36.398 {0.633}	30.421 {0.863}	28.580 {0.911}	43.595 {0.321}	44.861 {0.275}
Box-Pierce ² (40)	31.840 {0.817}	32.633 {0.789}	36.457 {0.63}	32.314 {0.801}	32.299 {0.801}
Fcst Test 1	107.567 {0.284}	76.579 {0.96}	81.931 {0.905}	78.806 {0.942}	89.254 {0.77}
Fcst Test 2	0.543{0.587}	-2.702 {0.006}	-1.59 {0.111}	-2.045 {0.04}	-0.909 {0.363}

Table 10 - System Results

	ASX200	KOSPI	HSI	JSX
Intercept	-4.836	-3.906	-3.987	-4.003
d	0.378	0.436	0.200	0.359
AR1	0.389	-0.167	N/A	N/A
MA1	0.607	N/A	N/A	N/A
(GARCH Intercept) ^{1/2}	0.415	N/A	0.354	0.415
GARCH AR1	0.508	N/A	0.739	0.928
GARCH MA1	0.431	N/A	0.690	0.902

	KLSE	NZSE	PSE	STI	TWI
Intercept	-4.140	-4.819	-4.097	-4.566	-4.049
d	0.525	0.412	0.388	0.449	0.291
AR1	0.491	0.365	N/A	0.469	N/A
MA1	0.678	0.592	0.152	0.618	N/A
(GARCH Intercept) ^{1/2}	0.350	0.422	0.496	0.338	0.350
GARCH AR1	0.955	0.854	0.898	0.978	0.778
GARCH MA1	0.924	0.809	0.910	0.957	0.708

Table 11 Equation Results

As a further test for long memory effects we estimate the d-parameters using both the Geweke/Porter-Hudak (1983) and Moulines-Soulier (2004) log-periodogram regression techniques. The results, shown in Table 35 and Figure 66, suggest estimates of fractional integration that in some cases differ widely, according to the estimation method used, with the Moulines-Soulier method generally providing the lowest parameter estimates and the model generally providing the highest estimates. It is noticeable that the series for which all three estimators are most closely in agreement, the HSI, JSX and TWI Indices, are estimated with ARFIMA-GARCH models which exclude AR and MA terms. This leads to the conjecture that it is the conflation of short- and long-memory effects which is the cause of the dispersion amongst the d-parameter estimates for the remaining series.

	<i>Model</i>	<i>G/P-H</i>	<i>M-S</i>
ASX200	0.378	0.351	0.245
KOSPI	0.436	0.466	0.326
CAS		0.309	0.309
HSI	0.200	0.202	0.175
JSX	0.359	0.347	0.365
KLSE	0.525	0.417	0.379
NZSE	0.412	0.300	0.226
PSE	0.388	0.350	0.293
STI	0.449	0.399	0.334
TWI	0.291	0.284	0.301

Table 12 d-Parameter Estimates

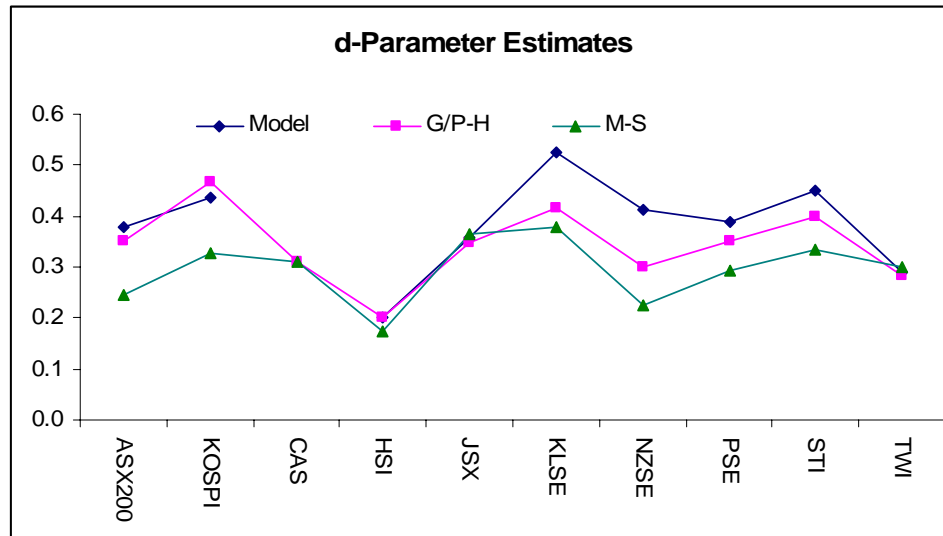


Figure 24 d-Parameter Estimates

We next consider the extension to the basic ARFIMA-GARCH model contemplated in equation 5.1 in which regressors are introduced in one of three possible ways. By way of illustration we use the simple bivariate system comprising the NZE and ASX 200 log volatility series, as it appears likely in principle that these two proximate markets might share commonalities in the index volatility processes – indeed, the preceding exploratory analysis suggest that to be the case. Time series and scatterplots of the series are shown in Figures 67 and 68 below.

Reference to the Akaike Information Criterion suggests models featuring Type 1 regressors provide the best description of the mechanism by which volatility in the NZSE Index is influenced by volatility in the ASX 200 Index.

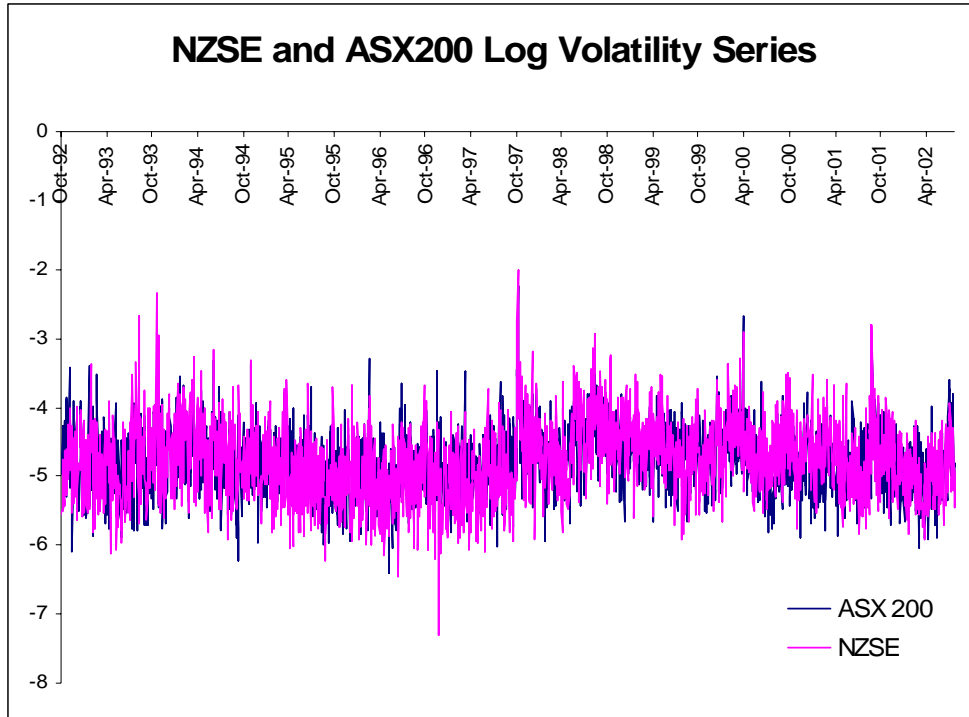


Figure 25 NZSE and ASX Index Log Volatility

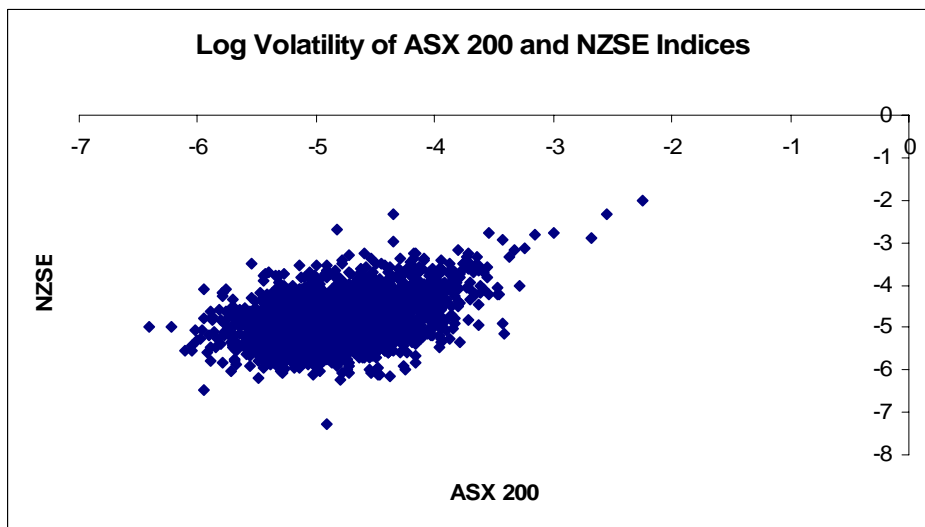


Figure 26 NZSE and ASX 200 Index Log Volatility

Model parameter estimates, shown in Tables 36, suggest a Granger-causality relationship in which volatility in the ASX 200 Index feeds concurrently and at one period lag into the NZSE volatility process. Table 37 shows a side-by-side comparison of the system results for models including and excluding the ASX 200 regression relationship. These demonstrate the clear improvement in the AIC and every other criterion of model fitness which results from the inclusion of the ASX 200 regressor.

	<i>Estimate</i>	<i>St. Err.</i>	<i>t-ratio</i>	<i>p-Value</i>
Intercept	-2.738	0.212	-12.918	0
ASX200	0.300	0.025	11.824	0
ASX200[-1]	0.122	0.023	5.278	0
ARFIMA d	0.377	0.054	7.014	0
AR 1	0.449	0.065	6.922	0
MA 1	0.661	0.066	10.061	0
(GARCH Intercept) ^{1/2}	0.434	0.019		
GARCH AR1	0.798	0.160	4.994	0
GARCH MA1	0.768	0.169	4.540	0

Table 13 Parameter Estimates for NZSE-ASX200 Model

	<i>With ASX 200</i>	<i>Without ASX 200</i>
Log Likelihood	-1515.29	-1625.970
Akaike	-1524.29	-1632.970
R-Sq	0.283	0.215
Residual SD	0.463	0.480
Residual Skewness	0.009	0.184
Residual Kurtosis	3.403	3.648
Jarque-Bera	15.796 {0}	54.998 {0}
Box-Pierce (40)	26.300 {0.953}	30.421 {0.863}
Box-Pierce ² (40)	32.612 {0.79}	32.633 {0.789}
Fcst Test 1	76.064 {0.964}	76.579 {0.96}
Fcst Test 2	-2.860 {0.004}	-2.702 {0.006}

Table 14 System Results for ARFIMA-GARCH Models With and Without Regressor

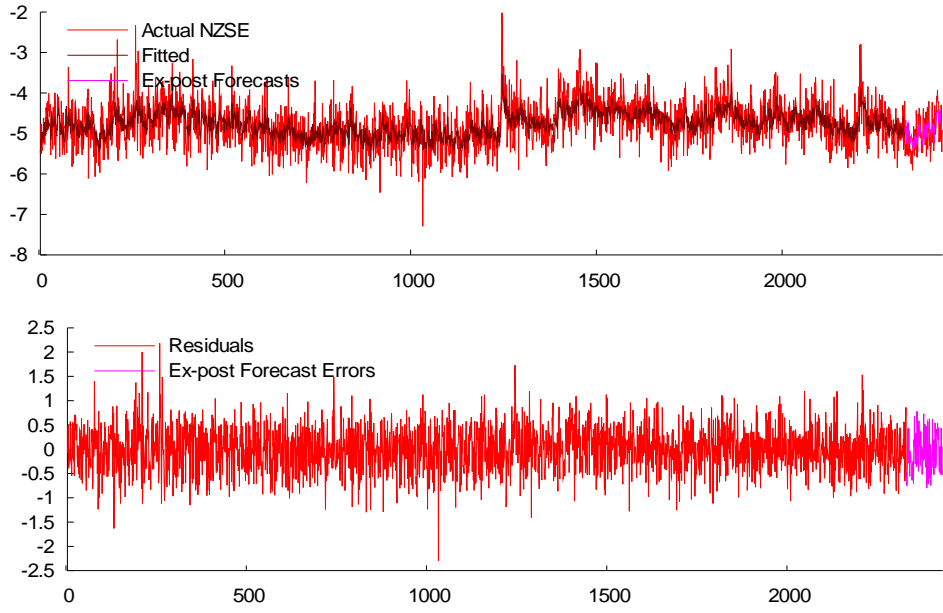


Figure 27 Forecasts and Residuals for NZSE-ASX200 ARFIMA-GARCH Model

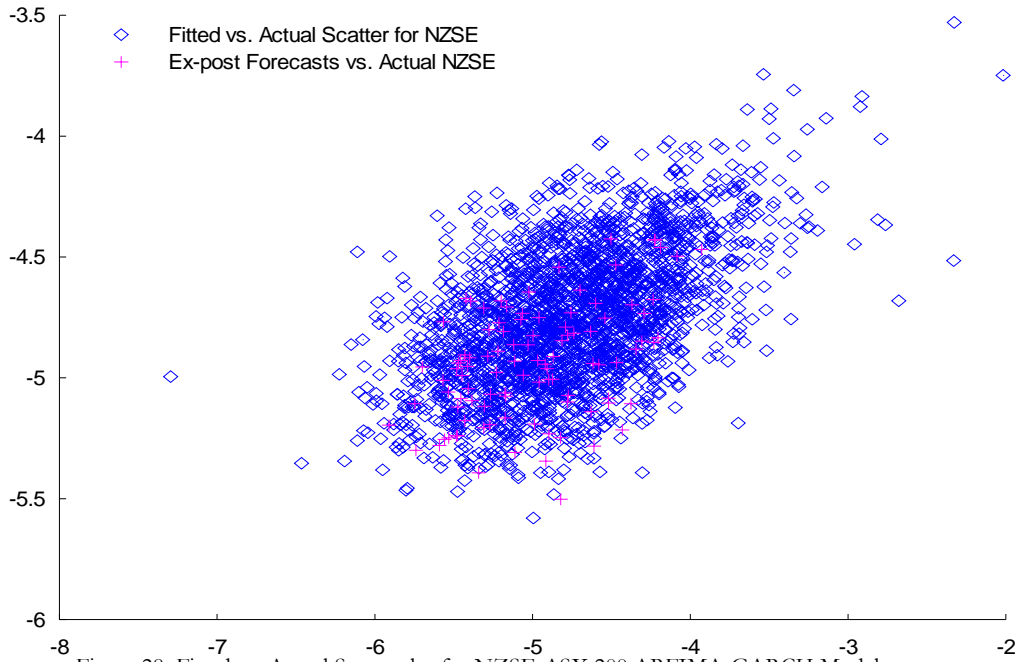


Figure 28 Fitted vs. Actual Scatterplot for NZSE-ASX 200 ARFIMA-GARCH Model

System of Equations Models

The preceding analysis suggests the possibility of cointegration behavior in the volatility processes under consideration and in this section of the analysis we consider applications of the Vector Auto Regressions and Vector Error Correction model frameworks described in the introduction. We begin by returning to the bi-variate NZSE and ASX 200 log volatility system and estimating a F-VECM model of the form described by equation 5.7. The results are set out in Tables 38-40. These indicate that the series are fractionally cointegrated with cointegrating vector close to (1, -1). The loading coefficient on the ECM is large but poorly determined in the case of the ASX equation, and smaller but better estimated in the NZSE equation. In contrast to the simple, one-way Granger causality (from ASX 200 to NZSE) found in the single equation model, here we find evidence of two-way Granger causality effects.

<i>Equilibrium Relation</i>	<i>Estimate</i>	<i>St. Err.</i>	<i>t-ratio</i>	<i>p-Value</i>
ASX200	1	Fixed		
NZSE	-0.93883	0.236	-3.981	0

Table 15 Equilibrium Relation NZSE-ASX 200

<i>Equation 1, for ASX200:</i>	<i>Estimate</i>	<i>St. Err.</i>	<i>t-ratio</i>	<i>p-Value</i>
[1]Intercept	-4.789	0.066	-72.538	0
ECM1	-0.258	0.138	-1.870	0
F-VECM d1	0.3201	0.02635	12.148	0
d3 for ECM 1	0.274	0.147	1.861	0.062
AR (1,1)	0.088	0.150	0.583	0.559
Ar (1,2)	-0.212	0.173	-1.222	0.222
Sum of Squares	459.190			
R-Squared	0.161			
Residual SD	0.435			
Residual Skewness	0.218			
Residual Kurtosis	3.323			
Jarque-Bera Test	29.9085	{0}		
Box-Pierce (12)	12.3802	{0.415}		
Box-Pierce ² (12)	39.072	{0}		

Table 16 System Equation fro ASX 200

<i>Equation 2, for NZSE:</i>	<i>Estimate</i>	<i>St. Err.</i>	<i>t-ratio</i>	<i>p-Value</i>
[1]Intercept	-4.77509	0.08017	-59.562	0
ECM1	0.07835	0.02777	2.821	0.004
AR (2,1)	0.11776	0.02459	4.788	0
Ar (2,2)	-0.13197	0.03342	-3.949	0
Sum of Squares	559.746			
R-Squared	0.23			
Residual SD	0.4805			
Residual Skewness	0.1736			
Residual Kurtosis	3.6877			
Jarque-Bera Test	60.0755	{0}		
Box-Pierce (12)	12.5743	{0.4}		
Box-Pierce ² (12)	28.8134	{0.004}		

Table 17 System Equation for NZSE

The cointegrating residual should be integrated to order $(d_3 - d_1)$, which is very close to zero (i.e. short memory only). We note, however, that estimates of d for the residual found from log-periodogram estimation techniques appear significantly different from zero. We find, too, that the absence of a mechanism for modeling residual GARCH effects leaves statistically significant patterning in the autocorrelations of the squares of the equation residuals.

<i>Log-Periodogram Regression</i>	
Geweke/Porter-Hudak Method	
Bandwidth = 300 (= $T^{0.82}$)	
Estimate of d	0.2862 -0.0807
Test of Significance: $N(0,1)$	3.54639 {0}
Bias Test: $N(0,1)$	-0.99339 {0.32}
Moulines/Soulier Broadband Method	
Estimate of d	0.1096 {0.0206}
Test of Significance: $N(0,1)$	5.31909 {0}

Table 18 Log-Periodogram Regressions for Equilibrium Residuals

For our second example we turn our attention to the Straights Times and Hang Seng Index log volatility series. As with the NZSE and ASX 200 Index volatility series, earlier analysis suggests that the volatility processes of these proximate markets are inter-related. Time series and scatter plots of the log-volatility processes are shown in the Figures 71 and 72.

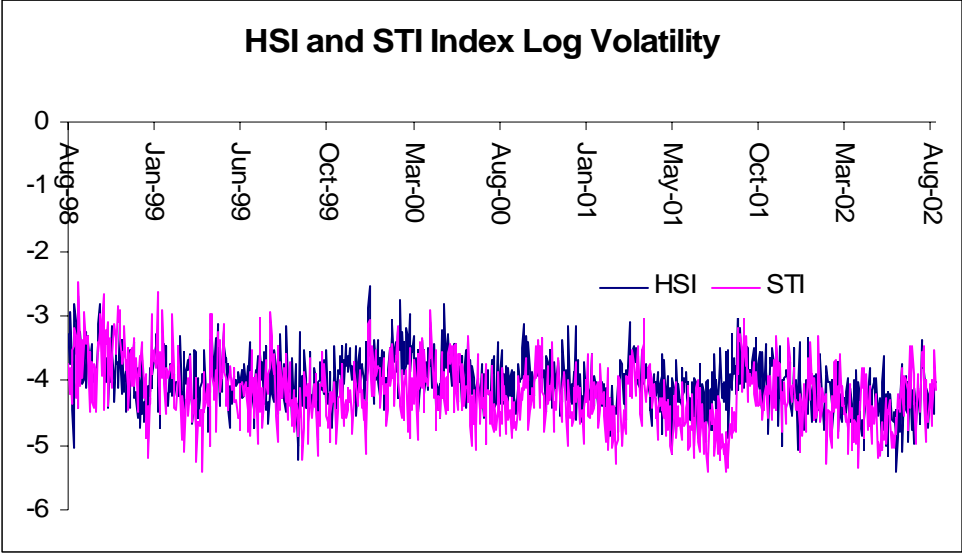


Figure 29 HSI and STI Index Log Volatility Time Series

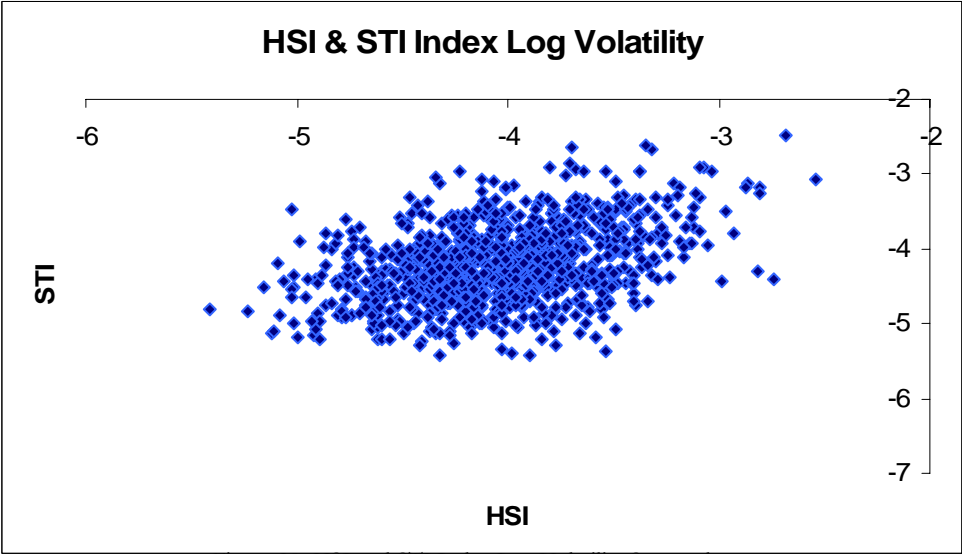


Figure 30 HSI and STI Index Log Volatility Scatterplot

The system and parameter estimates are shown in Tables 42-45.

The model estimates a Fractional VECM with cointegrating vector (1, -0.355), indicating an equilibrium relationship between the log volatility series which is significant at the 0.7% level. The loading coefficient on the ECM is large and well-estimated in the case of the HSI equation, but statistically insignificant for the STI index. AR and MA terms are not significant, and the model for each series is of the form ARFIMA(0,d,0), with $d=0.327$ (assumed identical for both series). Portmanteau tests on residual and squared-residual autocorrelations indicate no residual or GARCH effects and, for the HSI series at least, appear to be Normally distributed. The cointegrating residual process is integrated order ($d1 - d3$), approximately 0.12. To confirm this, we use log-periodogram regression to estimate residual long memory coefficient, using the Geweke/Porter-Hudak method (bandwidth 300) and Moulines/Soulier broadband method, yielding estimates of 0.147 {4.15%} and 0.12 {3.24%}. The conclusion is that the Hang Seng and Straights Times index volatility processes are fractionally cointegrated, albeit that we do not find evidence of Granger causality.

<i>Equilibrium Relation</i>	<i>Estimate</i>	<i>St. Err.</i>	<i>t-ratio</i>	<i>p-Value</i>
HSI	1	Fixed		
STI	-0.355	0.132	-2.686	0.007

Table 19 Equilibrium Relation HSI-STI F-ECM Model

<i>Equation 1, for HSI:</i>	<i>Estimate</i>	<i>St. Err.</i>	<i>t-ratio</i>	<i>p-Value</i>
[1]Intercept	-3.973	0.068	-58.205	0
ECM1	-0.235	0.043	-5.517	0
F-VECM d1	0.327	0.021	15.366	0
d3 for ECM 1	0.209	0.104	2.014	0.044
Sum of Squares	147.438			
R-Squared	0.204			
Residual SD	0.383			
Residual Skewness	-0.005			
Residual Kurtosis	2.965			
Jarque-Bera Test	0.055 {0.972}			
Box-Pierce (40)	32.824 {0.782}			
Box-Pierce ² (40)	48.236 {0.174}			

Table 20 Equation for HIS

<i>Equation 2, for STI:</i>	<i>Estimate</i>	<i>St. Err.</i>	<i>t-ratio</i>	<i>p-Value</i>
[1]Intercept	-4.08708	0.11148	-36.661	0
ECM1	0.06119	0.04675	1.309	0.19
Sum of Squares	171.244			
R-Squared	0.302			
Residual SD	0.413			
Residual Skewness	0.166			
Residual Kurtosis	3.229			
Jarque-Bera Test	6.844{0.032}			
Box-Pierce (40)	32.824 {0.782}			
Box-Pierce ² (40)	36.281 {0.638}			

Table 21 Equation for STI

<i>Log-Periodogram Regression</i>	
Geweke/Porter-Hudak Method	
Bandwidth = 300 (= T ^{0.82})	
Estimate of d	0.147 (0.0415)
Test of Significance: N(0,1)	3.536 {0}
Bias Test: N(0,1)	-1.442 {0.149}
Moulines/Soulier Broadband Method	
Estimate of d	0.120 (0.0324)
Test of Significance: N(0,1)	3.707 {0}

Table 22 Log Periodogram Regression for ECM Residuals

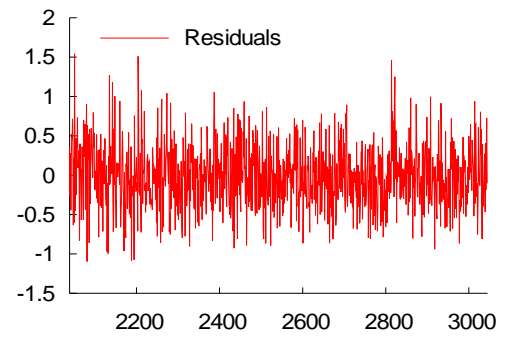
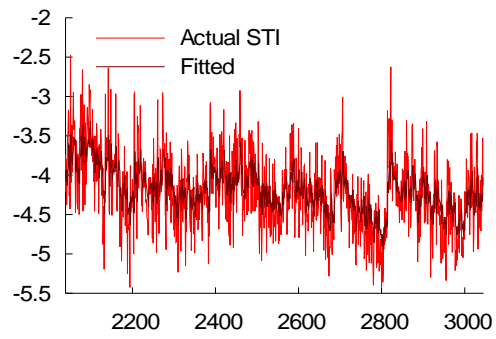
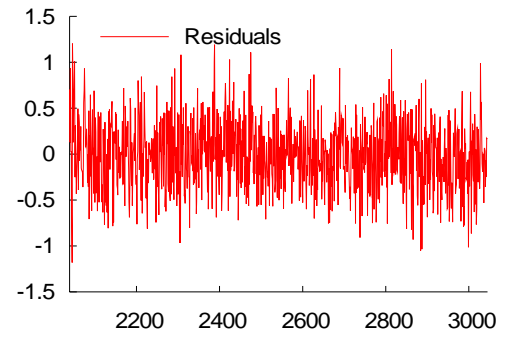
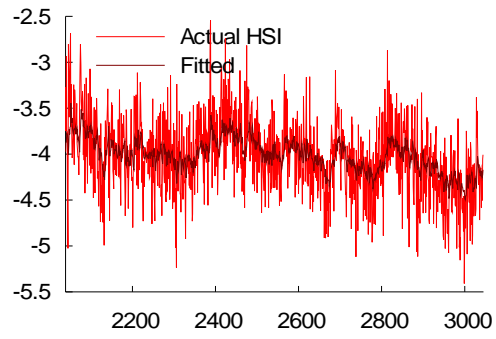


Figure 31 Forecasts and Residuals for HSI and STI

Summary and Conclusion

The research confirms the presence of a number of typical characteristics of volatility processes for emerging markets that have previously been identified in empirical research conducted in developed markets. These characteristics include volatility clustering, long memory, and asymmetry. There appears to be strong evidence of a region-wide regime shift in volatility processes during the Asian crises in 1997, and a less prevalent regime shift in September 2001. We find evidence from multivariate analysis that the sample separates into two distinct groups: a lower volatility group comprising the Australian and New Zealand indices and a higher volatility group comprising the majority of the other indices.

Models developed within the single- and two-factor REGARCH framework of Alizadeh, Brandt and Diebold (2002) provide a good fit for many of the volatility series and in many cases have performance characteristics that compare favorably with other classes of models with high R-squares, low MAPE and direction prediction accuracy of 70% or more. On the debit side, many of the models demonstrate considerable variation in explanatory power over time, often associated with regime shifts or major market events, and this is typically accompanied by some model parameter drift and/or instability.

Single equation ARFIMA-GARCH models appear to be a robust and reliable framework for modeling asset volatility processes, as they are capable of capturing both the short- and long-memory effects in the volatility processes, as well as GARCH effects in the kurtosis process. The available procedures for estimating the degree of fractional integration in the volatility processes produce estimates that appear to vary widely for processes which include both short- and long- memory effects, but the overall conclusion is that long memory effects are at least as important as they are for volatility processes in developed markets. Simple extensions to the single-equation models, which include regressor lags of

related volatility series, add significant explanatory power to the models and suggest the existence of Granger-causality relationships between processes.

Extending the modeling procedures into the realm of models which incorporate systems of equations provides evidence of two-way Granger causality between certain of the volatility processes and suggests that are fractionally cointegrated, a finding shared with parallel studies of volatility processes in developed markets.

Appendix 4

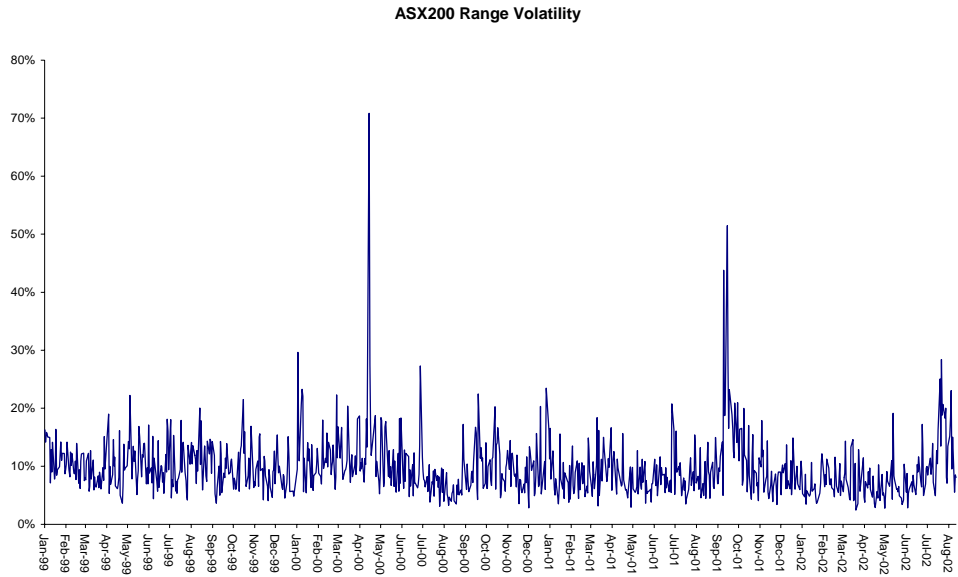


Figure 32 ASX 200 Index Volatility 1999-2002

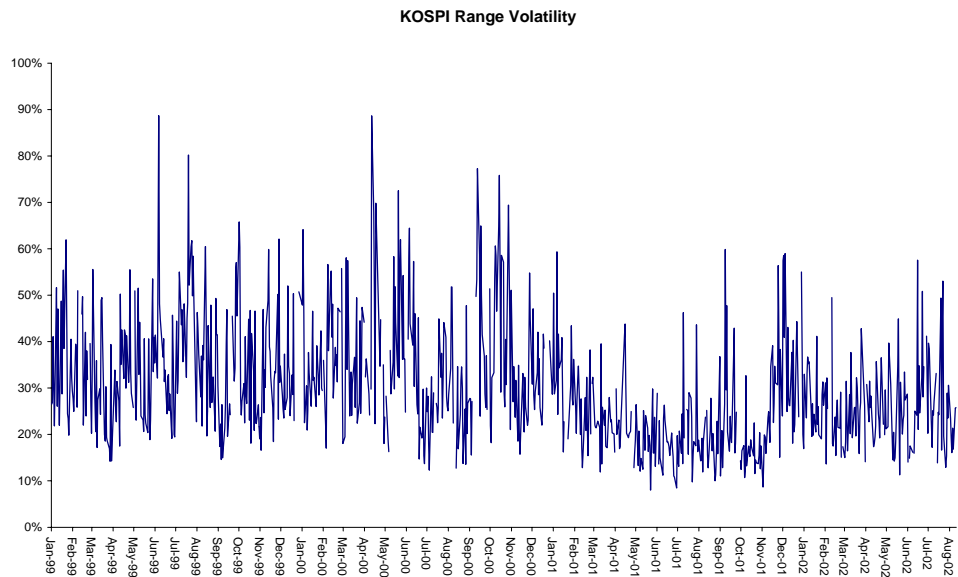


Figure 33 KOSPI Index Volatility 1999 - 2002

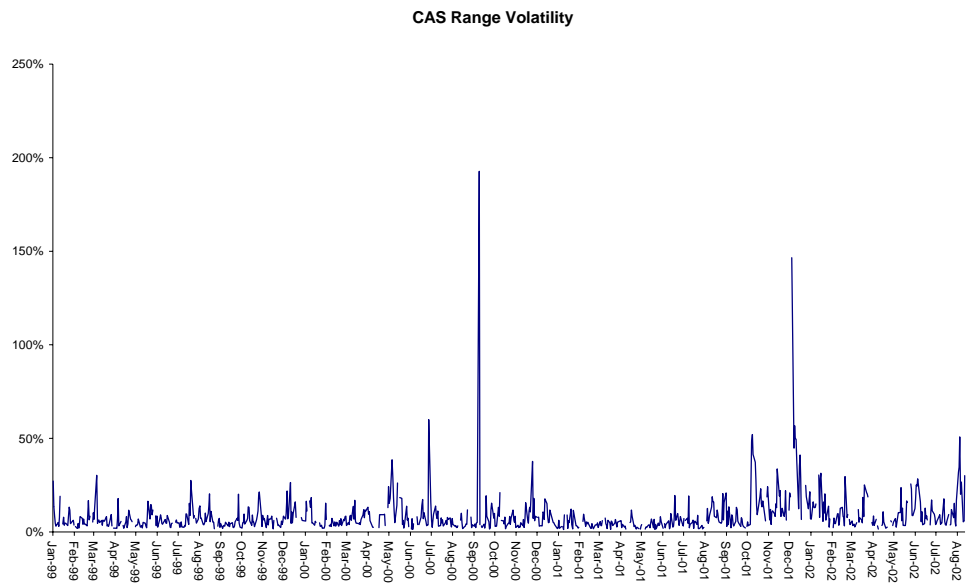


Figure 34 CAS Index Volatility 1999-2002

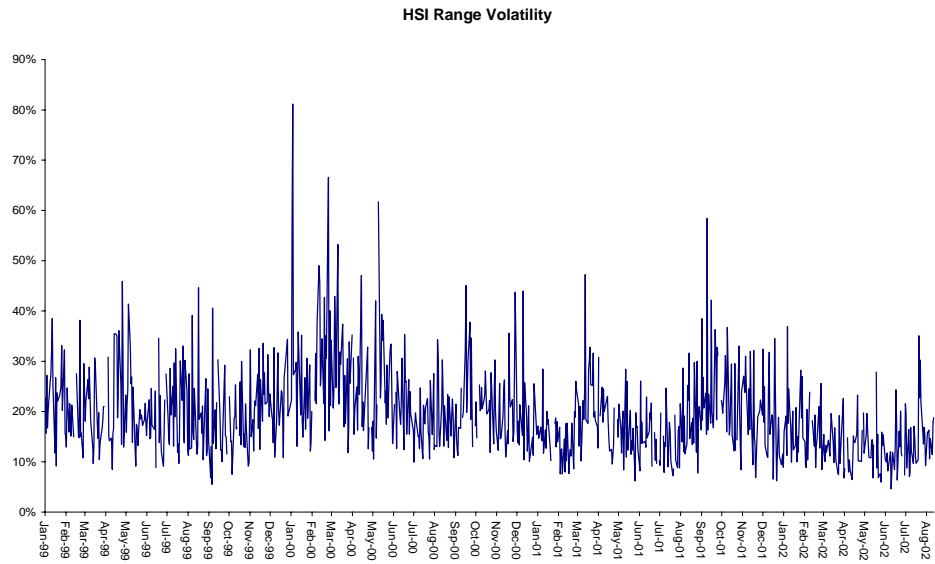


Figure 35 HSI Index Volatility 1999-2002

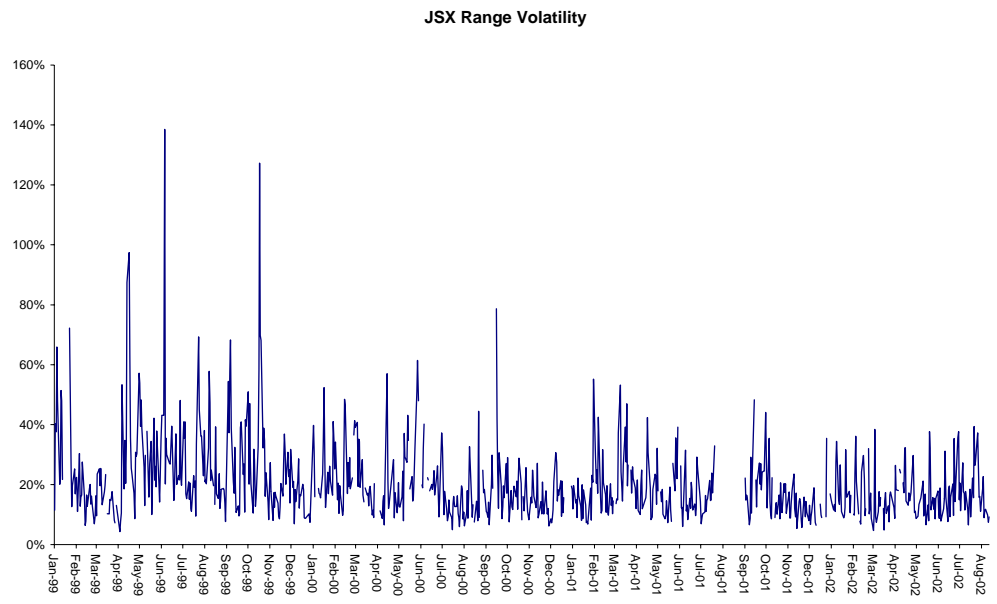


Figure 36 JSX Index Volatility 1999-2002

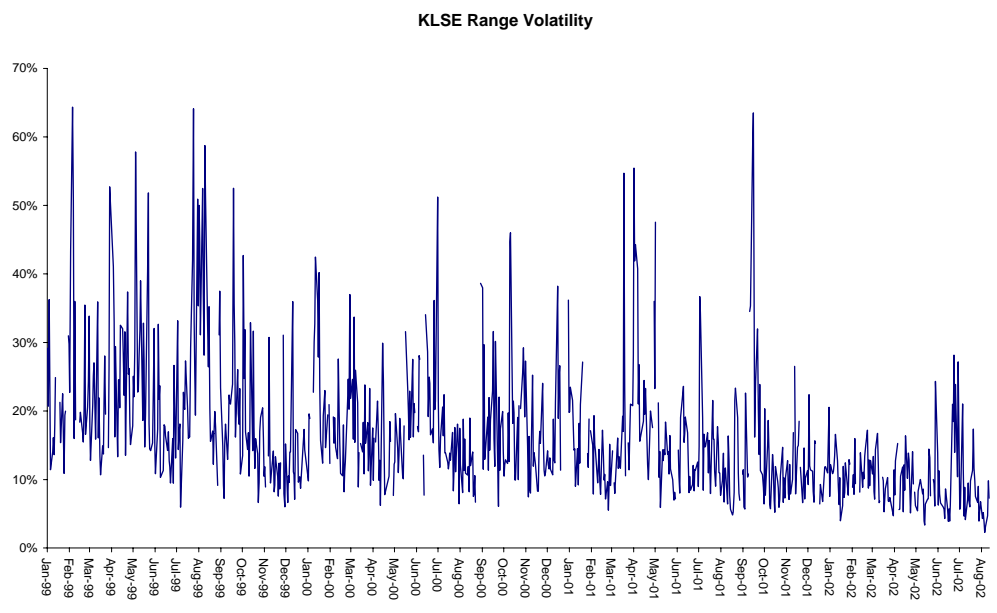


Figure 37 KLSE Index Volatility 1999-2002

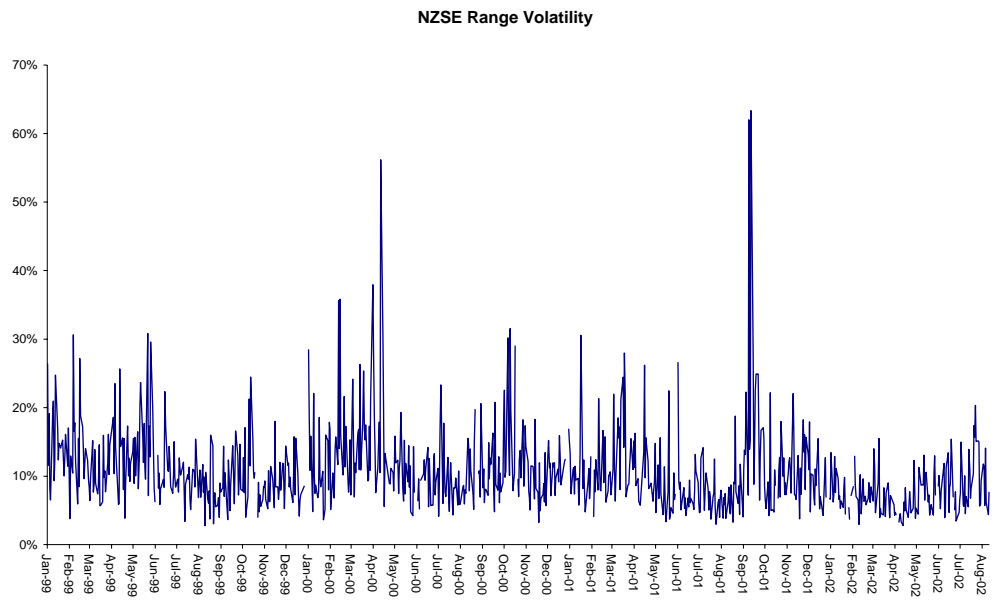


Figure 38 NZSE Index Volatility 1999-2002

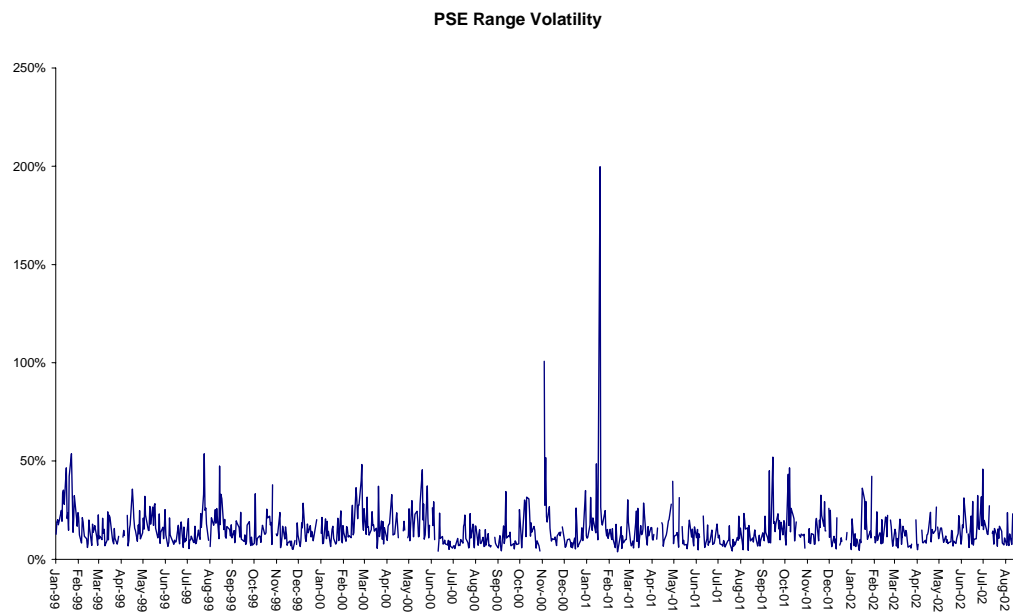


Figure 39 PSE Index Volatility 1999-2002

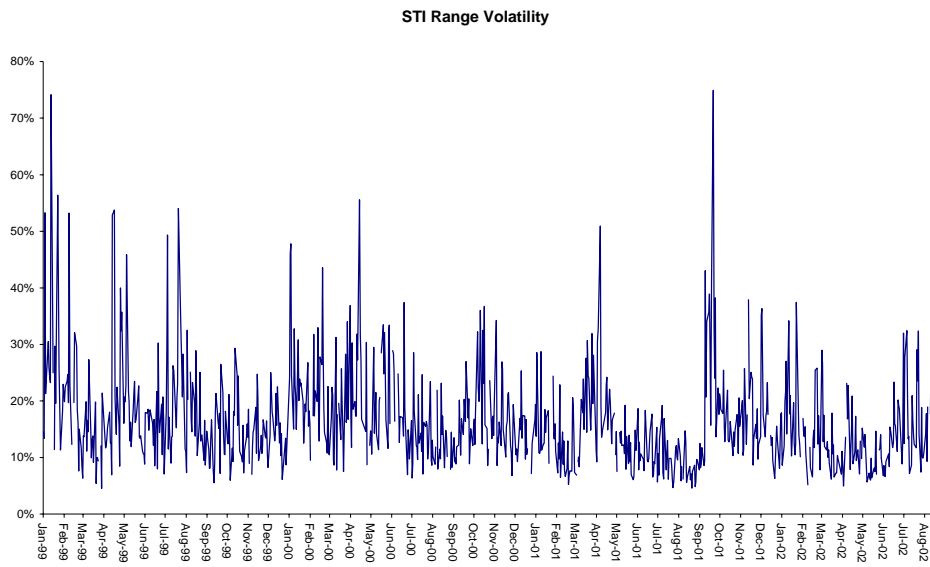


Figure 40 STI Index Volatility 1999-2002

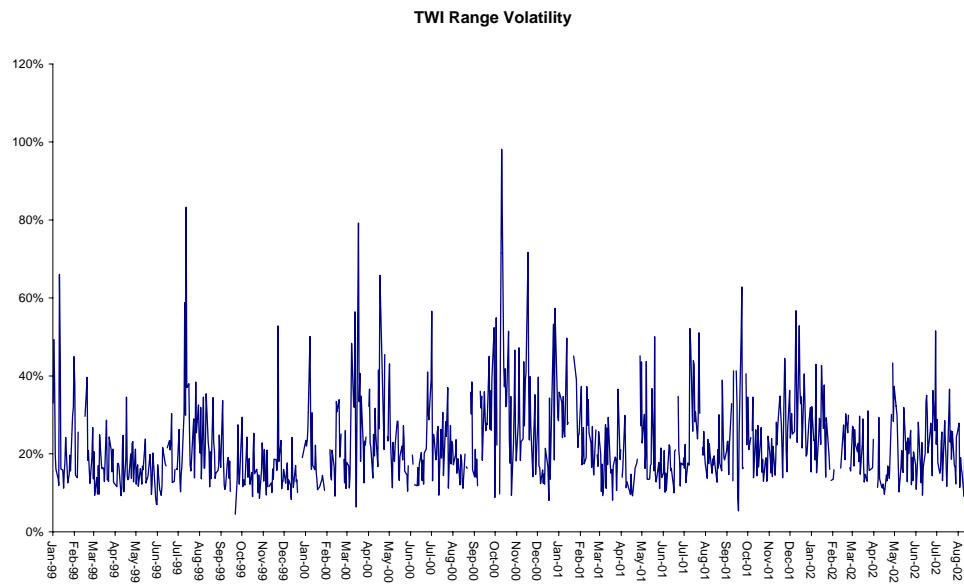


Figure 41 TWI Index Volatility 1999-2002

ICSS: ASX200

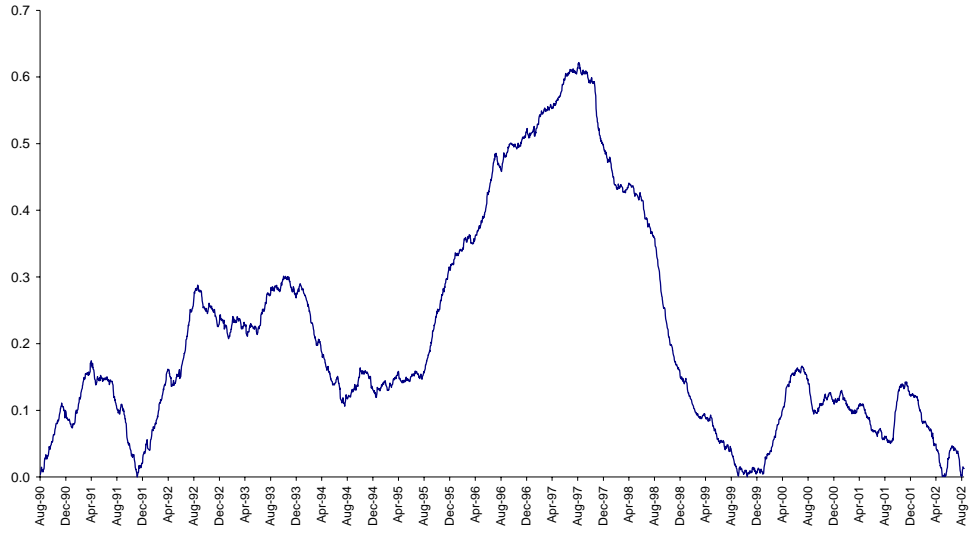


Figure 42 ICSS Test - ASX 200

ICSS: KOSPI

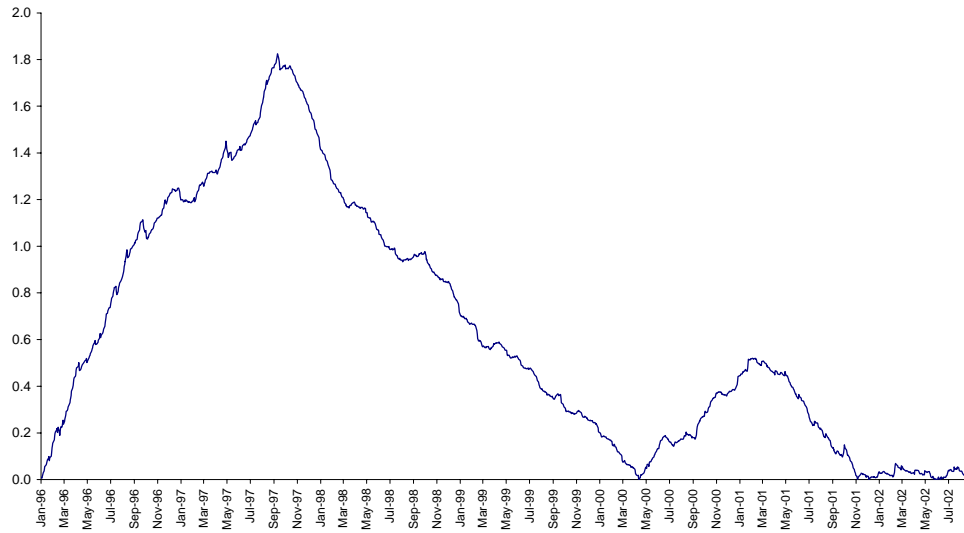


Figure 43 ICSS Test - KOSPI

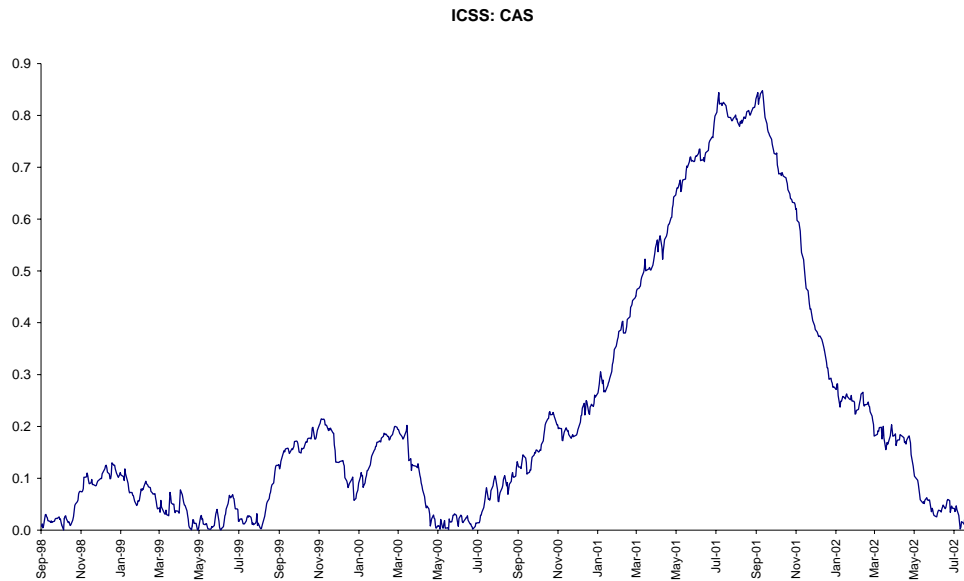


Figure 44 ICSS Test - CAS

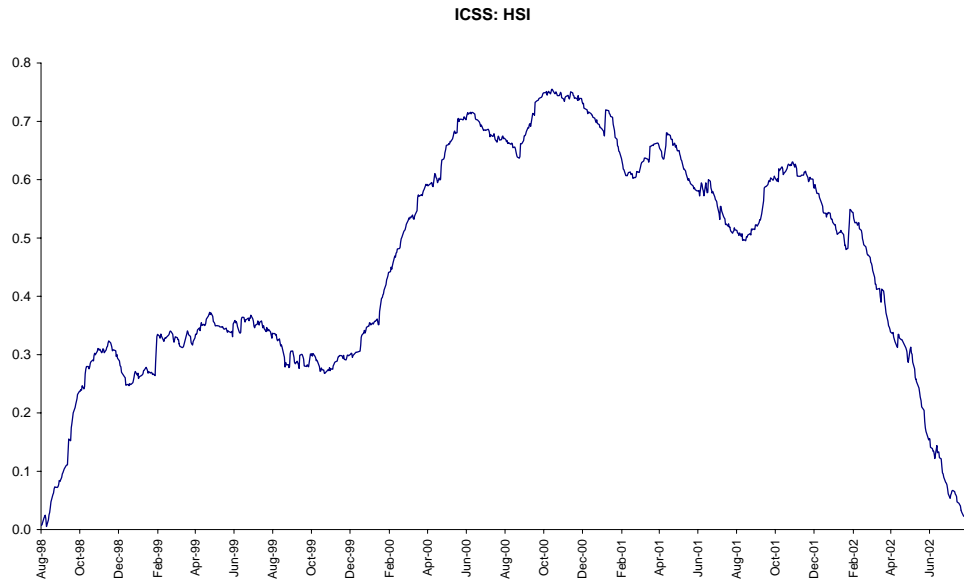


Figure 45 ICSS Test HSI



Figure 46 ICSS Test JSX

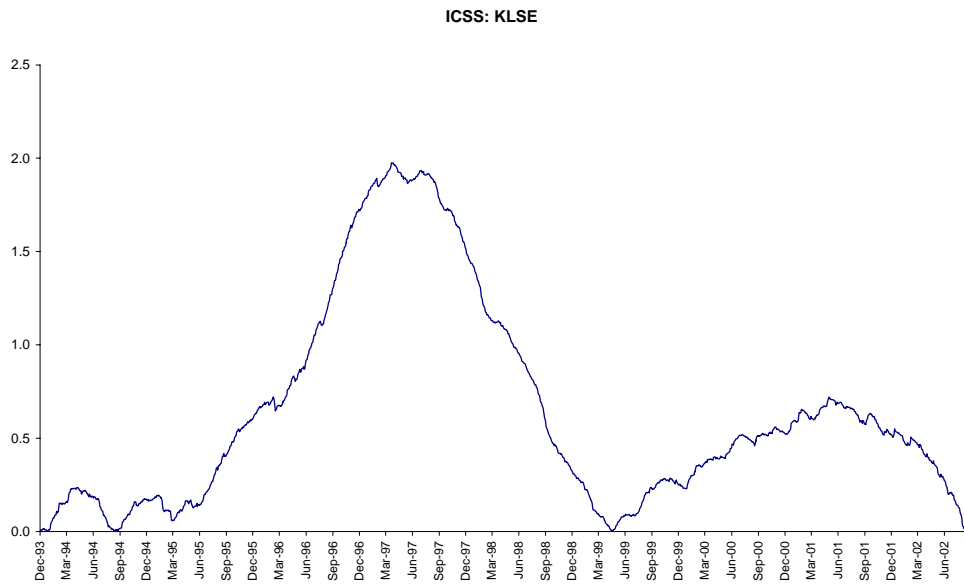


Figure 47 ICSS Test - KLSE

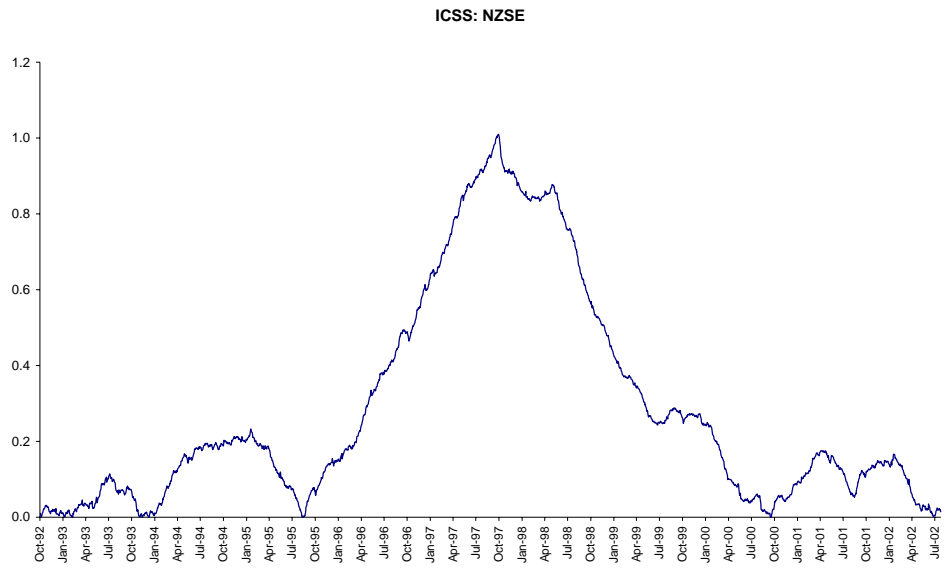


Figure 48 ICSS Test - NZSE

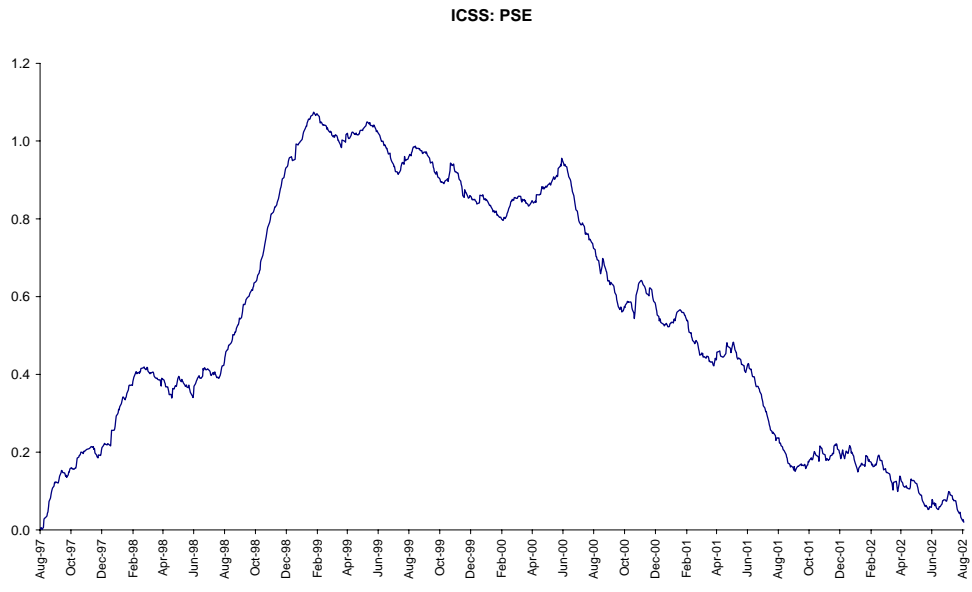


Figure 49 ICSS Test - PSE

ICSS: STI

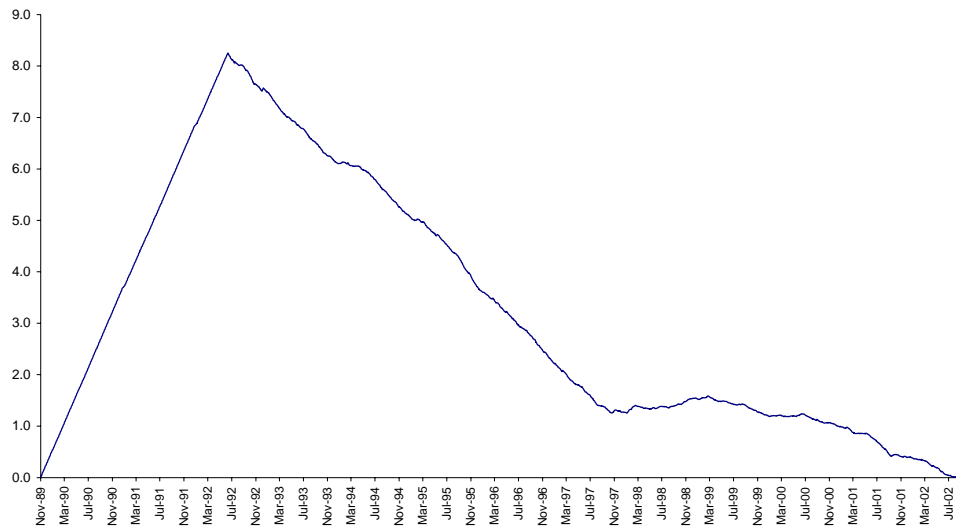


Figure 50 ICSS Test - STI

ICSS: TWI

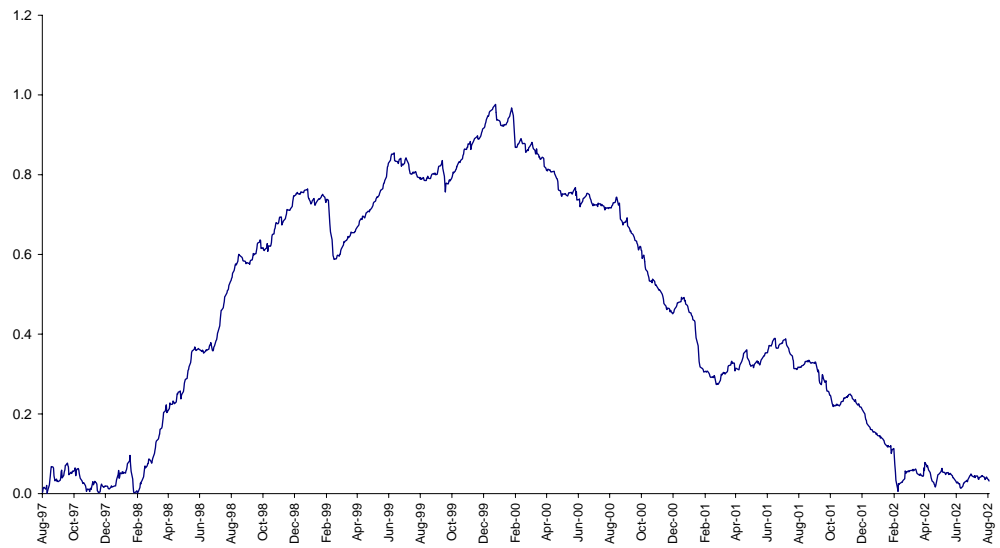


Figure 51 ICSS Test - TWI

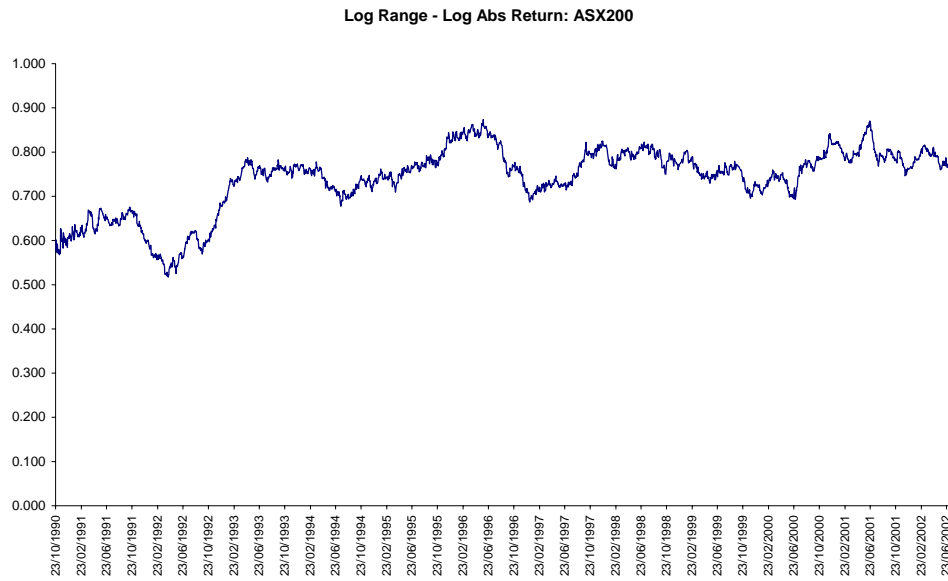


Figure 52 LR-LAR Test - ASX 200

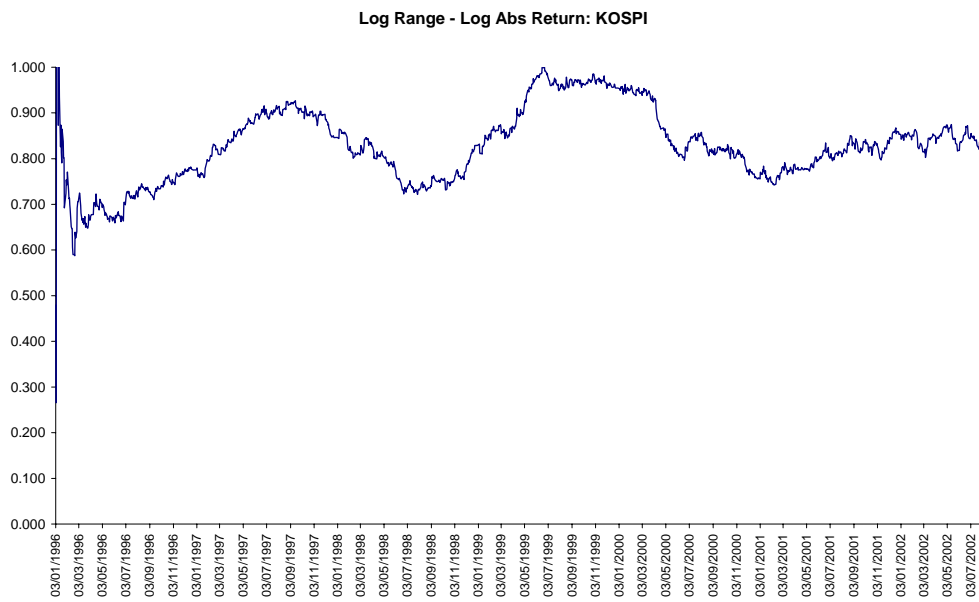


Figure 53 LR-LAR Test - KOSPI

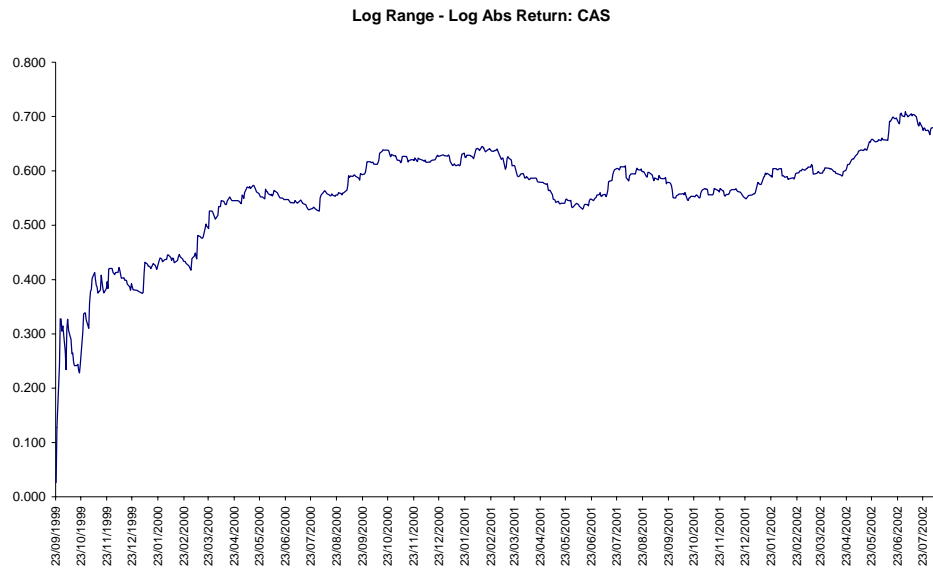


Figure 54 LR-LAR Test - CAS

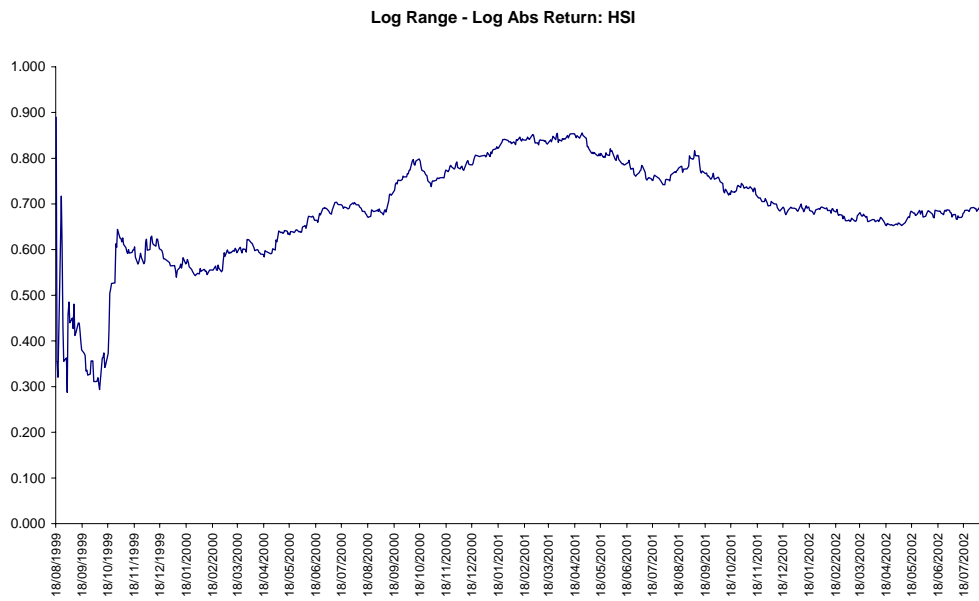


Figure 55 LR-LAR Test - HSI

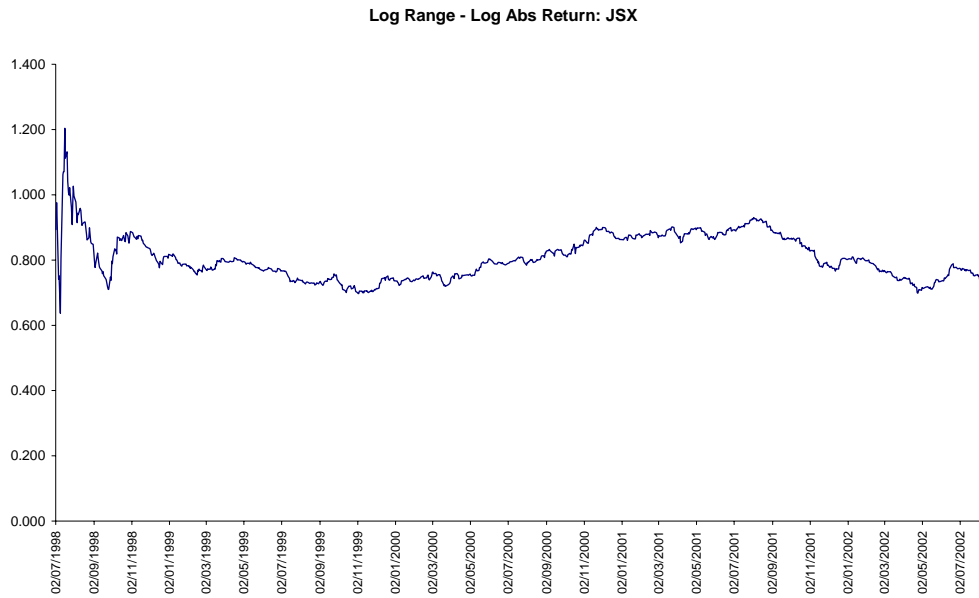


Figure 56 LR-LAR Test - JSX

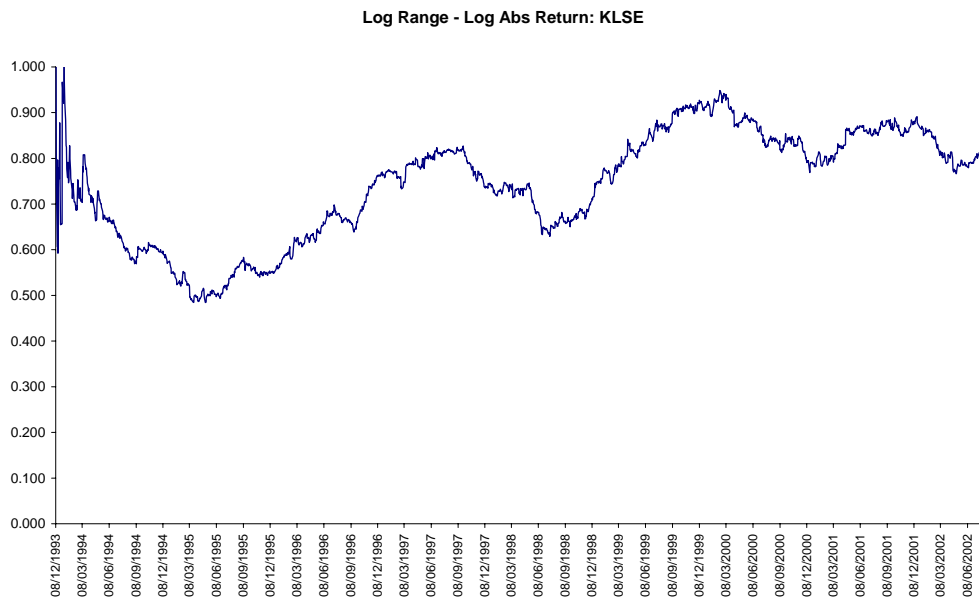


Figure 57 LR-LAR Test - KLSE

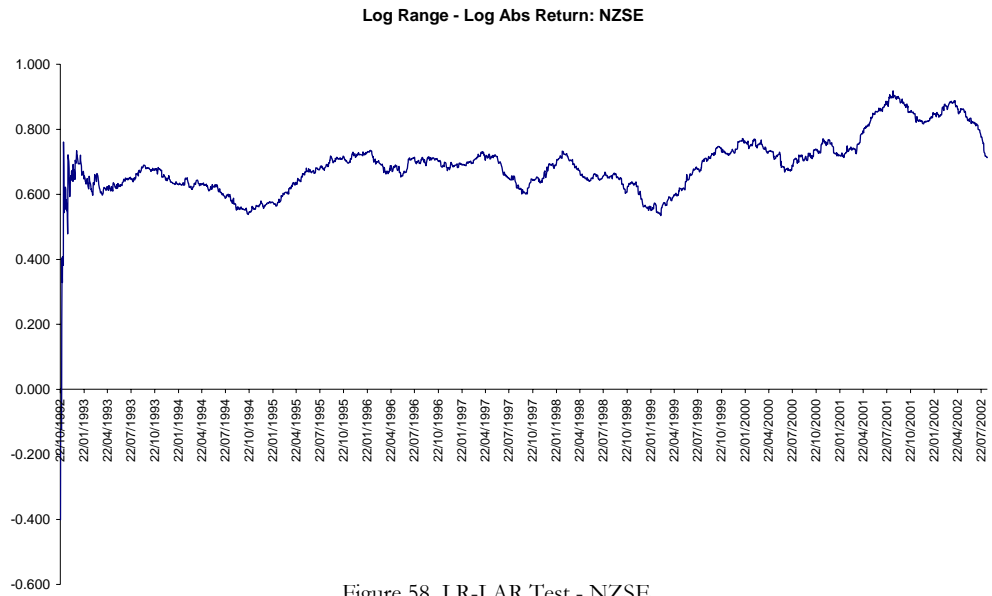


Figure 58 LR-LAR Test - NZSE

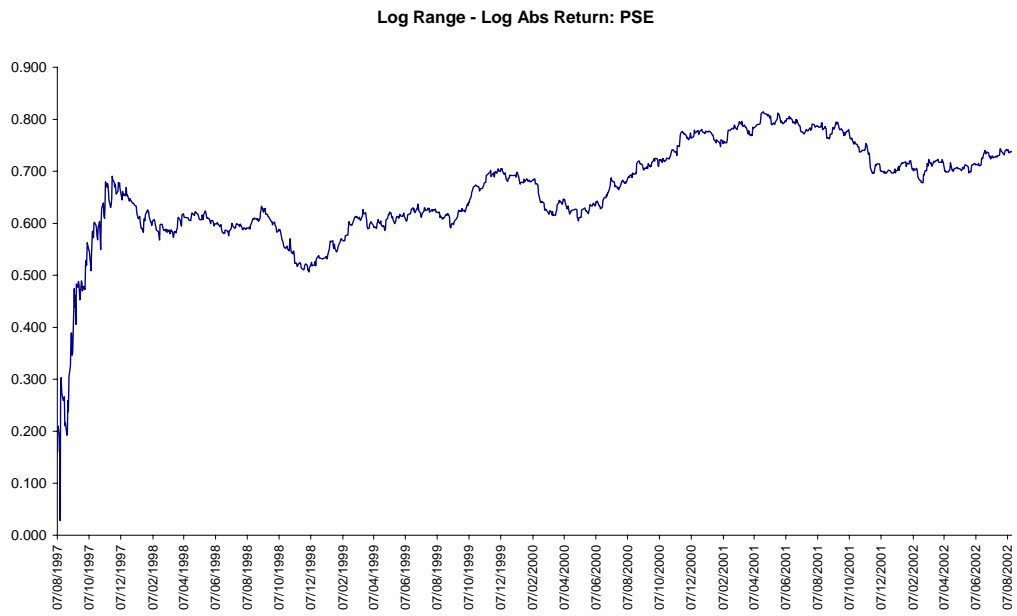


Figure 59 LR-LAR Test - PSE

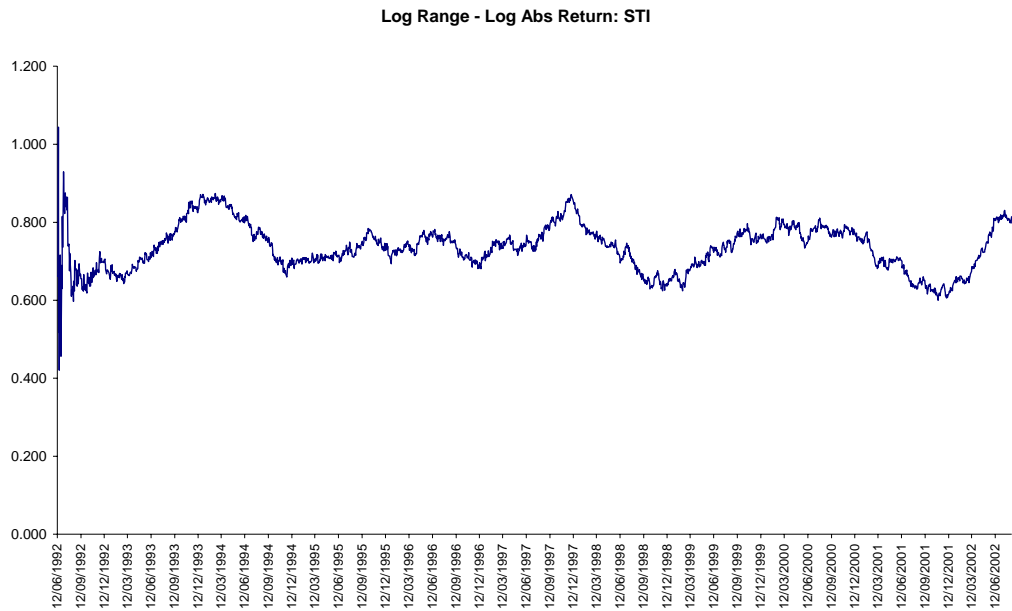


Figure 60 LR-LAR Test - STI

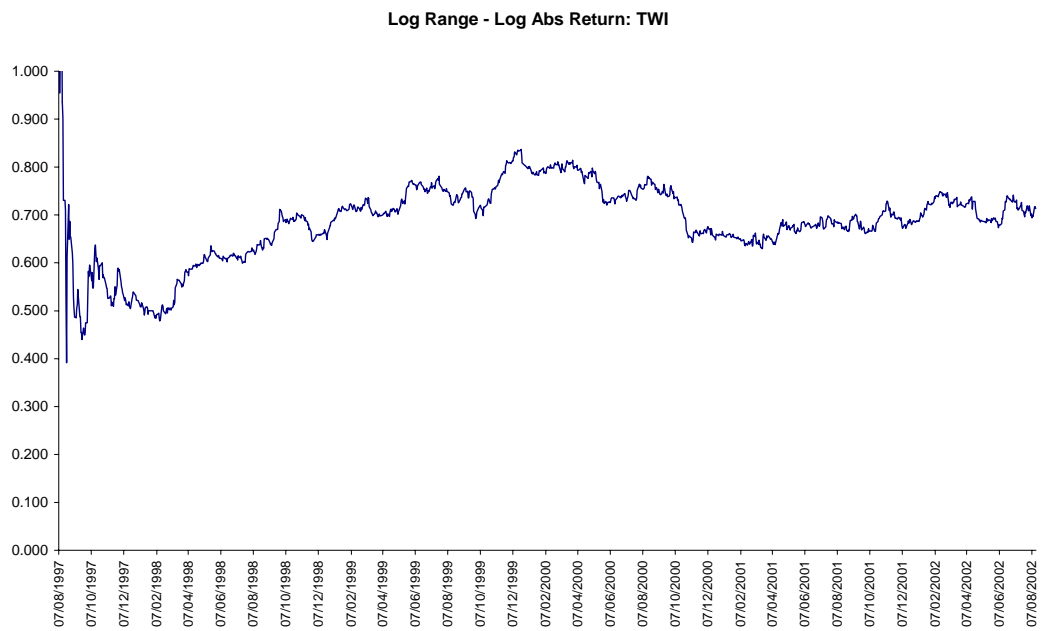


Figure 61 LR-LAR Test - TWI

MODEL: REGARCH 1

κ	0.0271		
θ	-5.1179		
ϕ	0.0264		
δ	-0.0252		
Sample Stats		Errors et	
T	1264	Mean	-0.001
SumSq Err	213.1	Stdev	0.411
Likelihood	5343.2	Skew	0.038
Adj R2	19.8%	Kurtosis	-0.082
AIC	-1.774	JB	1.6%
BIC	-1.758	Box-Pierce	7.5%
Av Dt	-4.712	ARCH-LM	0.6%
Av ln(ht)	-5.141	Sign Bias	0.99
Diff	0.429	Sign Bias -	-9.36
SD ln(ht)	0.204	Sign Bias +	2.27
Mean Xt	-0.005	D-W	1.87
SD Xt	1.417		
		Mean Rt/ht	0.017
MSE	16.9%	SD Rt/ht	1.352
MAD	33.0%	Sign Bias	1.85
MAPE	7.1%	Sign Bias -	-24.78
Theil's U	0.74	Sign Bias +	12.97
DP	72.8%	D-W	1.92

Figure 62 REGARCH 1-Factor Model - ASX 200

MODEL: REGARCH 2

$\kappa\eta$	0.1472		
$\phi\eta$	0.0383		
$\delta\eta$	-0.0260		
$\kappa\theta$	0.0020		
$\theta\theta$	-5.0012		
$\phi\theta$	0.0042		
$\delta\theta$	-0.0172		
Sample Stats		Errors et	
T	1262	Mean	0.007
SumSq Err	208.8	Stdev	0.407
Likelihood	5365.2	Skew	-0.029
Adj R2	19.7%	Kurtosis	-0.239
AIC	-1.793	JB	#NUM!
BIC	-1.776	Box-Pierce	18.9%
Av Dt	-4.715	ARCH-LM	1.2%
Av ln(ht)	-5.152	Sign Bias	0.56
Diff	0.437	Sign Bias -	-6.22
SD ln(ht)	0.202	Sign Bias +	3.44
Mean Xt	0.025	D-W	1.96
SD Xt	1.403		
		Mean Rt/ht	0.026
MSE	16.5%	SD Rt/ht	1.342
MAD	32.9%	Sign Bias	1.29
MAPE	7.1%	Sign Bias -	-20.48
Theil's U	0.74	Sign Bias +	16.87
DP	72.7%	D-W	1.92

Figure 63 REGARCH 2-Factor Model - ASX 200

MODEL: REGARCH 1

κ	0.0516		
θ	-3.9947		
ϕ	0.0635		
δ	-0.0136		
Sample Stats		Errors et	
T	1170	Mean	0.003
SumSq Err	149.3	Stdev	0.357
Likelihood	3468.0	Skew	0.176
Adj R2	33.7%	Kurtosis	-0.348
AIC	-2.052	JB	0.0%
BIC	-2.035	Box-Pierce	65.1%
Av Dt	-3.544	ARCH-LM	70.4%
Av ln(ht)	-3.976	Sign Bias	-0.27
Diff	0.433	Sign Bias -	-5.65
SD ln(ht)	0.256	Sign Bias +	4.25
Mean Xt	0.009	D-W	1.95
SD Xt	1.232		
		Mean Rt/ht	-0.010
MSE	12.8%	SD Rt/ht	1.423
MAD	29.0%	Sign Bias	0.75
MAPE	8.4%	Sign Bias -	-18.88
Theil's U	0.77	Sign Bias +	11.93
DP	70.7%	D-W	1.87

Figure 64 REGARCH 1-Factor Model - KOSPI

MODEL: REGARCH 2

$\kappa\eta$	0.5460		
$\phi\eta$	0.0729		
$\delta\eta$	-0.0096		
$\kappa\theta$	0.0123		
$\theta\theta$	-4.4832		
$\phi\theta$	0.0486		
$\delta\theta$	-0.0054		
Sample Stats		Errors et	
T	1170	Mean	0.034
SumSq Err	150.5	Stdev	0.357
Likelihood	3416.0	Skew	0.176
Adj R2	33.0%	Kurtosis	-0.343
AIC	-2.044	JB	0.0%
BIC	-2.027	Box-Pierce	68.4%
Av Dt	-3.544	ARCH-LM	85.9%
Av ln(ht)	-4.008	Sign Bias	-0.02
Diff	0.464	Sign Bias -	-6.73
SD ln(ht)	0.280	Sign Bias +	4.75
Mean Xt	0.118	D-W	2.00
SD Xt	1.232		
		Mean Rt/ht	-0.011
MSE	12.9%	SD Rt/ht	1.476
MAD	28.9%	Sign Bias	0.78
MAPE	8.5%	Sign Bias -	-18.06
Theil's U	0.78	Sign Bias +	11.06
DP	71.3%	D-W	1.87

Figure 65 REGARCH 2-Factor Model - KOSPI

MODEL: REGARCH 1

κ	0.0635		
θ	-4.2361		
ϕ	0.0958		
δ	-0.0108		
Sample Stats		Errors et	
T	1565	Mean	0.015
SumSq Err	215.3	Stdev	0.371
Likelihood	4929.1	Skew	0.053
Adj R2	49.8%	Kurtosis	-0.081
AIC	-1.978	JB	0.1%
BIC	-1.965	Box-Pierce	1.5%
Av Dt	-3.708	ARCH-LM	26.7%
Av ln(ht)	-4.153	Sign Bias	-0.19
Diff	0.445	Sign Bias -	-5.74
SD ln(ht)	0.365	Sign Bias +	4.05
Mean Xt	0.051	D-W	2.12
SD Xt	1.279		
		Mean Rt/ht	-0.040
MSE	13.8%	SD Rt/ht	1.417
MAD	29.8%	Sign Bias	0.78
MAPE	8.3%	Sign Bias -	-22.12
Theil's U	0.79	Sign Bias +	14.10
DP	70.8%	D-W	1.83

Figure 66 REGARCH 1-Factor Model - CAS

MODEL: REGARCH 2

$\kappa\eta$	0.1731		
$\phi\eta$	0.0714		
$\delta\eta$	-0.0213		
$\kappa\theta$	0.0016		
$\theta\theta$	-4.6644		
$\phi\theta$	0.0288		
$\delta\theta$	-0.0043		
Sample Stats		Errors et	
T	1565	Mean	0.009
SumSq Err	208.3	Stdev	0.365
Likelihood	4948.8	Skew	0.096
Adj R2	51.4%	Kurtosis	-0.189
AIC	-2.008	JB	0.0%
BIC	-1.984	Box-Pierce	42.0%
Av Dt	-3.708	ARCH-LM	48.2%
Av ln(ht)	-4.148	Sign Bias	-0.70
Diff	0.439	Sign Bias -	-5.41
SD ln(ht)	0.390	Sign Bias +	4.26
Mean Xt	0.032	D-W	2.01
SD Xt	1.258		
		Mean Rt/ht	-0.037
MSE	13.3%	SD Rt/ht	1.404
MAD	29.5%	Sign Bias	0.68
MAPE	8.2%	Sign Bias -	-21.09
Theil's U	0.78	Sign Bias +	13.45
DP	69.9%	D-W	1.83

Figure 67 REGARCH 1-Factor Model - CAS

MODEL: REGARCH 1

κ	0.1598		
θ	-5.5056		
ϕ	0.0973		
δ	0.0190		
Sample Stats		Errors et	
T	906	Mean	-0.002
SumSq Err	344.3	Stdev	0.617
Likelihood	3078.5	Skew	0.445
Adj R ²	29.0%	Kurtosis	1.180
AIC	-0.959	JB	0.0%
BIC	-0.937	Box-Pierce	0.3%
Av Dt	-5.081	ARCH-LM	27.2%
Av ln(ht)	-5.508	Sign Bias	-0.85
Diff	0.428	Sign Bias -	-2.37
SD ln(ht)	0.396	Sign Bias +	10.57
Mean Xt	-0.008	D-W	1.94
SD Xt	2.127		
		Mean Rt/ht	0.063
MSE	38.0%	SD Rt/ht	2.055
MAD	49.4%	Sign Bias	-1.64
MAPE	10.4%	Sign Bias -	-3.00
Theil's U	0.75	Sign Bias +	37.23
DP	68.5%	D-W	1.45

Figure 68 REGARCH 1-Factor Model - HSI

MODEL: REGARCH 2

$\kappa\eta$	0.5280		
$\phi\eta$	0.1036		
$\delta\eta$	0.0234		
$\kappa\theta$	0.0671		
$\theta\theta$	-5.4967		
$\phi\theta$	0.0469		
$\delta\theta$	0.0062		
Sample Stats		Errors et	
T	906	Mean	-0.003
SumSq Err	341.2	Stdev	0.614
Likelihood	3124.7	Skew	0.443
Adj R2	29.4%	Kurtosis	1.233
AIC	-0.961	JB	0.0%
BIC	-0.924	Box-Pierce	1.9%
Av Dt	-5.081	ARCH-LM	36.6%
Av ln(ht)	-5.508	Sign Bias	-0.91
Diff	0.427	Sign Bias -	-2.46
SD ln(ht)	0.403	Sign Bias +	10.14
Mean Xt	-0.009	D-W	2.00
SD Xt	2.117		
		Mean Rt/ht	0.055
MSE	37.7%	SD Rt/ht	2.030
MAD	49.1%	Sign Bias	-1.62
MAPE	10.3%	Sign Bias -	-3.48
Theil's U	0.75	Sign Bias +	37.31
DP	69.4%	D-W	1.45

Figure 69 REGARCH 2-Factor Model - HSI

MODEL: REGARCH 1

κ	0.0013		
θ	-4.0341		
ϕ	0.0258		
δ	-0.0068		
Sample Stats		Errors et	
T	965	Mean	-0.013
SumSq Err	144.1	Stdev	0.386
Likelihood	3219.6	Skew	0.067
Adj R2	21.7%	Kurtosis	-0.088
AIC	-1.893	JB	0.4%
BIC	-1.873	Box-Pierce	67.5%
Av Dt	-4.029	ARCH-LM	9.0%
Av ln(ht)	-4.445	Sign Bias	0.48
Diff	0.417	Sign Bias -	-4.38
SD ln(ht)	0.231	Sign Bias +	1.76
Mean Xt	-0.047	D-W	2.01
SD Xt	1.332		
		Mean Rt/ht	-0.005
MSE	14.9%	SD Rt/ht	1.490
MAD	31.1%	Sign Bias	0.11
MAPE	7.9%	Sign Bias -	-19.02
Theil's U	0.71	Sign Bias +	14.67
DP	70.9%	D-W	1.90

Figure 70 REGARCH 1-Factor Model - JSX

MODEL: REGARCH 2

$\kappa\eta$	0.2417		
$\phi\eta$	0.0323		
$\delta\eta$	-0.0102		
$\kappa\theta$	0.0005		
$\theta\theta$	-4.0166		
$\phi\theta$	0.0228		
$\delta\theta$	-0.0059		
Sample Stats		Errors et	
T	965	Mean	-0.012
SumSq Err	143.9	Stdev	0.386
Likelihood	3216.3	Skew	0.062
Adj R2	21.6%	Kurtosis	-0.091
AIC	-1.889	JB	0.6%
BIC	-1.853	Box-Pierce	72.3%
Av Dt	-4.029	ARCH-LM	9.3%
Av ln(ht)	-4.447	Sign Bias	0.47
Diff	0.418	Sign Bias -	-4.52
SD ln(ht)	0.230	Sign Bias +	1.76
Mean Xt	-0.040	D-W	2.06
SD Xt	1.331		
		Mean Rt/ht	-0.006
MSE	14.9%	SD Rt/ht	1.493
MAD	31.2%	Sign Bias	0.16
MAPE	7.9%	Sign Bias -	-19.21
Theil's U	0.71	Sign Bias +	14.36
DP	72.3%	D-W	1.90

Figure 71 REGARCH 2-Factor Model - JSX

MODEL: REGARCH 1

κ	0.1283		
θ	-4.3935		
ϕ	0.0978		
δ	-0.0013		
Sample Stats		Errors et	
T	1204	Mean	0.005
SumSq Err	298.4	Stdev	0.498
Likelihood	3822.7	Skew	0.310
Adj R2	31.7%	Kurtosis	0.138
AIC	-1.388	JB	0.0%
BIC	-1.371	Box-Pierce	0.8%
Av Dt	-3.943	ARCH-LM	44.3%
Av ln(ht)	-4.377	Sign Bias	-0.09
Diff	0.435	Sign Bias -	-13.15
SD ln(ht)	0.341	Sign Bias +	7.50
Mean Xt	0.016	D-W	1.88
SD Xt	1.717		
		Mean Rt/ht	-0.041
MSE	24.8%	SD Rt/ht	1.551
MAD	39.9%	Sign Bias	-0.23
MAPE	10.8%	Sign Bias -	-17.66
Theil's U	0.83	Sign Bias +	18.31
DP	68.4%	D-W	1.67

Figure 72 REGARCH 1-Factor Model - KLSE

MODEL: REGARCH 2

$\kappa\eta$	0.5075		
$\phi\eta$	0.1114		
$\delta\eta$	-0.0010		
$\kappa\theta$	0.0244		
$\theta\theta$	-4.4322		
$\phi\theta$	0.0326		
$\delta\theta$	-0.0141		
Sample Stats		Errors et	
T	1204	Mean	0.005
SumSq Err	292.4	Stdev	0.493
Likelihood	3846.2	Skew	0.299
Adj R2	32.9%	Kurtosis	0.106
AIC	-1.404	JB	0.0%
BIC	-1.374	Box-Pierce	50.5%
Av Dt	-3.943	ARCH-LM	49.1%
Av ln(ht)	-4.377	Sign Bias	-0.33
Diff	0.435	Sign Bias -	-12.29
SD ln(ht)	0.356	Sign Bias +	7.42
Mean Xt	0.016	D-W	1.99
SD Xt	1.700		
		Mean Rt/ht	-0.039
MSE	24.3%	SD Rt/ht	1.538
MAD	39.4%	Sign Bias	-0.34
MAPE	10.6%	Sign Bias -	-16.92
Theil's U	0.82	Sign Bias +	18.19
DP	69.6%	D-W	1.68

Figure 73 REGARCH 2-Factor Model - KLSE

MODEL: REGARCH 1

κ	0.0483		
θ	-5.1981		
ϕ	0.0446		
δ	-0.0106		
Sample Stats		Errors et	
T	2432	Mean	0.002
SumSq Err	570.4	Stdev	0.484
Likelihood	9681.5	Skew	0.151
Adj R2	21.5%	Kurtosis	0.655
AIC	-1.447	JB	0.0%
BIC	-1.437	Box-Pierce	5.9%
Av Dt	-4.765	ARCH-LM	0.0%
Av ln(ht)	-5.198	Sign Bias	-0.64
Diff	0.432	Sign Bias -	-18.22
SD ln(ht)	0.254	Sign Bias +	8.51
Mean Xt	0.008	D-W	1.87
SD Xt	1.670		
		Mean Rt/ht	0.036
MSE	23.5%	SD Rt/ht	1.560
MAD	38.5%	Sign Bias	1.00
MAPE	8.4%	Sign Bias -	-39.99
Theil's U	0.78	Sign Bias +	14.41
DP	71.7%	D-W	1.80

Figure 74 REGARCH 1-Factor Model - NZSE

MODEL: REGARCH 2

$\kappa\eta$	1.4191		
$\phi\eta$	0.0703		
$\delta\eta$	-0.0065		
$\kappa\theta$	0.0487		
$\theta\theta$	-5.1993		
$\phi\theta$	0.0473		
$\delta\theta$	-0.0113		
Sample Stats		Errors et	
T	2432	Mean	0.002
SumSq Err	567.1	Stdev	0.483
Likelihood	9717.6	Skew	0.140
Adj R2	21.9%	Kurtosis	0.637
AIC	-1.450	JB	0.0%
BIC	-1.434	Box-Pierce	42.9%
Av Dt	-4.765	ARCH-LM	0.1%
Av ln(ht)	-5.198	Sign Bias	-0.43
Diff	0.432	Sign Bias -	-17.76
SD ln(ht)	0.268	Sign Bias +	7.74
Mean Xt	0.008	D-W	2.04
SD Xt	1.665		
		Mean Rt/ht	0.034
MSE	23.3%	SD Rt/ht	1.551
MAD	38.4%	Sign Bias	1.11
MAPE	8.3%	Sign Bias -	-40.15
Theil's U	0.77	Sign Bias +	15.38
DP	71.9%	D-W	1.80

Figure 75 REGARCH 2-Factor Model - NZSE

MODEL: REGARCH 1

κ	0.0561		
θ	-4.6791		
ϕ	0.0593		
δ	-0.0016		
Sample Stats		Errors et	
T	1219	Mean	0.000
SumSq Err	269.9	Stdev	0.471
Likelihood	3516.3	Skew	0.548
Adj R2	27.5%	Kurtosis	0.973
AIC	-1.501	JB	0.0%
BIC	-1.484	Box-Pierce	82.6%
Av Dt	-4.244	ARCH-LM	21.0%
Av ln(ht)	-4.674	Sign Bias	0.29
Diff	0.430	Sign Bias -	-9.80
SD ln(ht)	0.291	Sign Bias +	14.69
Mean Xt	-0.001	D-W	1.94
SD Xt	1.623		
		Mean Rt/ht	-0.093
MSE	22.1%	SD Rt/ht	1.890
MAD	37.2%	Sign Bias	-1.13
MAPE	9.3%	Sign Bias -	-3.66
Theil's U	0.75	Sign Bias +	21.46
DP	70.3%	D-W	1.65

Figure 76 REGARCH 1-Factor Model - PSE

MODEL: REGARCH 2

$\kappa\eta$	0.2602		
$\phi\eta$	0.0653		
$\delta\eta$	0.0005		
$\kappa\theta$	0.0367		
$\theta\theta$	-4.6861		
$\phi\theta$	0.0371		
$\delta\theta$	-0.0051		
Sample Stats		Errors et	
T	1219	Mean	-0.001
SumSq Err	269.1	Stdev	0.470
Likelihood	3514.1	Skew	0.551
Adj R2	27.5%	Kurtosis	1.025
AIC	-1.499	JB	0.0%
BIC	-1.470	Box-Pierce	89.9%
Av Dt	-4.244	ARCH-LM	37.5%
Av ln(ht)	-4.673	Sign Bias	0.23
Diff	0.429	Sign Bias -	-9.62
SD ln(ht)	0.294	Sign Bias +	14.72
Mean Xt	-0.004	D-W	1.98
SD Xt	1.621		
		Mean Rt/ht	-0.093
MSE	22.1%	SD Rt/ht	1.891
MAD	37.0%	Sign Bias	-1.14
MAPE	9.2%	Sign Bias -	-3.61
Theil's U	0.75	Sign Bias +	21.65
DP	70.6%	D-W	1.65

Figure 77 REGARCH 2-Factor Model - PSE

MODEL: REGARCH 1

κ	0.0456		
θ	-4.9130		
ϕ	0.0684		
δ	-0.0161		
Sample Stats		Errors et	
T	2414	Mean	0.005
SumSq Err	550.6	Stdev	0.478
Likelihood	8913.7	Skew	0.135
Adj R2	40.9%	Kurtosis	0.205
AIC	-1.475	JB	0.0%
BIC	-1.465	Box-Pierce	0.0%
Av Dt	-4.453	ARCH-LM	0.0%
Av ln(ht)	-4.888	Sign Bias	-1.90
Diff	0.435	Sign Bias -	-0.70
SD ln(ht)	0.397	Sign Bias +	2.76
Mean Xt	0.016	D-W	1.83
SD Xt	1.647		
		Mean Rt/ht	-0.013
MSE	22.8%	SD Rt/ht	1.546
MAD	37.7%	Sign Bias	-0.03
MAPE	8.8%	Sign Bias -	-25.09
Theil's U	0.82	Sign Bias +	16.11
DP	69.0%	D-W	1.69

Figure 78 REGARCH 1-Factor Model - STI

MODEL: REGARCH 2

$\kappa\eta$	0.2454		
$\phi\eta$	0.0839		
$\delta\eta$	-0.0177		
$\kappa\theta$	0.0040		
$\theta\theta$	-5.0277		
$\phi\theta$	0.0177		
$\delta\theta$	-0.0049		
Sample Stats		Errors et	
T	2414	Mean	0.010
SumSq Err	538.5	Stdev	0.472
Likelihood	8909.3	Skew	0.181
Adj R2	42.2%	Kurtosis	0.234
AIC	-1.494	JB	0.0%
BIC	-1.478	Box-Pierce	38.8%
Av Dt	-4.453	ARCH-LM	0.0%
Av ln(ht)	-4.893	Sign Bias	-1.76
Diff	0.440	Sign Bias -	-0.41
SD ln(ht)	0.408	Sign Bias +	2.84
Mean Xt	0.033	D-W	1.96
SD Xt	1.629		
		Mean Rt/ht	-0.008
MSE	22.3%	SD Rt/ht	1.551
MAD	37.1%	Sign Bias	-0.18
MAPE	8.7%	Sign Bias -	-24.52
Theil's U	0.81	Sign Bias +	15.60
DP	70.0%	D-W	1.71

Figure 79 REGARCH 2-Factor Model - STI

MODEL: REGARCH 1

κ	0.1361		
θ	-4.4533		
ϕ	0.0737		
δ	-0.0252		
Sample Stats		Errors et	
T	1191	Mean	0.001
SumSq Err	197.9	Stdev	0.408
Likelihood	3865.7	Skew	0.116
Adj R2	23.8%	Kurtosis	0.217
AIC	-1.788	JB	0.0%
BIC	-1.771	Box-Pierce	49.3%
Av Dt	-4.009	ARCH-LM	0.4%
Av ln(ht)	-4.440	Sign Bias	1.36
Diff	0.431	Sign Bias -	-6.72
SD ln(ht)	0.228	Sign Bias +	1.96
Mean Xt	0.003	D-W	1.94
SD Xt	1.406		
		Mean Rt/ht	-0.061
MSE	16.6%	SD Rt/ht	1.545
MAD	32.4%	Sign Bias	-0.92
MAPE	8.3%	Sign Bias -	-19.29
Theil's U	0.78	Sign Bias +	17.05
DP	69.8%	D-W	1.84

Figure 80 REGARCH 1-Factor Model - TWI

MODEL: REGARCH 2

$\kappa\eta$	0.1731		
$\phi\eta$	0.0714		
$\delta\eta$	-0.0213		
$\kappa\theta$	0.0016		
$\theta\theta$	-4.6644		
$\phi\theta$	0.0288		
$\delta\theta$	-0.0043		
Sample Stats		Errors et	
T	1191	Mean	0.002
SumSq Err	198.1	Stdev	0.408
Likelihood	3860.8	Skew	0.154
Adj R2	23.5%	Kurtosis	0.328
AIC	-1.782	JB	0.0%
BIC	-1.752	Box-Pierce	47.6%
Av Dt	-4.009	ARCH-LM	0.5%
Av ln(ht)	-4.441	Sign Bias	2.50
Diff	0.432	Sign Bias -	-7.96
SD ln(ht)	0.267	Sign Bias +	0.76
Mean Xt	0.008	D-W	1.93
SD Xt	1.407		
		Mean Rt/ht	-0.067
MSE	16.6%	SD Rt/ht	1.548
MAD	32.2%	Sign Bias	-0.63
MAPE	8.3%	Sign Bias -	-19.11
Theil's U	0.79	Sign Bias +	15.69
DP	69.7%	D-W	1.83

Figure 81 REGARCH 2-Factor Model - TWI

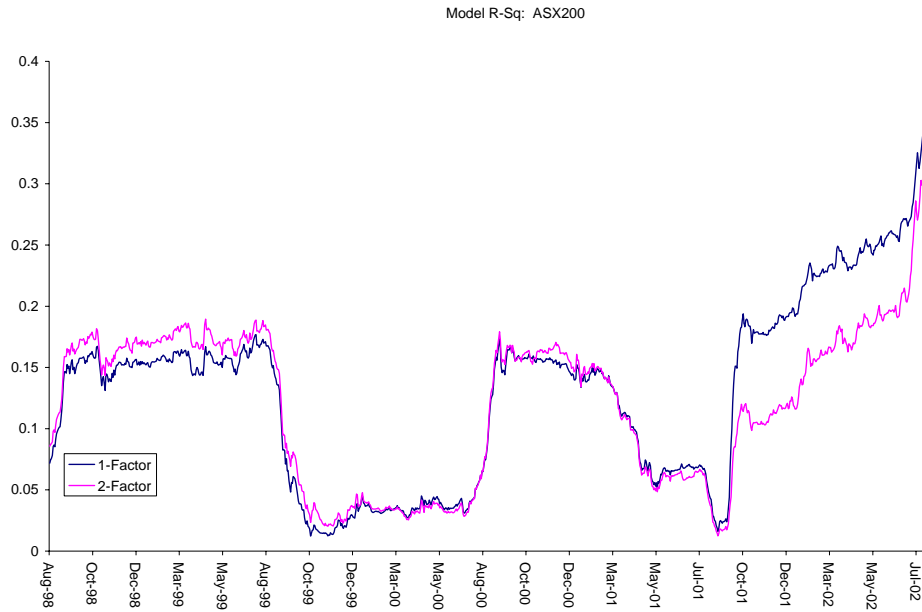


Figure 82 REGARCH Model R-Sq - ASX200

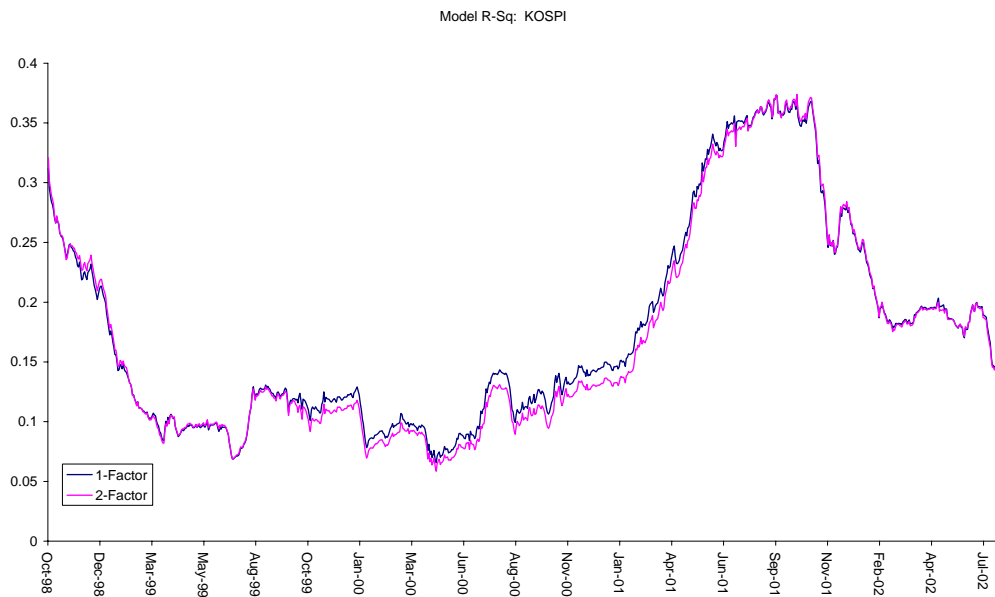


Figure 83 REGARCH Model R-Sq - KOSPI

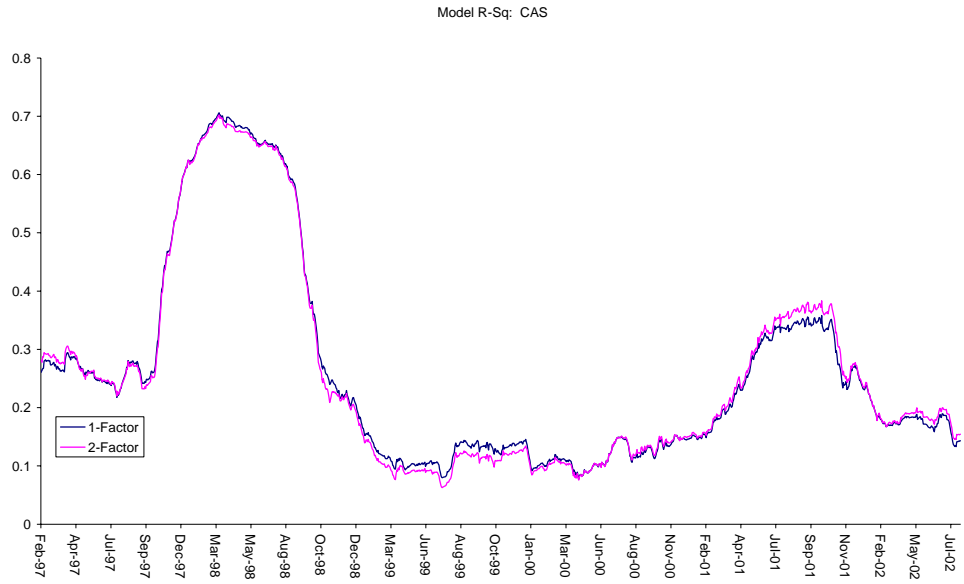


Figure 84 REGARCH Model R-Sq - CAS

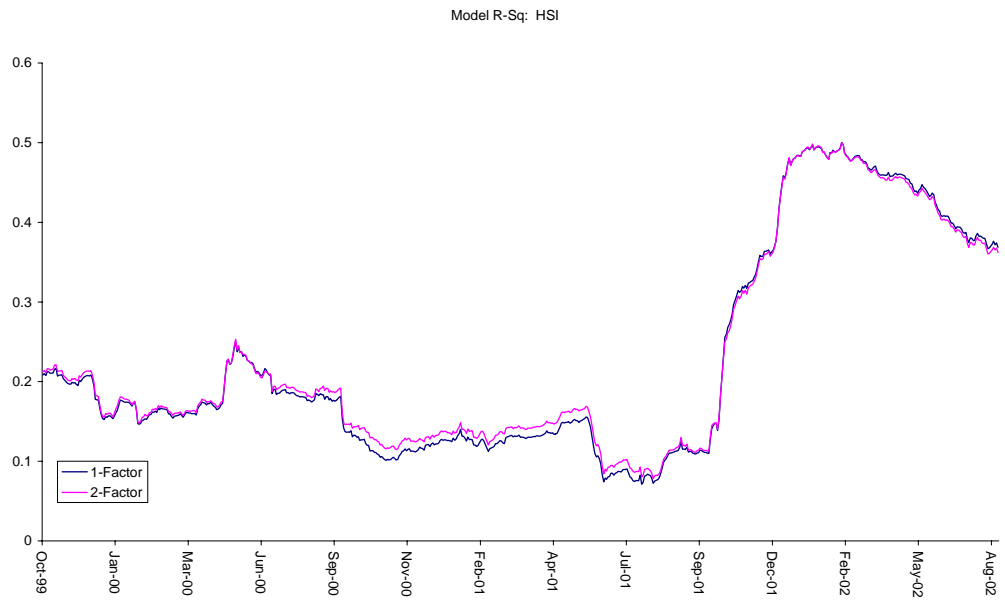


Figure 85 REGARCH Model R-Sq - HSI

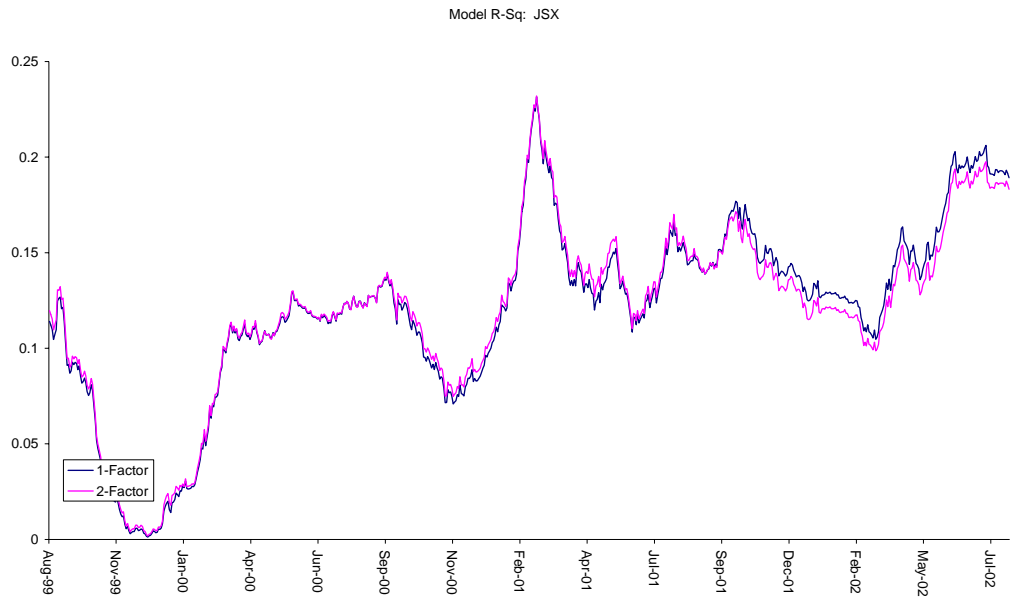


Figure 86 REGARCH Model R-Sq - JSX



Figure 87 REGARCH Model R-Sq - KLSE

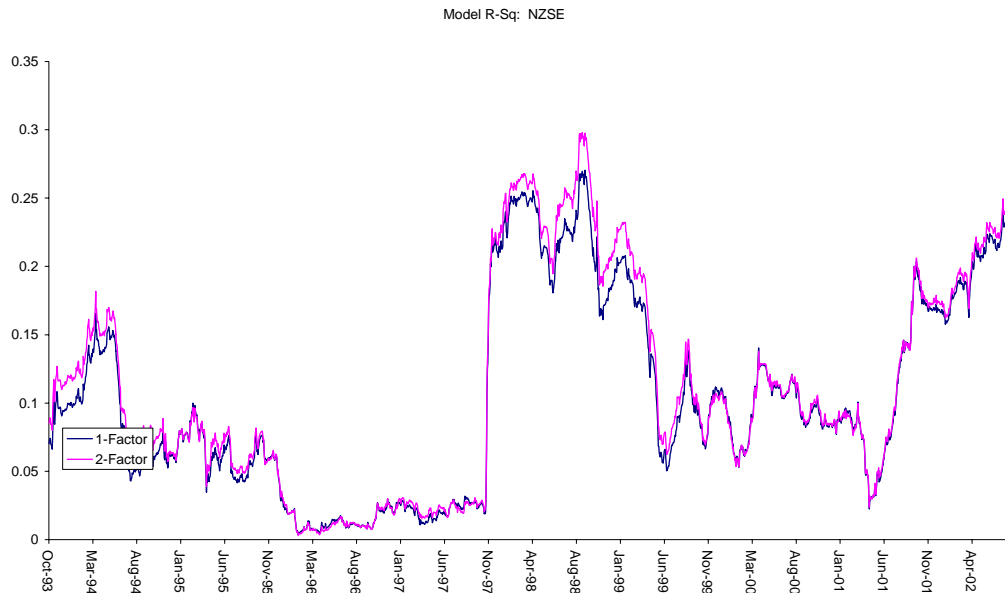


Figure 88 REGARCH Model R-Sq - NZSE



Figure 89 REGARCH Model R-Sq - PSE

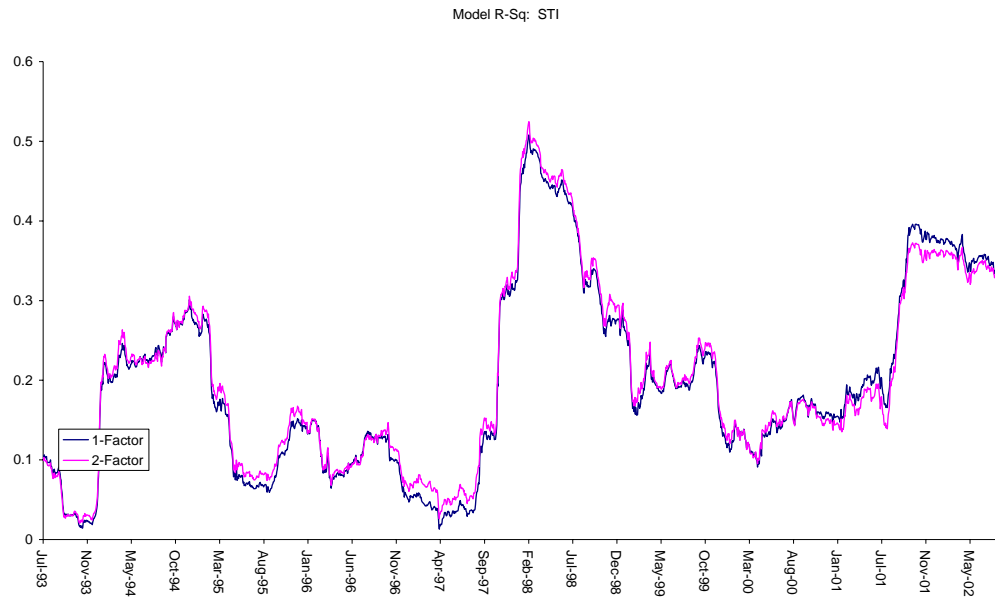


Figure 90 REGARCH Model R-Sq - STI

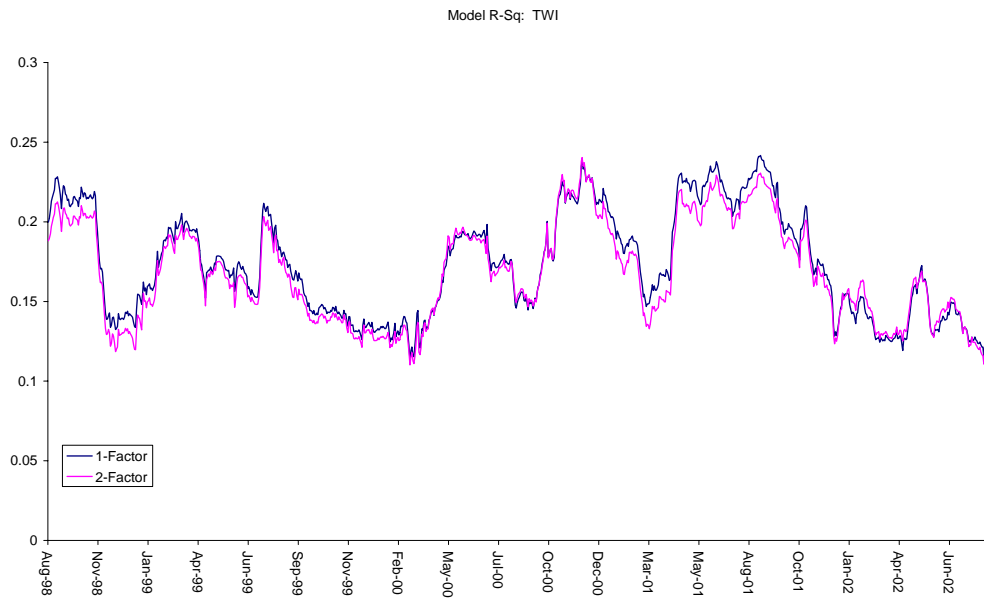


Figure 91 REGARCH Model R-Sq - TWI

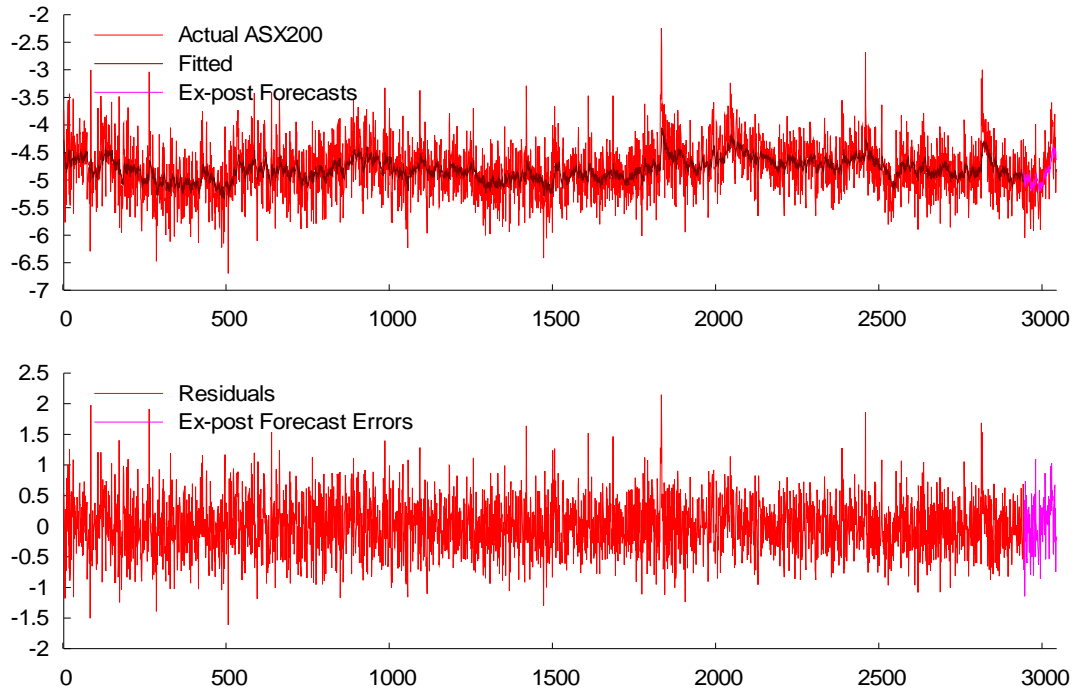


Figure 92 ARFIMA-REGARCH Model Forecasts and Residuals - ASX200

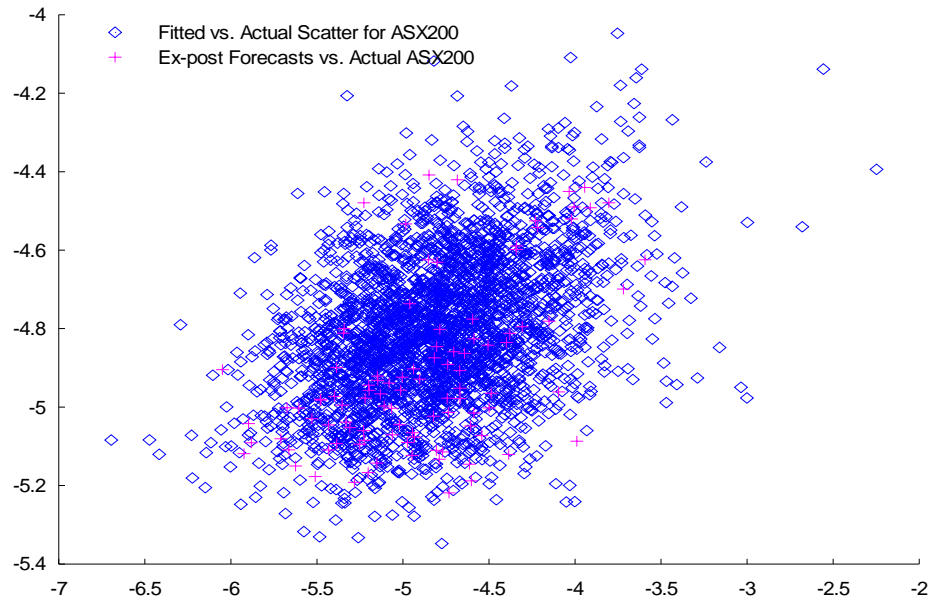


Figure 93 ARFIMA-REGARCH Model Forecast Scatterplot - ASX200

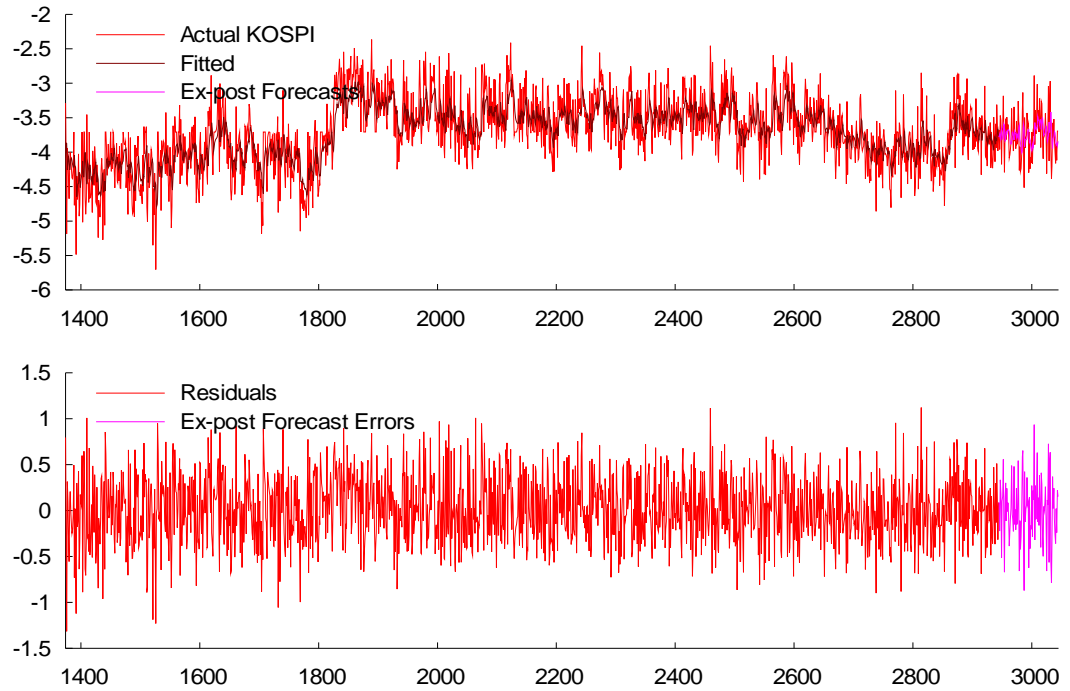


Figure 94 ARFIMA-REGARCH Model Forecasts and Residuals - KOSPI

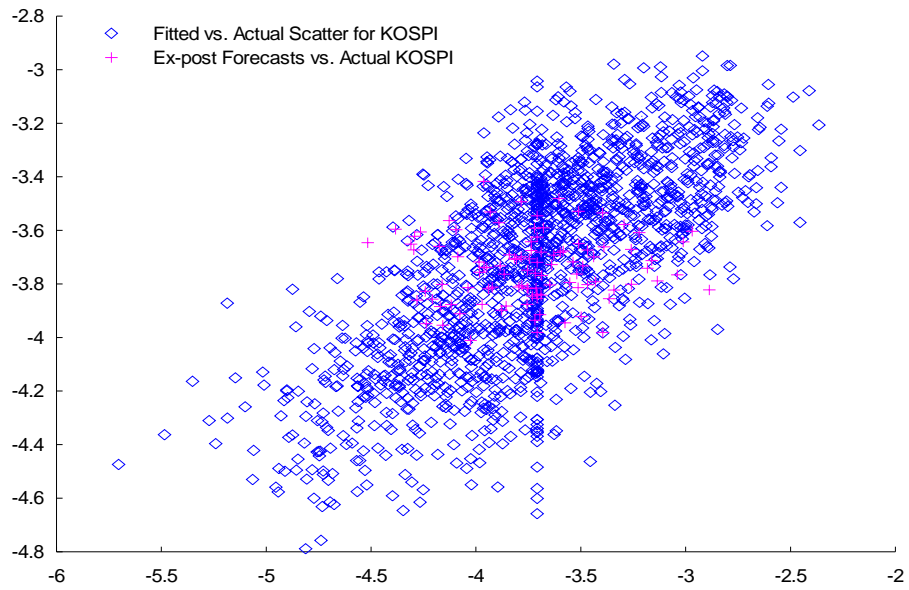


Figure 95 ARFIMA-REGARCH Model Forecasts Scatterplot - KOSPI

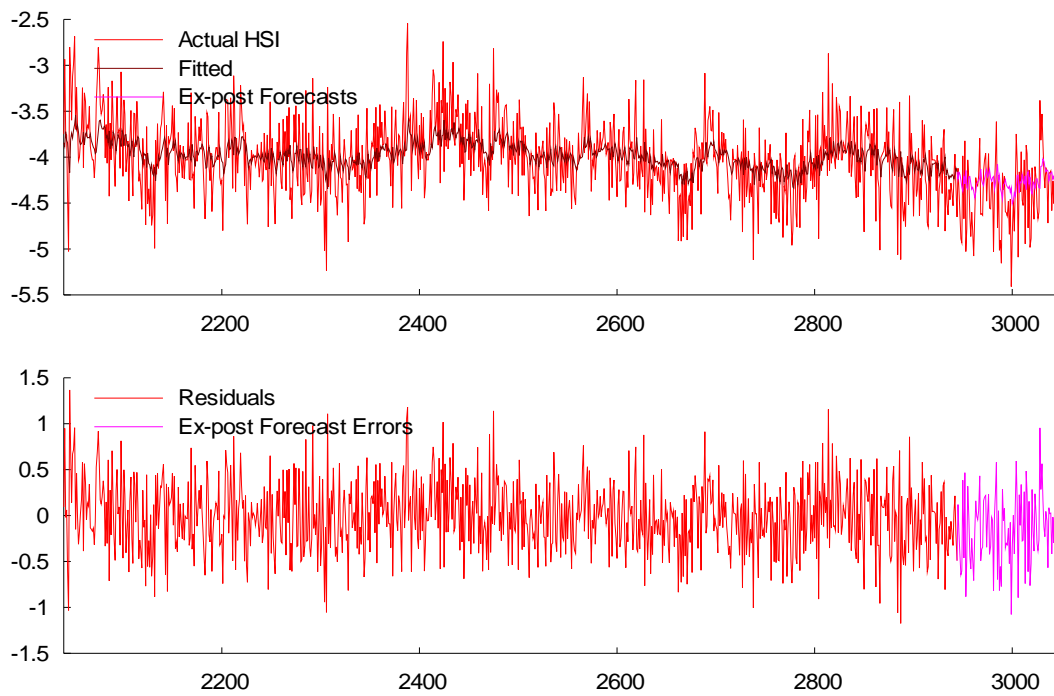


Figure 96 ARFIMA-REGARCH Model Forecasts and Residuals - HSI

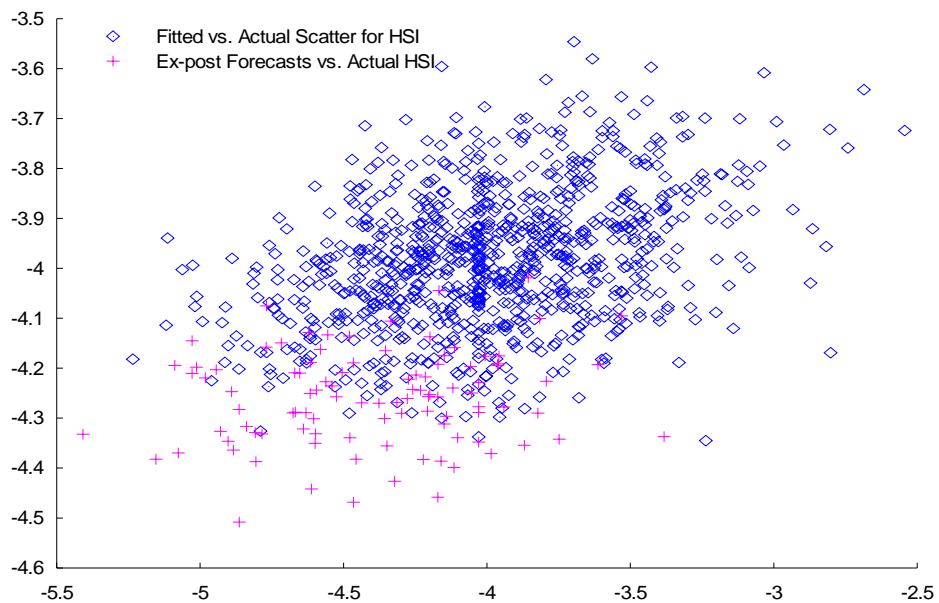


Figure 97 ARFIMA-REGARCH Model Forecasts Scatterplot - HSI

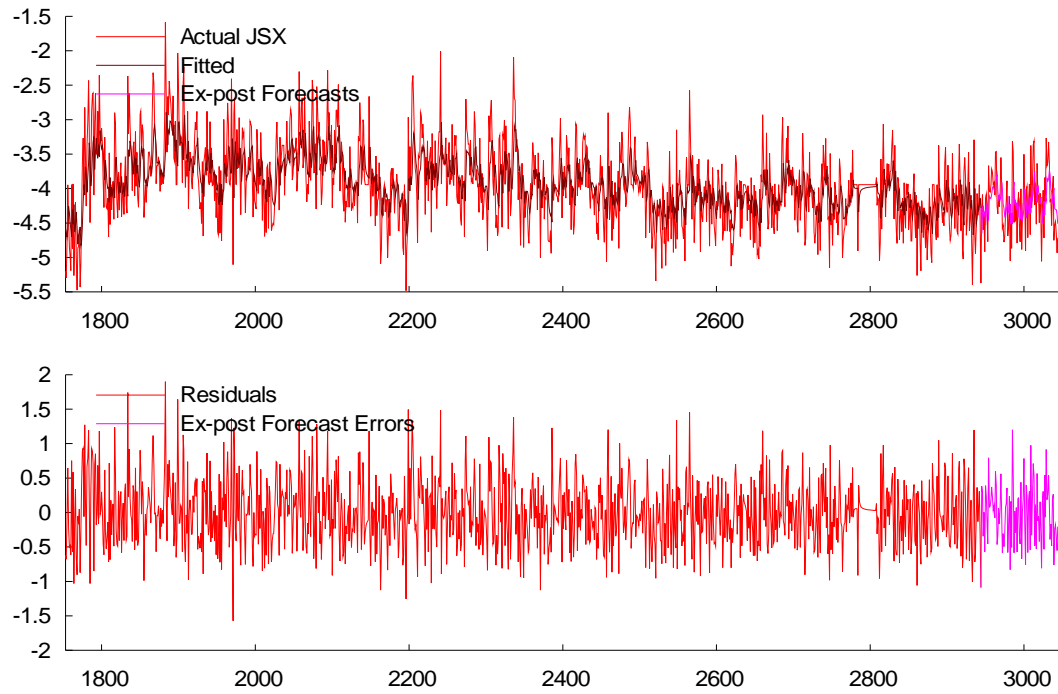


Figure 98 ARFIMA-REGARCH Model Forecasts and Residuals - JSX

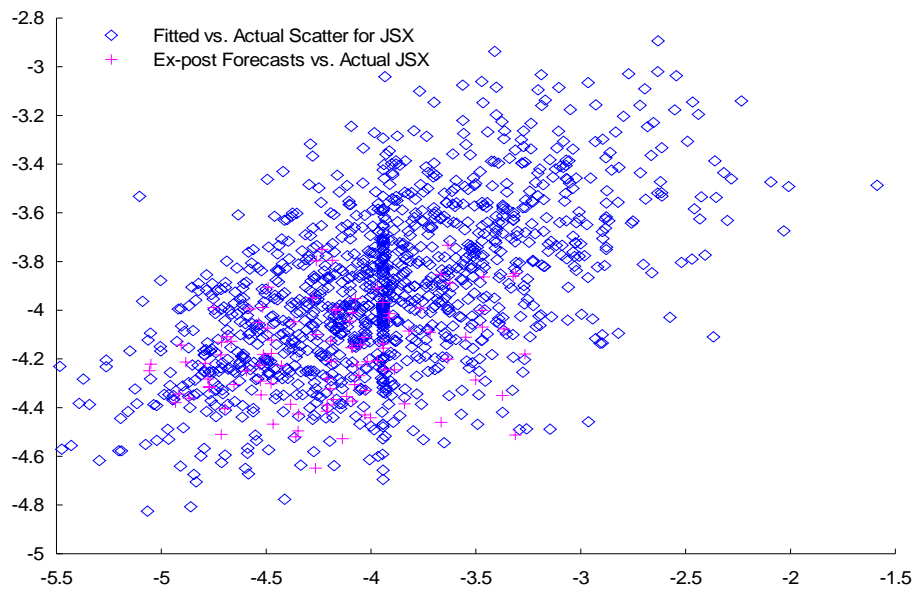


Figure 99 ARFIMA-REGARCH Model Forecasts Scatterplot - JSC

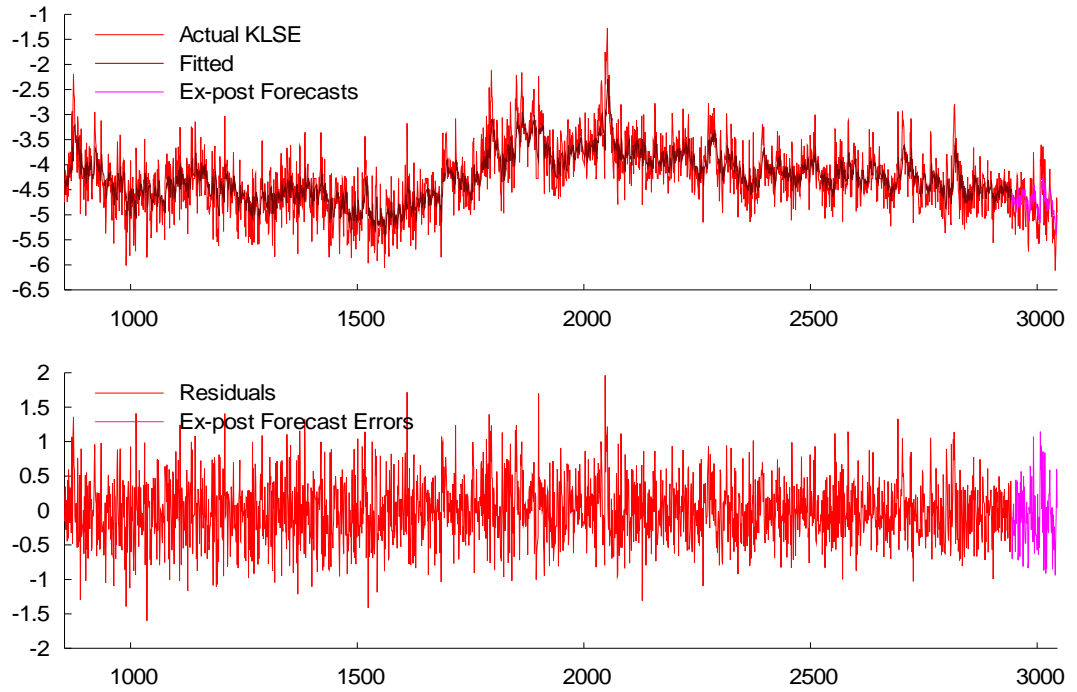


Figure 100 ARFIMA-REGARCH Model Forecasts and Residuals - KLSE

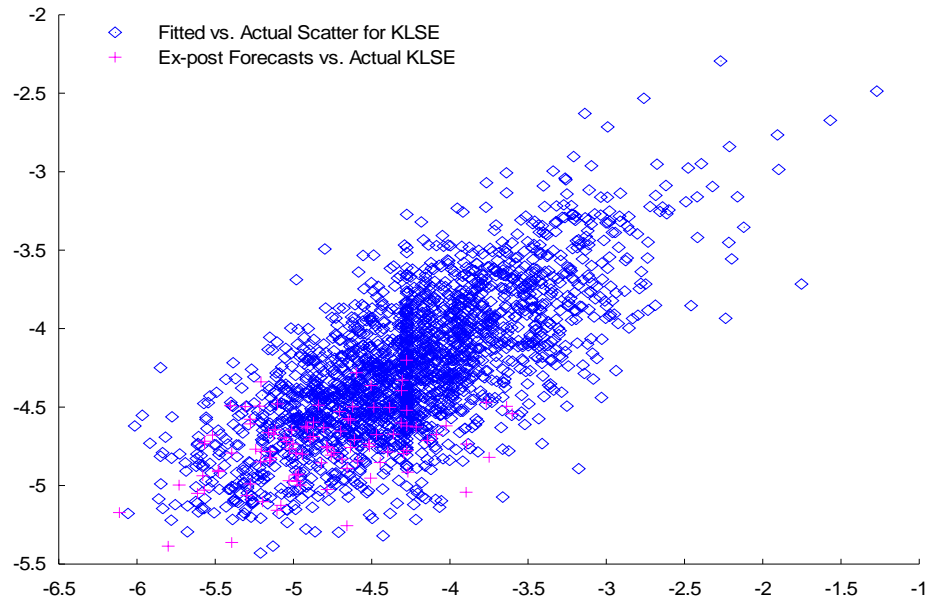


Figure 101 ARFIMA-REGARCH Model Forecasts Scatterplot - KLSE

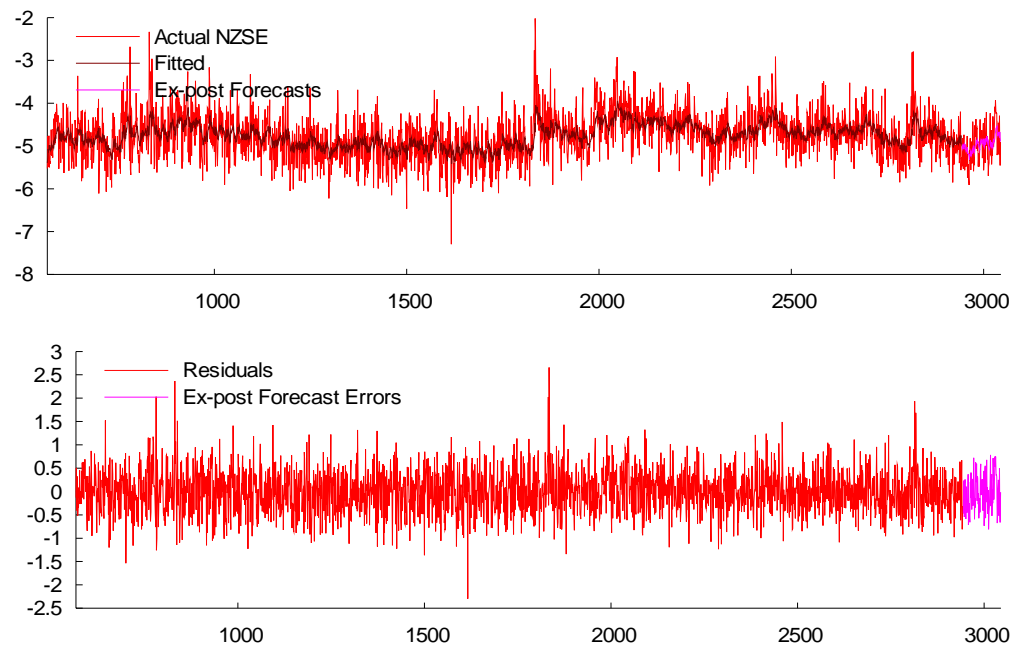


Figure 102 ARFIMA-REGARCH Model Forecasts and Residuals - NZSE

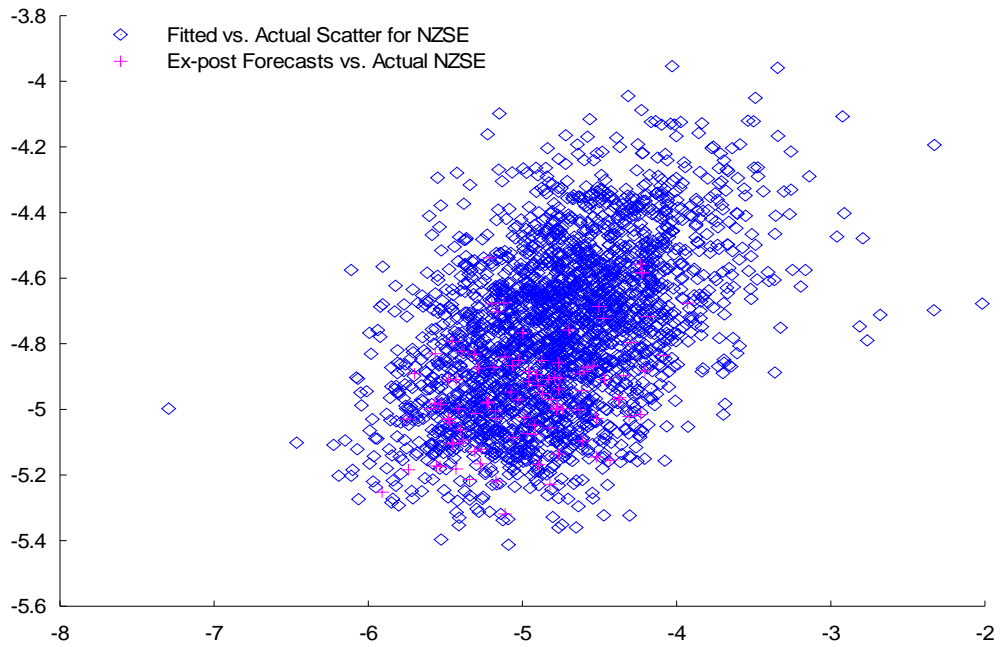


Figure 103 ARFIMA-REGARCH Model Forecasts Scatterplot - NZSE

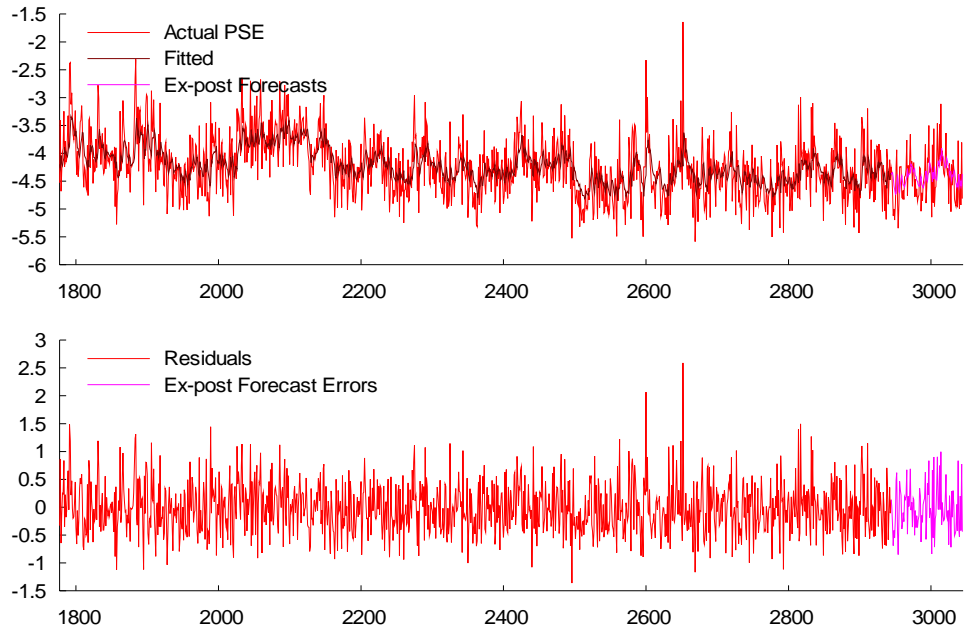


Figure 104 ARFIMA-REGARCH Model Forecasts and Residuals - PSE

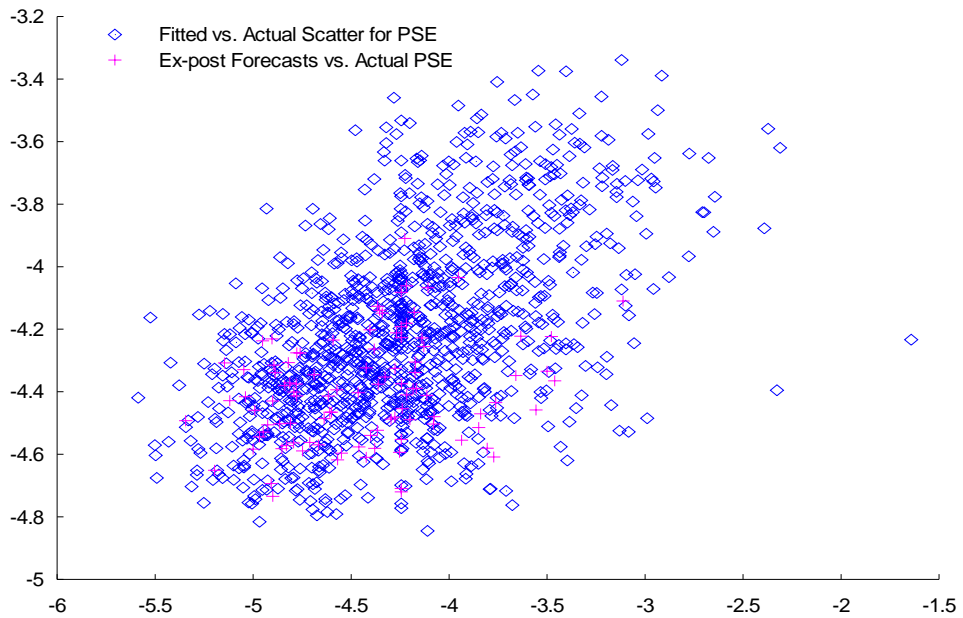


Figure 105 ARFIMA-REGARCH Model Forecasts Scatterplot - PSE

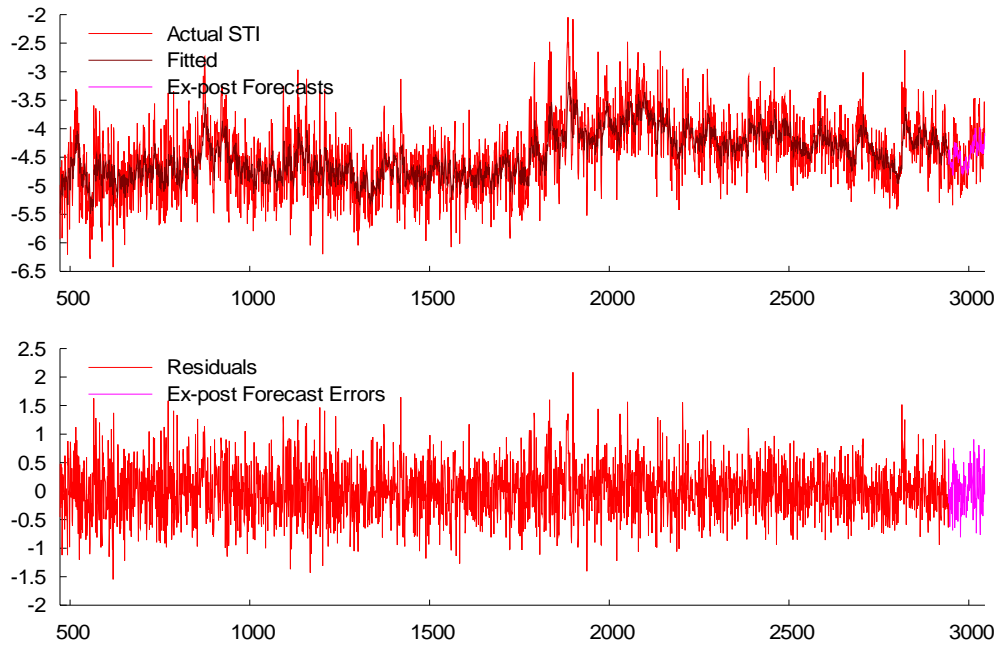


Figure 106 ARFIMA-REGARCH Model Forecasts and Residuals - STI

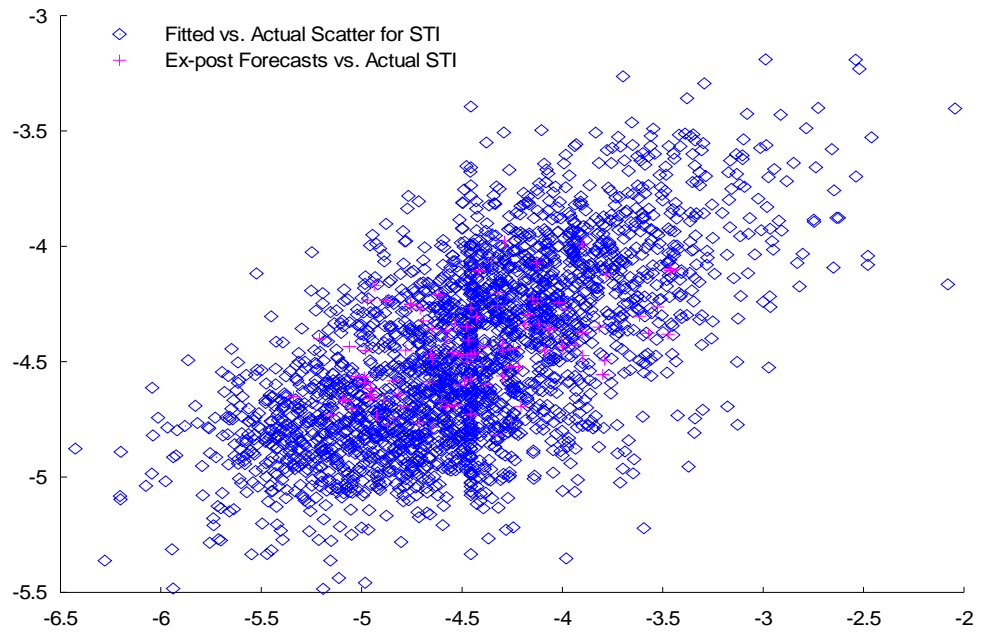


Figure 107 ARFIMA-REGARCH Model Forecasts Scatterplot - STI

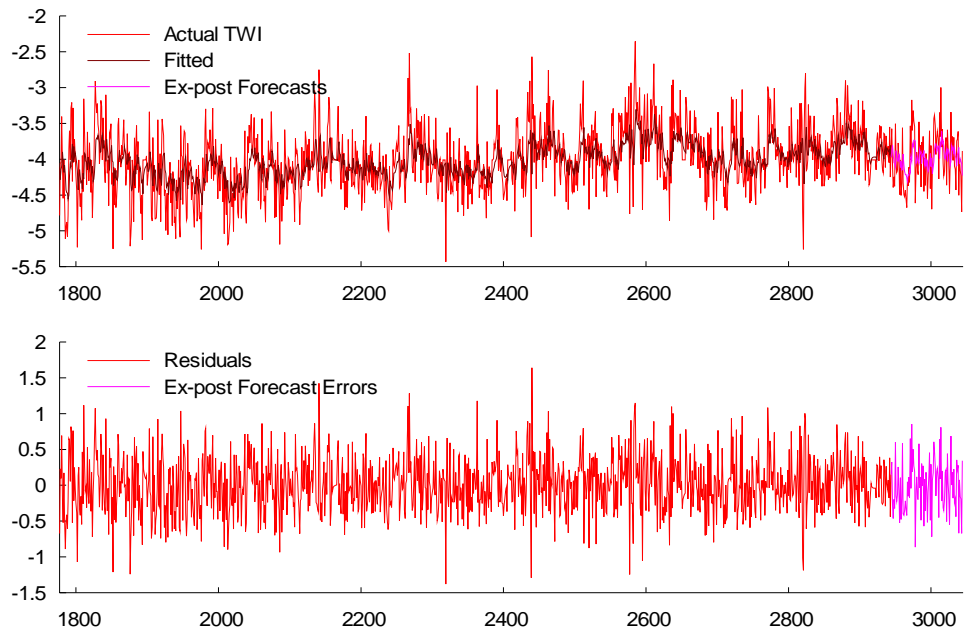


Figure 108 ARFIMA-REGARCH Model Forecasts and Residuals - TWI

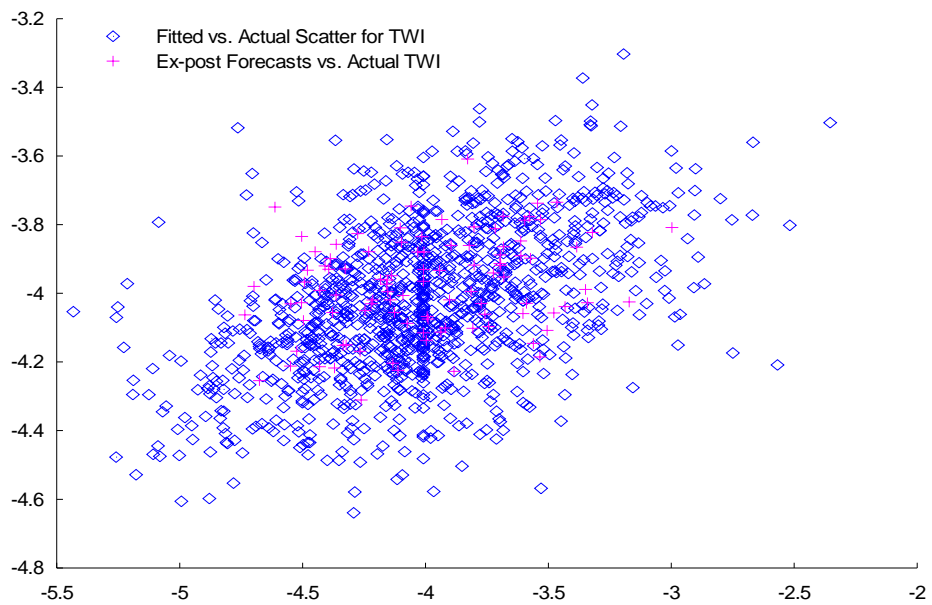


Figure 109 ARFIMA-REGARCH Model Forecasts Scatterplot – TWI